

*Characterization of Small Conductance Ca^{2+} -
activated K^+ Channel 2 Isoforms in Mouse Brain.*

**Dissertation
zur Erlangung des Doktorgrades
der Mathematisch-Naturwissenschaftlichen Fakultäten
der Georg-August Universität zu Göttingen**

**vorgelegt von
Saravana Radha Krishna Murthy
aus Bangalore, Indien**

Göttingen 2007

D7

Referent: Prof. Dr. Rüdiger Hardeland

Korreferent: Prof. Dr. Ernst Wimmer

Tag der mündlichen Prüfung: 1, November, 2007

For my mother Mrs.R.Geetha and
father Late Mr. K.L.Radha Krishna Murthy.

Contents

1.0 Abbreviations	6
2.0 Introduction	8
2.1 Synaptic plasticity	8
2.1.1 Hippocampal learning and memory	8
2.1.2 CRF	9
2.1.3 Long term potentiation (LTP)	11
2.1.4 Syntaxin	12
2.2 SK channels	14
2.2.1 SK channels and alternative splicing	15
2.3 Alternative splicing	16
2.3.1 Alternative splicing and function	18
2.3.2 Alternative splicing and neurotransmission	18
2.3.3 Alternative splicing and synapse function	20
2.3.4 Mechanism and Control of alternative splicing	22
2.3.5 Tools for deciphering alternative splicing	25
2.3.6 Mining databases	25
2.3.7 Tools for sequence alignment	25
2.3.8 Identification of alternatively spliced variants	28
3.0 Aim and outline of the thesis	31
4.0 Materials and Methods	33
4.1 Bioinformatics	33
4.2 Animal handling and tissue isolation	34
4.3 RNA preparation and cDNA synthesis	34
4.4 Reverse transcriptase PCR	34
4.5 Quantitative real-time PCR	35
4.5.1 Absolute quantification	35
4.5.2 Relative quantification	36
4.6 Rapid amplification of cDNA ends and cloning	37
4.7 Expression in HEK 293 cells	40
4.8 In-situ hybridization	41

Contents

4.9 Fluorescent in situ transcription (FIST)	42
4.10 Fear conditioning	42
4.11 Western blot	43
4.12 Excitotoxicity Experiment	43
4.13 Primary cortical neuronal culture	44
4.14 Protein analysis	45
5.0 Results	46
5.1 Bioinformatic analysis of SK2 alternative splice variants	46
5.1.1 Results of Expressed Sequence Tags (ESTs) analysis	48
5.2 Characterizations of SK2 splice variants	50
5.2.1 SK2P	50
5.2.2 SK2sh	61
5.2.3 SK2L	74
5.2.4 SK2CaMBD and SK2-N-terminus	77
6.0 Discussion	79
6.1 SK2P	79
6.2 Presence of SNARE domain in C-terminal region of SK2P	79
6.3 Specific expression of SK2P in CA3	81
6.4 Regulation of SK2P after stress	82
6.5 SK2sh	83
6.6 SK2L	84
6.7 SK2CaMBD	85
6.8 SK2-N-terminus and SK2R	85
6.9. Future perspectives	85
7.0 Summary	87
8.0 References	88
9.0 Curriculum vitae	113
10.0 Acknowledgements	114
11.0 Publications and abstract	117

1. Abbreviations

AD- Alzheimer's disease
AHP- AfterHyperPolarizations
AP- Alkaline Phosphatase
AS- Alternative Splicing
BLAST- Basic Local Alignment Search Tool
Blastn- Nucleotide-nucleotide BLAST
Blastp- Protein-protein BLAST
Blastx- Nucleotide 6-frame translation-protein
CaMBD-Calmodulin Binding Domain
cc-Corpus Callosum
CDD- Conserved Domain Database
cDNA-Complementary Deoxyribonucleic acid
cg-Cingulum
CNS-Central Nervous System
Cp- threshold Crossing Point
CRF-Corticotropin-releasing factor
CS- Conditional Stimulus
dbEST- Database for Expressed Sequence Tags
ec-External Capsule
EMBOSS- European Molecular Biology Open Software Suite
EST- Expressed Sequence Tag
E-value-Expectation Value
FC-Fear Conditioning
fi-Fimbria of the Hippocampus
FIST- Fluorescent *in situ* transcription
Glu-Glutamate
HEK cells-Human Embryonic Kidney cells
HPA-axis- Hypothalamo-Pituitary Adrenal axis
HPRT-Hypoxanthine-guanine PhosphoRibosylTransferase

Abbreviations

KDa-Kilodalton

LHbM-Lateral Habenular Nucleus

LTP- Long-Term Potentiation

MCLH Magnocellular Nucleus of the Lateral Hypothalamus

mt-Mammillothalamic Tract

NCBI-National Center for Biotechnology Information

ORF-Open Reading Frame

PC- Proprotein Convertases

PSI-BLAST- Position-Specific Iterative BLAST

PTC- Premature Termination Codon

RACE- Rapid amplification of cDNA ends

RT-PCR- Reverse Transcription Polymerase Chain Reaction

SK channel-Small conductance calcium-activated potassium channel

SK2CaMBD-Small conductance calcium-activated potassium channel 2-Calmodulin
Binding Domain

SK2P-Small conductance calcium-activated potassium channel 2- Parkinson

SK2sh-Small conductance calcium-activated potassium channel 2-Short

SK2std- Small conductance calcium-activated potassium channel 2-Standard

SMART-Simple Modular Architecture Research Tool

SNARE- Soluble N-ethylmaleimide-sensitive factor (NSF) attachment protein (SNAP)
receptors

STh-Subthalamic Nucleus

st-Stria Terminalis

tblastn- Protein-nucleotide 6-frame translation

tblastx- Nucleotide 6-frame translation-nucleotide 6-frame translation

TM- Transmembrane Domain

TNF-Tumor Necrosis Factor

UTR-Un-Translated Region

2. Introduction

2.1. Synaptic plasticity

2.1.1. Hippocampal learning and memory

The hippocampus is part of the limbic system, located in the medial temporal lobe of the mammalian brain. Anatomically, the hippocampus is composed of four regions, CA1, CA2, CA3 pyramidal cell regions and the dentate gyrus.

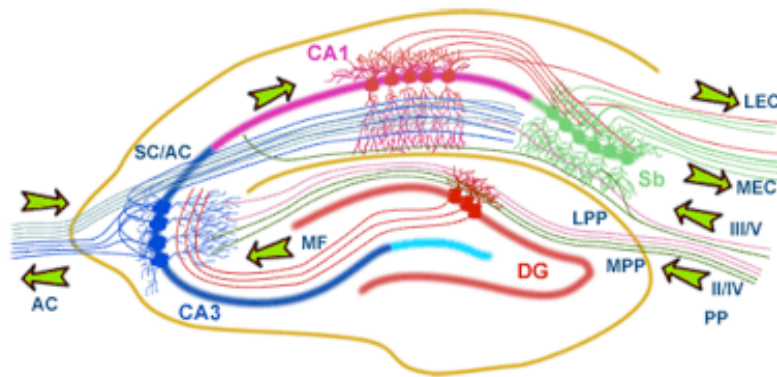


Fig. 1: Architecture of the hippocampus. The hippocampus forms a principally uni-directional network with input from the entorhinal-cortex (LEC/MEC) that forms connections with the dentate gyrus (DG) and CA3 pyramidal neurons via the perforant Path (PP – split into lateral and medial). CA3 neurons also receive input from the DG via mossy fibers (MF). They send axons to CA1 pyramidal cells via the Schaffer Collateral Pathway (SC), as well as to CA1 cells in the contralateral hippocampus via the associational Commissural pathway (AC). CA1 neurons also receive input directly from the perforant path and send axons to the Subiculum (Sb). These neurons in turn send the main hippocampal output back to EC, forming a loop. Inputs arrive to the CA3 area from the entorhinal cortex by the perforant path, both directly by the temporo-ammonic pathway and indirectly by the mossy fibre pathway (MF). The axons of the lateral perforant path synapse on the distal part of the apical dendrites of the CA3 pyramidal cells (green arrow at MF), whereas the axons of the dentate granule cells, the mossy fibers (MF), contact 'en passant' the proximal part of the apical dendrites and the basal dendrites of the CA3 cells, close to the cell body, through giant MF synapses. Collateral axons from the CA3 pyramids contact the median part of the apical dendrites

Introduction

of neighboring CA3 neurons by modifiable synapses and constitute the recurrent network.

The hippocampus plays a functional role in both navigation and memory processing (Sweatt et al, 2003). Hippocampal learning involves the formation of declarative or episodic memories about events and their relationships in the context of the organism's ongoing experience (Eichenbaum, 1999; Smith and Mizumori, 2006). This assumption is based on experiments, which report that hippocampal principal neurons - 'place cells' - exhibit location-specific firing (Winson et al., 1978). There is further evidence that hippocampal neurons are required for multi-modal sensory integration (Shapiro et al., 1997; Tanila et al., 1997). The hippocampus is also crucial for trace conditioning, a procedure where a period of no stimuli intervenes between the conditioned stimulus and the unconditioned stimulus (Mehta et al., 1997; Quirk et al., 2001). In support of this hypothesis, animals with a hippocampal lesion have problems associating two different episodes separated in time (Squire et al., 1991; Clark et al., 1998; Huerta et al., 2000).

2.1.2. Corticotropin-releasing factor (CRF)

Endocrine responses to stress are mediated by release of CRF. CRF is part of the body's stress axis, the hypothalamo-pituitary adrenal axis (HPA-axis) where it stimulates hypophyseal adrenocorticotrophic hormone (ACTH) secretion, which subsequently elicits adrenal glucocorticoid release (Spiess et al., 1981; Vale et al., 1981). Besides these neuroendocrine actions, CRF also acts in the brain to modulate behavioral, autonomic and neuroendocrine responses to stress (reviewed in: Owens and Nemeroff, 1991). Two CRF receptors, encoded by distinct genes, CRFR1 and CRFR2, which can exist in two alternatively spliced forms, have been cloned in rodents (Chang et al., 1993; Lovenberg et al., 1995). CRF receptors are members of a 7-transmembrane receptor family, whose actions are in most cases mediated through activation of adenylate cyclase. In addition to its interaction with membrane receptors, CRF binds with high affinity to a CRF binding protein (CRF-BP) (Cortright et al., 1995; Potter et al., 1991).

Introduction

Electrophysiological studies provide evidence for an excitatory action of CRF in several brain regions such as the locus coeruleus, solitary tract, hippocampus and some regions of the hypothalamus (Conti and Foote, 1996; Hollrigel et al., 1998; Siggins et al., 1985; Smith and Dudek, 1994; Yamashita et al., 1991). Exogenous application of CRF to hippocampal slices was shown to make the pyramidal neurons more excitable i.e., to reduce the slow afterhyperpolarizations and spike frequency accommodation (Aldenhoff et al., 1983; Haug and Strom, 2000; Smith and Dudek, 1994) and to enhance the amplitude of CA1 population spikes evoked by stimulation of the schaffer collateral pathway in rats (Hollrigel et al., 1998). CRF also increases the amplitude of orthodromically evoked (stratum radiatum stimulation) population spikes in the rat hippocampus (Smith and Dudek, 1994).

Like stress, CRF can modulate learning and memory, either enhancing or impairing retention in a time-, dose- and site-specific manner. Intracerebroventricular injections of CRF or its displacement from CRF-BP before or immediately after training improve memory in multiple learning tasks (Behan et al., 1995; Heinrichs et al., 1997; Koob and Bloom, 1995; Liang and Lee, 1988; Radulovic et al., 1999). CRF directly injected into the dentate gyrus consistently enhanced memory retention in rats in a one-way passive avoidance task (Lee et al., 1993). Intrahippocampal infusion of antisense oligodeoxynucleotides (ODNs) directed against CRF mRNA has been reported to impair performance of passive avoidance tasks (Wu et al., 1997). However, intracerebroventricular CRF injection before the memory test or overexpression of CRF in mice seems to impair memory (Diamant and De Wied, 1993; Heinrichs et al., 1996). Especially, the presence of CRFR1 in the hippocampus suggests a role for CRF in learning and memory processes (Radulovic et al., 1999).

The role of CRF in the hippocampus is further supported by electrophysiological data, which show that CRF induces a long-lasting enhancement of synaptic efficacy in the hippocampus (Wang et al., 1998). This finding appears to be critically dependent on protein synthesis (Wang et al., 2000). Wang and colleagues (1991) also found that application of CRF to the dentate gyrus increases the population excitatory postsynaptic potential as well as the population spike. Furthermore, pretreatment with CRF receptor antagonist dose-dependently diminishes tetanization induced LTP, while CRF and LTP

Introduction

have an additive effect on cell excitation in hippocampal neurons. On the basis of these findings, they suggest that CRF-induced potentiation and LTP may share some similar mechanisms and that CRF is probably involved in neuronal circuits underlying LTP.

2.1.3. Long-term potentiation (LTP)

The brain uses short- and long-lasting modifications in synaptic strength in critical neuronal circuits to process and store information. One such activity-dependent modification is long-term potentiation (LTP) in the hippocampus, a sustained increase in synaptic strength that is elicited by brief high frequency or theta-burst stimulation of excitatory afferents. Mechanisms underlying LTP have been proposed as possible mechanisms for memory formation in the brain. This conclusion is in part due to the properties LTP displays (Bliss and Lomo, 1973; Nicoll et al., 1988; Bliss and Collingridge, 1993) and is further supported by the observation that an LTP-like phenomenon can be seen in brains of animals successfully learning a behavioral task (Berger, 1984; Moser et al., 1994; Sharp et al., 1985; Skelton et al., 1985). LTP exhibits input specificity, in that LTP occurs only at synapses stimulated by afferent activity but not at adjacent synapses of the same postsynaptic cell. Temporal pairing of a weak input with activation of strong input results in LTP of weak input. Furthermore, pharmacological blocking of LTP interferes with the acquisition of behavioral learning (Davis et al., 1993; Morris et al., 1986) and targeted gene knockouts of various genes, which impair LTP generation also impair spatial learning (Abeliovich et al., 1993; Grat and Silva, 1994).

Although LTP mechanisms have been shown to be an attractive candidate as a mechanism for memory formation, it is important to note that there is little empirical evidence that directly links LTP to the storage of memories (Barnes, 1995; Goda and Stevens, 1996; Holscher, 1999; Martin et al., 2000). For example, Gu and colleagues (2002) observed impaired conditioned fear but enhanced LTP in *Fmr2* knockout mice. Instead of being a learning mechanism, LTP has also been suggested to rather serve as a neural equivalent to an arousal or attention device in the brain. Thus, LTP could act to facilitate and maintain learning indirectly by altering the organism's responsiveness to, or perception of environmental stimuli (Shors and Matzel, 1997).

2.1.4. Syntaxin

Syntaxins are membrane integrated Q-SNARE (soluble NSF attachment receptor) proteins participating in exocytosis (Teng et al., 2001). Syntaxins possess a single C-terminal transmembrane domain, a SNARE domain (known as H3), and an N-terminal regulatory domain (Habc). The SNARE (H3) domain binds to both synaptobrevin and SNAP-25 forming the core SNARE complex. Formation of this extremely stable SNARE core complex is believed to generate the free energy required to initiate fusion between the vesicle membrane and plasma membrane.

The N-terminal Habc domain is formed by 3 α -helices and when collapsed onto its own H3 helix forms an inactive "closed" syntaxin conformation (Sutton et al., 1998).

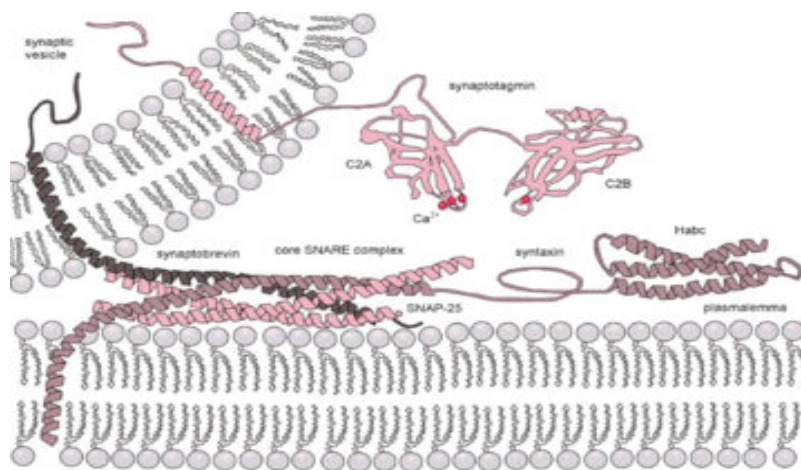


Fig. 2: Molecular machinery driving exocytosis in neuromediator release. The core SNARE complex is formed by four α -helices contributed by synaptobrevin, syntaxin and SNAP-25, synaptotagmin serves as a calcium sensor and regulates intimately the SNARE zipping. This closed conformation of syntaxin is believed to be stabilized by binding to *nSec1* (*Munc18*) (Togneri et al., 2006), although more recent data suggests that *nSec1* may bind to other conformations of syntaxin as well. The "open" syntaxin conformation is the conformation that is competent to form into SNARE core complexes (Sutton et al., 1998, Fasshauer et al., 1998).

Proposed mechanism of membrane fusion

Assembly of the SNAREs into the "trans" complexes likely bridges the apposed lipid bilayers of membranes belonging to the cell and the secretory granule, bringing them in proximity and inducing their fusion. The influx of calcium into the cell triggers the completion of the assembly reaction, which is mediated by an interaction between the putative calcium sensor, synaptotagmin, with membrane lipids and/or the partially assembled SNARE complex.

According to the "zipper" hypothesis, the complex assembly starts at the N-terminal parts of SNARE motifs and proceeds towards the C-termini that anchor interacting proteins in membranes. Formation of the "trans"-SNARE complex proceeds through an intermediate complex composed of SNAP-25 and syntaxin-1, which later accommodates synaptobrevin-2 (the quoted syntaxin and synaptobrevin isotypes participate in neuronal neuromediator release).

Based on the stability of the resultant cis-SNARE complex, it has been postulated that energy released during the assembly process serves as a means for overcoming the repulsive forces between the membranes. There are several models that propose explanations of a subsequent step – the formation of stalk and fusion pore, but the exact nature of these processes remains debated. It has, however, been proved that in vitro syntaxin is sufficient to drive spontaneous calcium independent fusion of synaptic vesicles containing v-SNAREs (Woodbury et al., 2000). This suggests that in Ca²⁺-dependent neuronal exocytosis synaptotagmin is a dual regulator. In absence of Ca²⁺ ions synaptotagmin inhibits SNARE dynamics, while in presence of Ca²⁺ ions it acts as an agonist in the membrane fusion process.

2.2. SK Channels

Small conductance calcium-activated potassium channels (SK channels) are potassium selective and voltage independent channels, which are activated by intracellular calcium during an action potential and play an important role in excitable cells (Kohler, M. et al., 1996). Although calcium ions do not interact directly with the SK channel α subunits, calcium gating is due to a constitutive interaction with calmodulin and subsequent calcium-dependent conformational alterations (Xia et al., 1998; Keen et al., 1999; Schumacher et al., 2001). Activation of SK channels causes membrane hyperpolarization, which inhibits cell firing and limits the firing frequency of repetitive action potentials. The intracellular calcium increase evoked by action potential firing decays slowly, allowing SK channel activation to generate a long-lasting hyperpolarization termed the slow afterhyperpolarization (sAHP) in some types of neurons. In hippocampal neurons SK channels are not involved in sAHPs and their role in medium AHP is currently discussed with controversy (Vogalis et al., 2003). This spike-frequency adaptation protects the cell from the deleterious effects of continuous tetanic activity and is essential for normal neurotransmission (Sah et al., 1996; Madison et al., 1984; Lancaster et al., 1986; Hille et al., 1992).

Slow AHPs can be classified into two groups, based on sensitivity to the bee venom toxin apamin. In general, apamin-sensitive sAHPs activate rapidly following a single action potential and decay with a time constant of approximately 150 ms. In contrast; apamin-insensitive sAHPs rise slowly and decay with a time constant of approximately 1.5 s. The basis for this kinetic difference is not yet understood. (Bond et al., 1999). SK1, SK2, and SK3 are the three sub types of the SK channel family and are expressed in overlapping yet distinct patterns throughout the central nervous system with SK2 being the most highly expressed (Kohler et al., 1996; Stocker et al., 2000; Sailer et al., 2004)

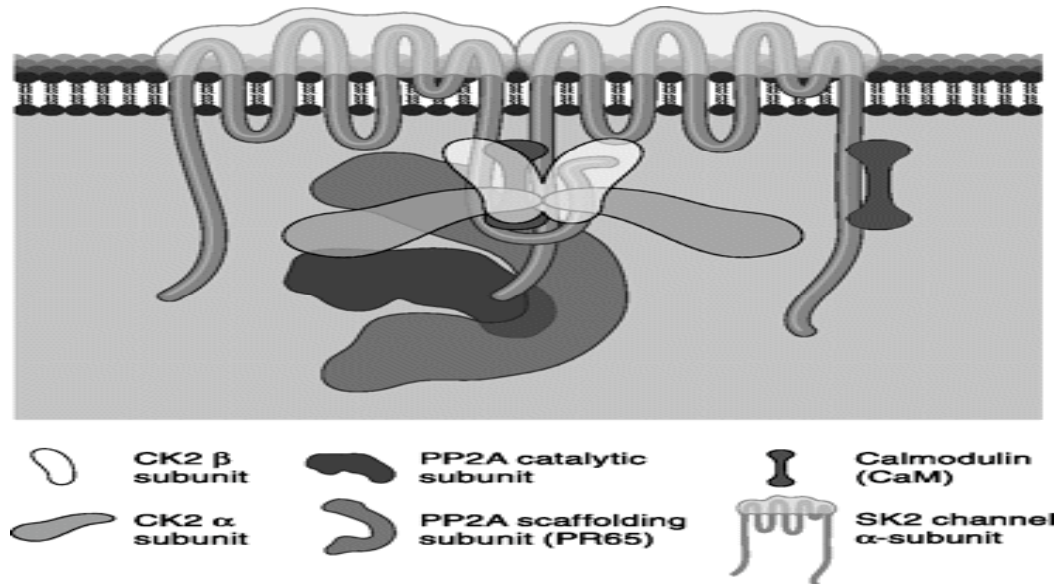


Fig. 3: Model for coassembled SK2, CaM, CK2, and PP2A. The model represents two of the four SK2 subunits and invokes an intersubunit interaction. CK2 and PP2A are drawn approximately to scale. (Adapted from Allen et al., 2007)

2.2.1 SK channel and alternative splicing

All three SK channel subunits, SK1, SK2 and SK3 have been shown to undergo alternative splicing (Shmukler et al., 2001; Tomita et al., 2003; Kolski et al., 2004; Barfod ET et al., 2001). Twenty mouse SK1 transcripts are expressed in brain at levels sufficient to allow consistent detection, and these encode 16 SK1 polypeptide variants. Only four of these 16 polypeptides preserve the ability to bind calmodulin in a Ca²⁺-independent manner (Shmukler et al., 2001). Four different splice variants of SK3 have been identified, SK3-1B, SK3-1C, SK3EX4 and SK3 liver isoform (Tomita et al., 2003; Kolski et al., 2004; Barfod ET et al., 2001). SK3-1B and SK3-1C are found to be non-channel forming, and selectively suppress endogenous SK3 currents in a dominant-negative fashion (Tomita et al., 2003; Kolski et al., 2004), whereas SK3_ex1c has similar characteristic but was non-neuronal in expression (Wittekindt et al., 2004). The SK2 gene encodes two subunit proteins and suggests that native SK2-L subunits may preferentially divide up into heteromeric channel complexes with other SK subunits (Strassmaier et al., 2005).

2.3. Alternative mRNA Splicing

Promptly after the discovery of RNA splicing in 1977, the question, ‘why genes in pieces?’ was addressed by a proposal that multiple mRNAs, and consequently multiple protein functions, could be encoded from a single gene (Gilbert, 1978). This concept is now termed ‘alternative RNA splicing’. Genome sequencing of diverse species has indicated that the number of protein-coding genes in an organism does not correlate with its overall cellular complexity. This, in turn, suggests that mechanisms acting to regulate and diversify gene functions must have played a major role in the evolution of the specialized cell types and multiple activities that are typically associated with complex metazoans. The question then arises: how do organisms generate a substantially larger number of functional proteins than the number of available genes? In particular, how are the hundreds of thousands of proteins generated that are expressed in mammalian brains? Although post-translational modifications, RNA editing, alternative polyadenylation, and multiple start sites of transcription can contribute to answering this question, alternative splicing seems the major mechanism for generating isoform diversity. Alternative splicing (AS), the process by which the exons of primary transcripts (pre-mRNAs) from genes can be spliced in different arrangements to produce structurally and functionally distinct mRNA and protein variants, may be one of the most extensively used mechanisms that accounts for the greater macromolecular and cellular complexity of higher eukaryotic organisms.

Alternative splicing is often regulated in a temporal or tissue-specific fashion, giving rise to different protein isoforms in different tissues or at different developmental stages. Thus, at the organism level, specific protein isoforms are expressed at certain developmental stages or in specific tissues or as a consequence of regulation by extracellular signaling mechanisms (Matter et al., 2002).

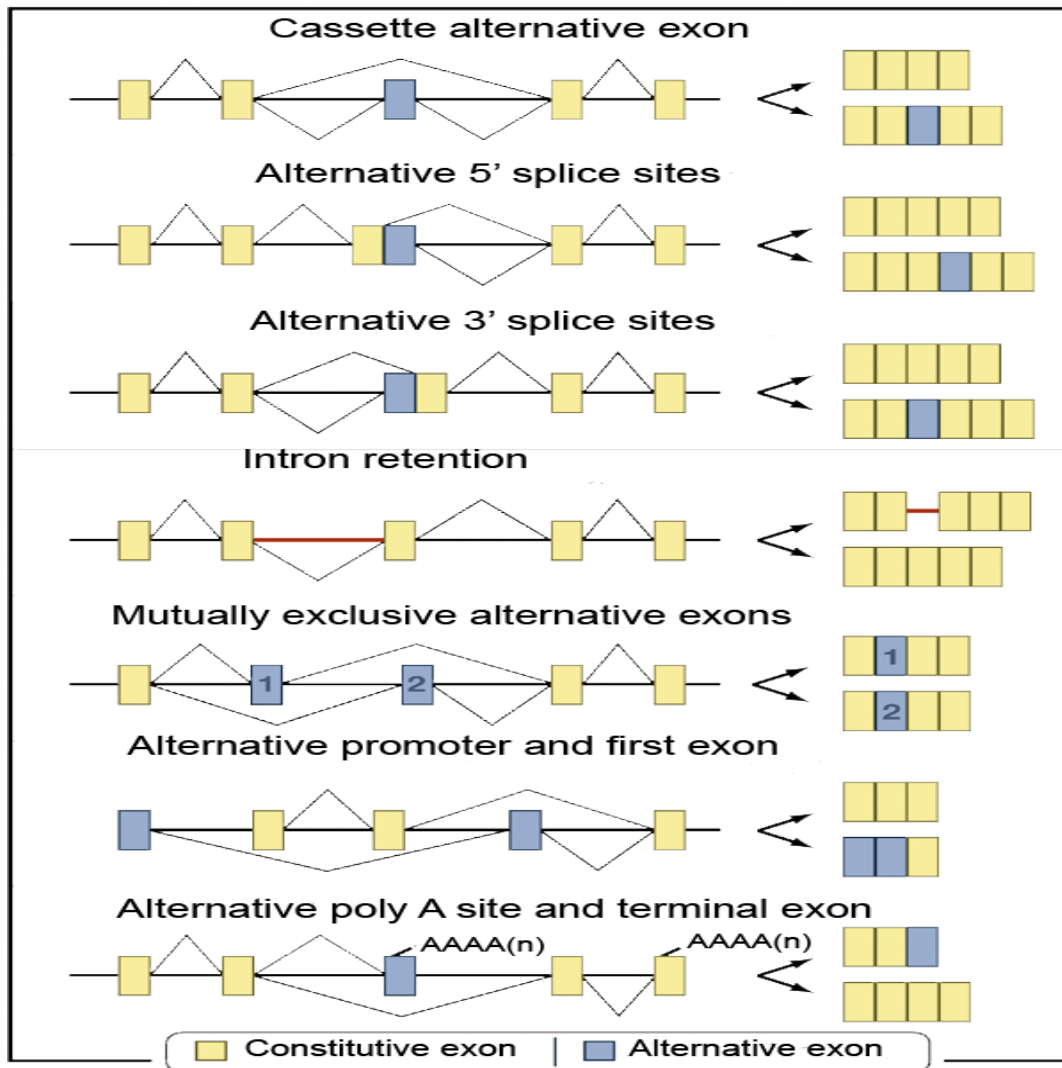


Fig. 4: Types of alternative splicing. The types of alternative splicing alteration that have been observed include exon skipping, intron retention and use of alternative splice donor or acceptor sites. The figure depicts different types of AS, which are responsible for the generation of functionally distinct transcripts. Blue boxes indicate alternative exons (Adapted from Blencowe, 2006).

The most common mechanisms are alternative inclusion or exclusion (“skipping”) of individual exons (Black, D. L et al., 2003; Maniatis, T et al., 2002; Lopez, A. J et al., 1998). It is thought that at least half of all the genes in the human genome undergo alternative splicing.

Introduction

Alternative splicing is controlled by the binding of trans-acting protein factors to cis-acting sequences within the pre-mRNA leading to differential use of splice sites. Many such sequences have been identified and are grouped as either enhancer or suppressor elements (Ladd and Cooper, 2002). These elements are generally short (8-10 nucleotides) and are even less conserved than those sequences present at exon-intron junctions.

Control of alternative splice site recognition is mediated by members of the SR (serine rich) protein family of splicing factors, which bind to the splicing enhancer and inhibitor elements. The interactions of these proteins with the pre-mRNA substrate and with snRNP proteins have been intensively studied. Their role in regulating splice site selection is believed to occur in two (perhaps non-exclusive) modes – arginine-serine (RS) domain-dependent and RS domain-independent (Cartegni et al., 2002).

2.3.1. Alternative splicing and function

In the nervous system, thousands of alternatively spliced mRNAs are translated into their protein counterparts where specific isoforms play roles in learning and memory, neuronal cell recognition, neurotransmission, ion channel function, and receptor specificity. The essential nature of this process is underscored by the finding that its altered regulation is a common characteristic of human disease. It is evident that even a small change in the coding region of the mRNA can lead to a substantial switch in protein function, and that alternative splicing is used extensively as a way of increasing proteomic diversity particularly in the nervous system (Black et al., 2003; Stamm et al., 2000 and Claverie et al., 2001).

2.3.2. Alternative splicing and neurotransmission

Alternative splicing can generate immense diversity of proteins involved in forming specific synaptic connections and in mediating synaptic transmission. Proper tuning of induction and propagation of action potentials requires the coordination of many different types of ion channels and transporters. The functional diversification of these proteins seems usually achieved by alternative splicing. Electrophysiological properties of numerous proteins involved in cell excitation are affected by changes in

Introduction

splicing. These changes can regulate the voltage- or ligand-dependence of ion channel gating, the ion conductance and the activation or inactivation kinetics of the channel, as well as its coupling to intracellular signaling pathways.

Alternative splicing specifies this localization of many proteins at the synapse, which are key to many functions of the receptors. This is very well illustrated by the C1 exon cassette (exon 21) of the N-methyl--aspartate R1 (NMDA R1) receptor. Splice variants of NMDAR1 transcripts containing the C1 cassette exon were shown to guide the receptor to the plasma membrane (Ehlers et al., 1995; Zhang et al., 1999). Neurofilament L binding site and the phosphorylation site for high/low affinity binding of calcium/calmodulin for the receptor requires the presence of this C1 exon (Ehlers et al., 1996; Hisatsune et al., 1997). In $\alpha 1B$ subunit of N type calcium channel, which regulates neurotransmitter release presence or absence of two amino acids, ET (glutamic acid, threonine) generated by alternative splicing affects the slower activation kinetics on the channel (Lin et al., 1999) and the splicing is tissue specific (Lin et al., 1997).

Optimization of neurotransmitter release in the central compared with the peripheral nervous system is a consequence of alternative splicing of the $\alpha 1B$ ET encoding exon. $\gamma 2L$ and $\gamma 2S$ are alternatively spliced forms of GABAA $\gamma 2$ subunit, which mediate regulation of the ligand-gated chloride channel in response to the binding of benzodiazepine agonists (Wafford et al., 1993). These variants increase affinity for benzodiazepines, and show increased sensitivity in behavioral responses to these agonists compared with parent strains (Quinlan et al., 2000). The increase in affinity is caused by the variants having an eight amino acid segment which contains a protein kinase C phosphorylation site that is believed to modulate channel function in response to ethanol (Krishek et al., 1994; Whiting et al., 1990). Alternatively spliced forms are similarly involved in selective coupling of G proteins with dopamine receptors. Alternatively spliced isoforms of the D2 and D3 dopamine receptor subtypes have been characterized and found to vary in a tissue specific manner and to elicit differential effects on adenylyl cyclase activity. One of the D2 receptor isoforms, a D2L insert, plays a critical role in the selectivity for the G-proteins interacting with the receptor (Dal Toso et al., 1989; Giros et al., 1989; Grandy et al., 1989, Xie et al., 1998; Guiramand et al., 1995).

Introduction

More importantly as far as this study is concerned, alternative splicing in the Ca²⁺ and voltage activated K⁺ Channel (also called BK or slo channels) modulates function of a particular cell type (Vergara et al., 1998). Five hundred different variants are generated with inclusion of numerous cassette exons in BK transcripts, which are very carefully regulated to allow Cochlea cells to be tuned for low or high frequency responses (Coetzee et al., 1999; Lingle et al., 1996; Fettiplace and Fuchs, 1999; Jones et al., 1999; Navaratnam et al., 1997; Rosenblatt et al., 1997).

2.3.3. Alternative splicing and synapse function

Alternative splicing plays a very important role in synaptic connectivity and nervous system development, in which transcription, cell adhesion, axon guidance and programmed cell death are some of the key functions. In the case of agrin, an extracellular matrix protein involved in signaling of synapse formation at the neuromuscular junction, there are many brain specific exons termed Y and Z exons. These neural specific spliced isoforms induce synaptic differentiation at the neuromuscular junction (Denzer et al., 1997; Ruegg et al., 1992; Godfrey et al., 1999; Burgess et al., 1999; Gautam et al., 1996). Neurexins a neural surface receptor thought to function in synapse formation (Missler and Sudhof, 1998) also show multiple alternative splice variants (Ullrich et al., 1995).

Around 3000 predicted and 596 experimentally validated splice variants of neurexin have been observed in mammalian brain. All these variants and their specific functions in differential neuronal cell recognition events are still poorly understood (Scheiffele et al., 2000; Ichtchenko et al., 1995, Puschel and Betz, 1995). The *Drosophila* axon guidance receptor, Dscam, a homolog of the human Down syndrome cell adhesion molecule interacts with an SH3/SH2 adaptor protein Dock, required for axon guidance (Schmucker et al., 2000). Thirty eight thousand splice variants of Dscam were predicted by comparing Dscam cDNA with the genomic locus. Combinatorial patterns of exons 4, 6, 9, and 17 of the Dcsam gene provide a very good example of mutually exclusive alternative exons, which perform immense array of functions. Alternative spliced forms of Bcl-x and Caspase-2 have contrasting functions in apoptosis pathways (Boise et al., 1993; Jiang et al., 1998 and Jiang and Wu, 1999). A method employed by *Caenorhabditis*

Introduction

elegans to regulate apoptosis is the exclusion of a short RNA region, encoding 24 amino acids, which leads to the production of an activator of programmed cell death, Ced-4S. By contrast, inclusion of this sequence produces an inhibitor of that pathway, Ced-4L (Shaham and Horvitz, 1996). Here alternative splicing plays the role of a switch that determines life or death for the cell.

Alternative spliced variants from a single transcription factor gene can function both as activators and repressors of transcription (Foulkes and Sassone-Corsi, 1992). A very good example for such contrasting function was shown by tissue specific splice variants of NRSF/REST a neuron-restrictive silencer factor and modular protein which containing an amino terminal repressor domain followed by a zinc finger DNA binding domain. Alternative splicing causes attenuation of DNA binding at the zinc-finger-DNA-binding-domain (Chong et al., 1995; Schoenherr et al., 1995 and Palm et al., 1998). Another very interesting example of alternative splicing and transcription, is the brain specific antagonistic function of CRE modulator protein (CREM) splice variants (De Cesare et al., 2000) and alteration of learning and memory function by CRE binding protein (CREB) splice variants (Lopez, 1995 and Lopez, 1998).

Alternative splicing is also involved in modulation of sensitivity to inactivation during trains of action potential waveforms brought about by an exon in a cytoplasmic region of the CaV2.2 channel (Thaler et al., 2004). Modification of synaptic strength by alternative splicing was shown in many studies. Alterations in facilitation of synaptic transmissions were developmentally regulated by SNAP-25 isoforms (Bark et al., 2004). Addition of a single "L27" motif in an alternatively spliced variant of PSD95, PSD95 β , played a very critical role for L27 domain interactions and Hrs regulated vesicular trafficking in postsynaptic protein clustering (Chetkovich et al 2002). Alternative splice forms can also play the roles of molecular signals responsible for trafficking of metabotropic glutamate receptor 1 to different neuronal compartments. Francesconi et al. (2002) showed that targeting of mGluR1 to dendrites and axons of transfected retina neurons is controlled by alternative splicing and identified in the tail of the receptor a tripeptide motif, which is necessary and sufficient to exclude the splice variant mGluR1b from distal dendrites and to drive it to the axon. A similar kind of study was carried out by Mu et al. (2003) in which they showed compelling evidence that alternative splicing

Introduction

of the NMDA receptor drives bidirectional modification of synaptic strength, as neuronal activity is turned up or down. Splice variants of NMDA that control NMDA receptor accumulation are controlled at the level of receptor export from the endoplasmic reticulum (ER) to the plasma membrane. Changes in the electrical activity of cortical cultures result from changes in surface expression of the NMDA receptor.

An additional post-translational modification site in a splice variant can also contribute to the synaptic strength. This was demonstrated in a variant of ABP-L (seven PDZ form of AMPA receptor-binding protein) called pABP-L that is palmitoylated at a cysteine residue at position 11 within a novel 18 amino acid N-terminal leader sequence encoded through differential splicing. The palmitoylation contributed to the synaptic and intracellular sites for the anchorage of AMPA receptors during receptor trafficking to and from the synapse (DeSouza et al., 2002). Alternative splicing also regulates membrane trafficking of Kainate Receptors as shown by Jaskolski et al. (2004). Alternative splicing can also be controlled by neural excitation as shown by many studies (Chalfant et al., 1995; Collett and Steele, 1993; Rodger et al., 1998; Shifrin and Neel, 1993; Smith et al., 1997; Wang et al., 1991; Zacharias et al., 1996).

2.3.4. Mechanism and Control of alternative splicing

Splicing is carried out by the spliceosome, which recognizes splicing signals and catalyzes the removal of noncoding intronic sequences to assemble protein-coding sequences into mature mRNA (Black et al., 2003). Splicing signals are sequence elements that are located at the 5'- and 3'-splice sites, the polypyrimidine tract, and the branchpoint sequence upstream of the 3'-splice site (Burge et al., 1999). The spliceosome is assembled in a stepwise manner from the small nuclear ribonucleoproteins (snRNPs), U1, U2, and U4/U5/U6 (triple snRNP).

Introduction

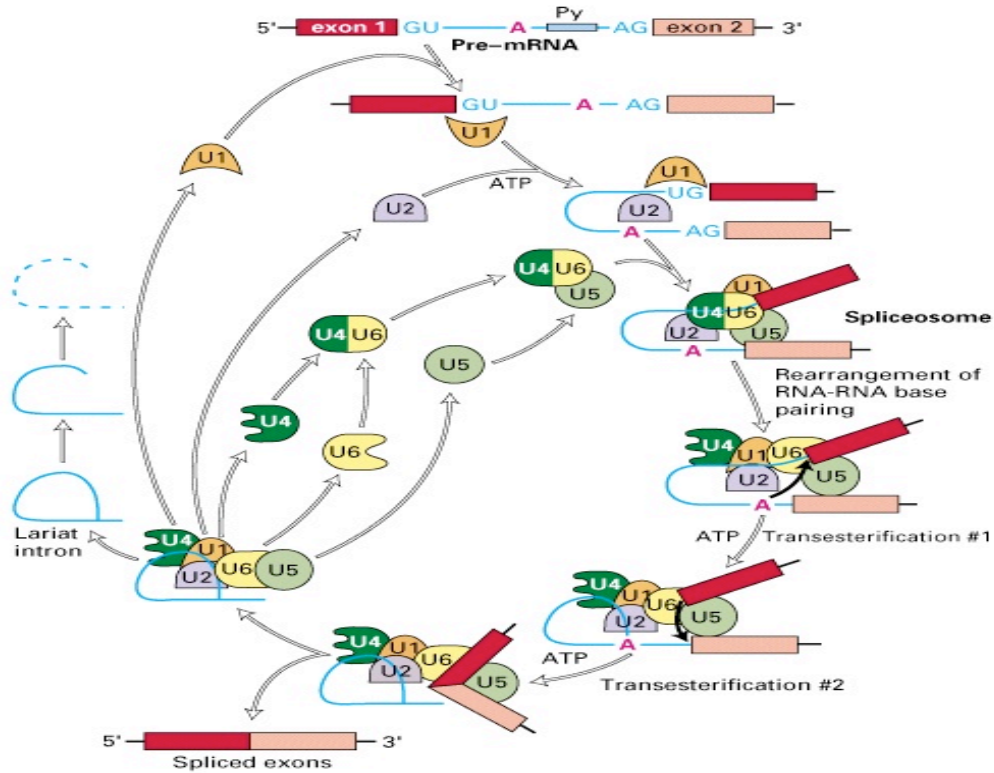


Fig. 5: The spliceosomal splicing cycle. The splicing snRNPs (U1, U2, U4, U5, and U6) associate with the pre-mRNA and with each other in an ordered sequence to form the spliceosome. This large ribonucleoprotein complex then catalyzes the two transesterification reactions that result in splicing of the exons (light and dark red) and excision of the intron (blue) as a lariat structure. Although ATP hydrolysis is not required for the transesterification reactions, it is thought to provide the energy necessary for rearrangements of the spliceosome structure that occur during the cycle. Note that the snRNP proteins in the spliceosome are distinct from the hnRNP proteins discussed earlier. In higher eukaryotes, an hnRNP protein called U2AF, which binds to the pyrimidine-rich region near the 3' splice site, assists the association of U2 snRNP with pre-mRNA. U2AF also probably interacts with other proteins required for splicing through a domain containing repeats of the dipeptide serine-arginine (the SR motif). The branch-point A in pre-mRNA is indicated in boldface.

Assembly and catalytic activation of the spliceosome is a complex process requiring the sequential pairing and unpairing of specific snRNA helices and binding of a host of accessory proteins (Staley and Guthrie, 1998). These accessory factors play important

Introduction

roles in sequence specific RNA recognition, RNA annealing, RNA duplex unwinding (by RNA helicases), and snRNP biogenesis/recycling (Krämer A., 1996).

The spliceosome assembles onto each intron from a set of five small nuclear ribonucleoproteins (snRNPs U1, U2, U4-U6) and numerous accessory proteins that bind specifically to locations at or within the vicinity of the splice sites, and catalyze the excision of the intron (Black et al., 2003). While the 5' (donor) and 3' (acceptor) splice sites have well characterized consensus sequences that are recognized to play a major role in splicing, an increasing body of evidence reveals that previously unknown RNA elements located outside the splice signals, in exons and introns, contribute to the exon's inclusion or exclusion in the mature mRNA, in a network of interactions that appear to be centered on exons, rather than introns. These m-regulatory elements can promote (splicing enhancers) or repress (splicing silencers) the inclusion of the exon in the mRNA through the activity of the bound regulatory proteins, and can be located in the exons-exonic splicing enhancers (ESEs) and silencers (ESS), or introns-intronic splicing enhancers (ISE) and silencers (ISS). They can act from both within the proximity of the exon or from 300 to 1000 bp away. It is becoming increasingly evident that many exons, constitutive or alternative, and their surrounding introns harbor both silencing and enhancing elements, and that the exon's inclusion/exclusion is the result of competition between these two effects (Smith and Valcarcel, 2003).

2.3.5. Tools for deciphering alternative splicing

Approaches for identifying full-length splice variants or just splice forms typically involve the comparison of two or more expressed DNA or protein sequences of different isoforms to detect differences caused by insertions or deletions of genetic material.

2.3.6. Mining databases

Database mining is the process of finding and extracting useful information from raw datasets. Computational approaches rely on cDNA and protein sequences collected in large repositories in GenBank and around the world. Database for expressed sequence tags (dbEST) (Boguski et al., 1993) contains single-pass EST sequences from direct submissions to GenBank. RefSeq (Pruitt et al., 2003) is an NCBI effort to collect, review and curate full-length mRNA sequences from submissions or gene prediction projects. More recently, the Mammalian Gene Collection (MGC) project (Strausberg et al., 1999) was started as an NIH initiative to clone and sequence full-length open reading frames (ORFs) for human, mouse and rat genes. Protein sequences can be obtained from databases such as SwissProt, TrEMBL and PIR, currently united into the Universal Protein Knowledgebase UniProt (Bairoch et al., 2005). The quality and characteristics of the data may differ significantly, and thus in judging the potential for identified differences to represent true alternative splicing events considerations about the type, quality and reliability of data are important.

2.3.7. Tools for sequence alignment

In bioinformatics, Basic Local Alignment Search Tool, or BLAST (Altschul et al., 1990), is an algorithm for comparing primary biological sequence information, such as the amino-acid sequences of different proteins or the nucleotides of DNA sequences. A BLAST search enables a researcher to compare a query sequence with a library or database of sequences, and identify library sequences that resemble the query sequence above a certain threshold. For example, following the discovery of a previously unknown gene in the mouse, a scientist will typically perform a BLAST search of the human genome to see if humans carry a similar gene. BLAST will identify sequences in the human genome that resemble the mouse gene based on similarity of sequence.

Introduction

BLAST searches for high scoring sequence alignments between the query sequence and sequences in the database using a heuristic approach that approximates the Smith-Waterman algorithm. The Smith-Waterman algorithm compares segments of all possible lengths and optimizes the similarity measure. However, an exhaustive Smith-Waterman approach is too slow for searching large genomic databases such as GenBank. Therefore, the BLAST algorithm uses a heuristic approach that is slightly less accurate than Smith-Waterman but over 50 times faster. The speed and relatively good accuracy of BLAST are the key technical innovations of the BLAST programs and arguably explain why the tool is the most popular bioinformatics search tool. The BLAST algorithm can be conceptually divided into three stages. In the first stage, BLAST searches for exact matches of a small fixed length W between the query and sequences in the database. For example, given the sequences AGTTAC and ACTTAG and a word length $W = 3$, BLAST would identify the matching substring TTA that is common to both sequences. By default, $W = 11$ for nucleic seeds, also known as the initial hit parameter. The hit probability of different seeds varies with the minimum length and similarity of sequences desired to be retrieved. In the second stage, BLAST tries to extend the match in both directions, starting at the seed. The ungapped alignment process extends the initial seed match of length W in each direction in an attempt to boost the alignment score. Insertions and deletions are not considered during this stage. For our example, the ungapped alignment between the sequences AGTTAC and ACTTAG centered on the common word TTA would be:

```
..AGTTAC..
```

```
  |  || |
```

```
..ACTTAG..
```

If a high-scoring ungapped alignment is found, the database sequence is passed on to the third stage. In the third stage, BLAST performs a gapped alignment between the query sequence and the database sequence using a variation of the Smith-Waterman algorithm. Statistically significant alignments are then displayed to the user.

BLAST is actually a family of programs. Nucleotide-nucleotide BLAST (blastn): This program, given a DNA query, returns the most similar DNA sequences from the DNA database that the user specifies.

Introduction

Protein-protein BLAST (blastp): This program, given a protein query, returns the most similar protein sequences from the protein database that the user specifies.

Position-Specific Iterative BLAST (PSI-BLAST): One of the more recent BLAST programs is used for finding distant relatives of a given protein. First, a list of all closely related proteins is created. Then these proteins are combined into a "profile" that is a sort of average sequence. A query against the protein database is then run using this profile, and a larger group of proteins found. This larger group is used to construct another profile, and the process is repeated.

By including related proteins in the search, PSI-BLAST is much more sensitive in picking up distant evolutionary relationships than the standard protein-protein BLAST.

Nucleotide 6-frame translation-protein (blastx): This program compares the six-frame conceptual translation products of a nucleotide query sequence (both strands) against a protein sequence database.

Nucleotide 6-frame translation-nucleotide 6-frame translation (tblastx): This program is the slowest of the BLAST family. It translates the query nucleotide sequence in all six possible frames and compares it against the six-frame translations of a nucleotide sequence database. The purpose of tblastx is to find very distant relationships between nucleotide sequences.

Protein-nucleotide 6-frame translation (tblastn): This program compares a protein query against the six-frame translations of a nucleotide sequence database.

Large numbers of query sequences (megablast): When comparing large numbers of input sequences via the command-line BLAST, "megablast" is much faster than running BLAST multiple times. It basically concatenates many input sequences together to form a large sequence before searching the BLAST database, and then post-analyzes the search results to glean individual alignments and statistical values.

A number of specialized programs have been developed to align cDNA sequences to genomic sequences allowing for sequencing errors, polymorphisms and introns, such as EST_GENOME (Mott et al., 1997), Sim4 (Florea et al., 1998), Spidey (Wheelan, 2001), and GeneSeqer (Usuka et al., 2000). These programs were designed specifically to compare a cDNA with the restricted genomic range encompassing the gene. With the availability of whole genome sequences, new generation tools were developed to

Introduction

efficiently map large cDNA data sets to large chromosomal sequences and whole genomes. Examples include Blat (Kent, 2002), ESTmapper (Florea et al., 2005), MGAalignIt (Lee et al., 2003), and GMAP (Wu et al., 2005). Given a cDNA sequence, each of these programs generates a spliced alignment of the cDNA and the genomic sequence. The alignment clearly marks the locations of exons and introns in the two sequences and gives additional information about the match, such as the predicted strand and alignment quality statistics. Although all of these programs have reached a high level of accuracy, challenges remain in dealing with non-canonical splice junctions, high EST sequencing error rates or specific types of sequencing errors, detecting small exons and/or large introns, and correctly determining the true location of the cDNA on the genome from among multiple paralogous matches.

2.3.8. Identification of alternatively spliced variants

Annotating full length splice variants is more complex and involves methods such as gene indices, which assemble putative splice variants from overlapping EST and mRNA sequences without resorting to a reference genome, and includes genome-based methods for clustering spliced alignments and inferring gene models.

Gene indices

Gene indices are gene- or transcript-oriented collections of EST and mRNA sequences grouped by sequence similarity. Traditional methods compare all EST and mRNA sequences against each other to identify significant overlaps, then group and assemble sequences with compatible overlaps into disjoint clusters. The term 'gene indices' may be used to refer to the annotated collections of sequences [UniGene (Schuler .GD, 1997)], to the multiple alignments of sequences in the clusters, or to the consensus sequences generated from the multiple alignments (TIGR Gene Indices (Liang et al., 2000), GeneNest (Haas et al., 2000)). Constructing gene indices is complicated by a number of factors. Over-clustering may occur when differences between paralogs are interpreted as sequencing errors, forcing paralogs into a same cluster, or when contamination of ESTs with vector or linker sequences or residual polyA tails creates

Introduction

false appearances of overlaps. Other times, insufficient EST sampling may result in under clustering, where several disconnected clusters are produced for a same gene. Furthermore, the process is computationally expensive, as the time required by the pair wise comparisons increases quadratically with the number of sequences in the set. To alleviate these problems, methods were developed to trim the vector and low-quality ends of the EST sequences prior to the comparison, pre-cluster the sequences by aligning EST sequences against the known primary mRNA form (also known as “seeded clustering”), and to a priori cluster almost identical or contained sequences to reduce the complexity of the clustering (Lee et al., 2005).

Genome-based clustering and assembly

In the genome-based approach, the spliced alignments of cDNA and protein sequences are clustered at loci along the genomic sequence. To distinguish among possibly different genes sharing the same genomic locus, including overlapping genes and sense-antisense transcripts (Kiyosawa et al., 2005), clustering is often refined to group alignments separately on each strand of the genomic sequence, and requires that the sequences share common splice junctions in addition to overlapping exons. One recent innovation in alternative splicing annotation has been the concept of a splice graph, as a model for concisely capturing splice variations within a gene. The splice graph represents a gene as a directed acyclic graph in which exons are represented as vertices, introns are the arcs connecting the exons, and splice variants are the paths obtained by traversing the graph from a source vertex (with no incoming arcs) to a sink vertex (with no outgoing arcs). With this set of rules, cDNA and protein spliced alignments at a genomic locus can be consolidated into a spliced graph and candidate full-length splice variants can be enumerated from the graph in a combinatorial fashion. The combinatorial nature of the splice graph is also the main limitation of the model since some of the exon combinations it encodes may be artificial constructs without biological relevance.

Different methods have been proposed to select or prioritize candidate transcripts in order to differentiate between those most likely to be biologically relevant and those likely to be artefactual. For instance, the annotation integrated resource AIR annotation

Introduction

pipeline (Florea et al., 2005) assigns splice variants confidence scores based on a set of four characteristics measuring the strength of the supporting cDNA and protein evidence, such as the quality and length of the supporting alignments, accuracy of splice signals and the level of fragmentation of the evidence. High-scoring candidates are later selected and promoted into the annotation. The ECgene (Kim et al., 2005) system classifies candidate transcripts into three categories, high-, medium- and low confidence, based on the number of cDNA alignments that were stitched together to construct it. Other methods simply defer the task of transcript selection to the users, but provide additional information and visualization to aid in the analysis (Leipzig et al., 2004, Sugnet et al., 2004).

Genome-based approaches solve a number of deficiencies observed with the gene indices. By mapping the ESTs to the genome, contamination from foreign matter, such as vector and linker sequences, or from polyA tails are removed. In addition, the sequencing errors that were compounded between the cDNA sequences in the gene indices method are now resolved by aligning the sequence against the genome, used as reference. As a result, fewer sequences are misplaced along the genome, resulting in considerably less clustering of paralogs. However, genome-based clustering has set of limitations of its own. Some of the remaining issues that have to be resolved involve the contamination of ESTs with genomic fragments or incompletely spliced forms that could produce over-clustering of neighboring or overlapping genes, errors in the alignment, particularly inaccuracy of splice junctions and missing short exons, and strand prediction. Other limitations of the splice graph model include its inability to fully capture splicing variations where one variant is a 5' or 3' extension of another, and its sensitivity to alignment errors, as one spurious exon may double the number of candidates.

3. Aim and Outline of the thesis

Corticotropin-releasing factor (CRF) is a 41 amino acid neuropeptide (Spiess et al., 1981) that has been implicated in both physiological and behavioral responses to stress. CRF modulates the currents underlying slow afterhyperpolarization (sAHP) and neuronal excitability by suppressing the slow Ca^{2+} -activated K^+ current, I_{sAHP} , in CA1 hippocampal pyramidal neurons (Nicoll et al., 1988; Gorelova et al., 1996; Haug et al., 2000). It was also shown by Blank et al. (2003) that CRF activates additional intracellular signaling pathways in the mouse hippocampus and exhibits distinct effects on associative learning. It was unclear which ion channel would mediate the CRF-modulated sAHP. One candidate was the small conductance Ca^{2+} -activated K^+ channel 2 (SK2), an apamin-sensitive SK channel subtype, which plays a critical role in the regulation of neuronal excitability.

However, the findings reported so far regarding the role of SK2 channel function in the hippocampus seem controversial. It was found in our laboratory that SK2 antisense oligonucleotides, which reduced SK2 expression in mouse hippocampus, enhanced basal synaptic efficacy and enhanced long-term potentiation (LTP) at Schaffer collateral-CA1 synapses. On the other hand, the same antisense treatment introduced deficits in contextual fear conditioning, a hippocampus-dependent learning task. In agreement with these data, a reduction in contextual fear conditioning was observed after injection of the selective SK2 channel antagonist Lei-Dab7 into the dorsal hippocampus. These data indicate opposite contributions of SK2 channels to hippocampal LTP and contextual fear memory (data not published). Consistent with these findings, it was shown that SK2 overexpression reduced long-term potentiation after high-frequency stimulation (Hammond et al., 2006), although LTP has generally been used as a model to understand the mechanism by which strengthening of synaptic connections can be achieved (Lynch, 2004).

Nevertheless, a definitive demonstration indicating that memory consolidation requires induction of changes that resemble those necessary for initiation of LTP remains elusive. However, it has become increasingly evident that the hippocampus uses a number of additional mechanisms, such as changes in spiking, to process, store, and recall information (Giese et al., 2001). Mpari et al (2005) showed that SK3 subunits

appeared to be a decisive component in hippocampal AHP generation, which is a negative learning regulator. This was consistent with data shown by Blank T et al (2003). So the question now arises, if SK3 subunit is the major contributor of hippocampal AHP and blocking or down regulating SK2 impairs hippocampal learning and memory, is there involvement of any other mechanisms, which could contribute to the contradictory role of the SK2 channel in hippocampal LTP and contextual fear memory?

In previous studies it has been shown that neuronal excitability can be modulated by posttranscriptional regulation in voltage-gated KV3.1 and KV3.2 potassium channels (Surmeier et al., 2003). **Based on these data, we here investigated whether the described contradictory roles of SK2 channels in hippocampal LTP and contextual fear memory are due to regulation at the post-transcription level.** At the post-transcriptional level a key regulatory process is alternative splicing, by which different mature RNAs can be generated from the same primary transcript. The resulting combinatorial complexity may generate multiple alternative SK2 channel functions. It has been shown in other genes that alternative splicing alters fear memory and LTP (Nijholt et al., 2004). Moreover, alternatively spliced variants of other SK channel subunits (SK1 and SK3) have been shown to exhibit non-channel functions (Tomita et al., 2003; Kolski et al., 2004, Barfod et al., 2001; Wittekindt et al., 2004; Shmukler et al., 2001). We hypothesize that alternative splice variants of SK2 may play specific roles in memory consolidation and modulation of LTP. **The central aim of the present study was to identify and characterize new SK2 splice variants, which might contribute to hippocampal plasticity and function.**

It was also shown in our laboratory that SK2 mRNA expression was highly up regulated in mouse hippocampus after immobilization stress (data not published). **Thus, a second aim of this study was to define the modulations among SK2 splice variants at the mRNA level, which might contribute to the observed up regulation of SK2 after stress.**

Bioinformatics was the initial and key technique to identify novel splice variants of the SK2 gene. Reverse transcriptase PCR, fluorescent in situ transcription, Western blots, cloning, in situ hybridization and behavioral experiments provided experimental evidence for the identification of potential novel variants in mouse brain.

4. Material and Methods

4.1. Bioinformatics

The NCBI databases were used as a search engine for nucleotide and protein sequences. ClustalW (EMBL) was used to perform the BLAST (Altschul et al., 1990) sequence alignments as well as the phylogenetic tree analysis. The cDNA and protein sequence of SK2 channel of human, mouse and rat were used as queries and a BLAST (Basic Local Alignment Tool) (Altschul et al., 1990) search was done against human, mouse and rat EST (Expressed Sequence Tag) databases (<http://www.ncbi.nlm.nih.gov/dbEST/index.html>) respectively with expect value of 0.01 and low complexity filters as parameters. Blastx was then performed to search the human, mouse and other mammalian protein databases using a translated SK2 nucleotide query. tblastn was performed to search translated mammalian EST databases (using SK2 protein query) and tblastx (to search translated nucleotide database using a translated nucleotide sequence as query). The resulting sequence alignments were manually examined for insertions or gaps in the alignment. Differences in exon alignments of the EST against the query cDNA or protein sequence were analyzed by bl2seq (to align two sequences). The screened ESTs were further aligned against human, mouse and other mammalian genomic sequences by genomic BLAST tools (<http://www.ncbi.nlm.nih.gov/mapview/>). BLAST searches were carried out against EST databases to find conservation of the splice variants across other species. Splice variant prediction was followed by ORF (Open reading frame) analysis using EMBOSS Transeq (<http://www.ebi.ac.uk/emboss/transeq/>). Protein domains and motifs analyses were performed using CDD (Conserved Domain Database) (<http://www.ncbi.nlm.nih.gov/Structure/cdd/wrpsb.cgi>), SMART (<http://smart.embl-heidelberg.de/>), PFam (<http://www.sanger.ac.uk/Software/Pfam/>) and PHI-BLAST (<http://caps.ncbs.res.in/campass/phi-blast.html>). Literature evidence was used to evaluate the functional relevance of the predicted motifs.

4.2. Animal handling and tissue isolation

Male C57BL/6J mice aged 3-6 months (The Jackson Laboratory, Maine, USA) were kept in air-conditioned rooms (12 h dark/light cycle) at 22–23°C in an air humidity

Materials and Methods

of 55%. The mice had free access to water and food pellets. For brain tissue isolation animals were sacrificed by decapitation between 3 and 6 h into the light period. After isolation of different brain regions and peripheral tissue samples, they were immersed into RNA-later solution (Qiagen, USA), kept at room temperature (22–23°C) for 1 h and thereafter stored at +4°C until further processed.

4.3. RNA preparation and cDNA synthesis

Total RNA from individual tissue samples was isolated using sv total RNA isolation system (Promega). DNA contamination was removed by treatment with DNase I (Roche Diagnostics, USA) at 37°C for 4 h. DNase I was inactivated by heating the samples at 75°C for 15 min. cDNA was synthesized from 1 μ g of total RNA with Transcriptor First Strand cDNA Synthesis Kit (Roche applied science, USA), using random hexamers as primers according to the manufacturer's instructions. RNA and DNA concentration and yield was determined by optical density (OD) measurements at wavelengths of 260 and 280 nm using a GeneQuant *pro* spectrophotometer (Amershem, England).

4.4. Reverse transcriptase PCR

Primers were designed to produce overlapping PCR-products corresponding to junctions of the SK2P, SK2sh, SK2L and SK2 primary standard isoform (SK2std) open reading frames for human, mouse and rat (listed in Table 1A). RT-PCR was performed with 0.5 μ g total RNA, 5 pmol primers using OneStep RT-PCR Kit (Invitrogen, Germany). The thermal cycling conditions were 55 °C for 30 min, 95 °C for 15 min, 38 cycles of 95 °C for 30 s, 60 °C for 30 s and 72 °C for 10 s. The amplified products were monitored by electrophoresis in a 2% agarose gel with TAE buffer. A negative control was included for every reaction without the RNA. To analyze the amplicons, the amplified products were cloned into the pCR2.1-TOPO vector (Invitrogen). Subcloned fragments were reamplified using the same primers and the insert was confirmed by sequencing.

4.5. Quantitative real-time PCR

Materials and Methods

The cDNA was analyzed in quantitative real-time PCR on Roche Lightcycler 2 (Roche Applied science, Indianapolis, IN, USA) and at-least one was flanking in a primer pair. All primers were designed with Roche Probe Design 2 software (Roche Applied science, Indianapolis, IN, USA): primers are given in the TABLE (1A). Each real-time PCR reaction was prepared with a total volume of 20 μ l contained 1 μ l cDNA; 0.25 μ mol/L of each primer, 4 μ l of LightCycler FastStart DNA Master-PLUS SYBR Green I master mix (Roche Applied science, Indianapolis, IN, USA). The following conditions were utilized for real-time PCR: initial denaturation for 3 min at 95°C, followed by 45 cycles of 15 s at 95°C, 15 s at 54–61°C (optimal annealing temperature) and 5 s at 72°C. This was followed by 1 cycle of melting and subsequently cooled to 15°C. All real-time PCR experiments were performed in duplicate and repeated twice. A negative control for each primer pair and a positive control with 25 ng of mouse genomic DNA was included in each tube.

The sensitivity of reactions and amplification of contaminant products such as primer dimers, indiscriminately detected by the SYBR green chemistry, was evaluated by amplifying serial dilutions of cDNA (1, 1:10, 1:100, 1:1000) and one sample containing reaction mixture without cDNA. The amplicons were further verified by gel electrophoresis. The threshold cycle, Ct, which correlates inversely with the target mRNA levels, was measured as the cycle number at which the reporter fluorescent emission increased above a pre-set threshold level.

4.5.1. Absolute quantification was obtained by plotting the standard curves for every assay that were generated using defined concentrations of mSK2std cloned in (pcDNA3.1His vector, Invitrogen, USA), mSK2P and mSK2sh cDNA cloned in (pCR2.1 vector, Invitrogen, USA). The PCR products were run on 3% agarose gel x 1 TAE, fragments were excised and purified using SV gel and PCR clean-up system (Promega). The concentrations were determined spectrophotometrically and the conversion of microgram value to picomoles was performed using the formula: pmol of dsDNA = μ g(of dsDNA) X 10⁶ pg/1 μ g X 1pmol/660 pg X1/Nbp (Nbp = length of the amplicon in bp, dsDNA = double standard DNA). Equimolar dilutions of the PCR fragments were used to generate the standard curve of at least three orders of magnitude. Standard curves for

Materials and Methods

each amplicon were run in triplicates and plotted from eight different concentrations of standards.

4.5.2. Relative quantification. The following conditions were utilized for real-time PCR: initial denaturation for 3 min at 95°C, followed by 45 cycles of 15 s at 95°C, 15 s at 54-61°C (optimal annealing temperature) and 5 s at 72°C. The PCR reaction was followed by a melting curve program (65–95°C with a heating rate of 0.1°C per second and a continuous fluorescence measurement) and a cooling program at 40°C. Negative controls consisting of no-template (water) reaction mixtures were run with all reactions. PCR products were also run on agarose gels to confirm the formation of a single product of predicted size. Crossing points for each transcript were determined using the 2nd derivative maximum analysis with the arithmetic baseline adjustment. Crossing point values for each transporter were normalized to the respective crossing point values for the reference gene hypoxanthine-guanine phosphoribosyltransferase (HPRT). Data are presented as a fold change in gene expression using the 2 delta delta Ct method (Livak and Schmittgen, 2001).

Table (1A): Primers for Real-time PCR

Type	Primer name	Sequence
Human HPRT	hHPRTFwd	5' GACCAGTCAACAGGGGACAT 3'
	hHPRTRev	5' CCTGACCAAGGAAAGCAAAG 3'
Human SK2short (SK2sh)	hSK2shFwd	5' GGGAAATACAGTACCATGATC 3'
	hSK2shRev	5' TATCAACCACATCGCTCCAA 3'
Human SK2 primary isoform (SK2std)	hSK2stdFwd	5' GCGTCGCTGTATTCCTTAGC 3'
	hSK2stdRev	5' TCCAGTCATCTGCTCCATTG 3'
Mouse HPRT	mHPRTFwd	5' CCTGCTGGATTACATTAAGCACTG 3'
	mHPRTRev	5' CCTGAAGTACTCATTATAGTCAAGG 3'

Materials and Methods

Mouse SK2short (SK2sh)	mSK2shFwd	5' GGGAAATACAGTACCATGATC 3'
	mSK2shRev	5' CTGCACCCATGATTCCAGTA 3'
Mouse SK2 primary isoform (SK2std)	mSK2stdFwd	5' CTTGGAAATACTGGTGTGTGC 3'
	mSK2stdRev	5' CACATCTGCGGTGGTTG 3'
Human SK2P	hSK2PFwd	5' GTGCACAATTCATGATGGAT 3'
	hSK2PRev	5' TTAATTTCCGAGCTTGATGA 3'
Mouse SK2P	mSK2PFwd	5' GTGCACAATTCATGATGGAT 3'
	mSK2PRev	5' TTAATTTCCGAGCTTGATGA 3'
Mouse SK2L	mSK2LFwd	5' CCTGCAGTTTCAGCACTGTC 3'
	mSK2LRev	5' GAAACATCCCTTGCCTCAA 3'
Mouse SK2CaMBD	mSK2CaMBDFwd	5' CGGATTCCGGGATTCAATA 3'
	mSK2CaMBDRev	5' CACACTTCTTAATTCTTTTGGTC 3'
Mouse SK2R	mSK2RFwd	5' TGAGTCCTGTGAAGAAAGAAATTG 3'
	mSK2RRev	5' GCCACCAACTTCATCAGAGAG 3'
Mouse SK2-N- Terminus	mSK2NFwd	5' TTGCTCCATTTTGTGTTTGGAT 3'
	mSK2NRev	5' TCATCTGCTCCATTGTCCAC 3'

4.6. Rapid amplification of cDNA ends and cloning

To determine the full-length nucleotide sequence of mSK2P and mSK2sh mRNA, cDNA was amplified by reverse transcription-PCR (RT-PCR) and 5' and 3' rapid amplification of cDNA ends (RACE) (Fig. 6a) using a GeneRacer kit (Invitrogen, USA) according to the manufacturer's instructions. GeneRacer-oligo(dT) primer, GeneRacer 3' primer, and GeneRacer 5' primer were provided with the kit, gene specific primers SK2PAS1 primer (5' GCT ATT CAT CAA GCT CGG AAA TTA AGA AG 3') and

Materials and Methods

SK2PAS2 primer (5' CTT CTT AAT TTC CGA GCT TGA TGA ATA GC 3') were designed for mSK2P and SK2shAS1 primer (5' CTG CAC CCA TGA TTC CAG TA 3') and SK2shAS2 primer (5' TAC TGG AAT CAT GGG TGC AG 3') were designed for mSK2sh.

To obtain the 3' ends, polyadenylated RNA was isolated from C57BL/6j mouse hippocampal tissue, using the sv total RNA isolation system (Promega). The first-strand cDNA was synthesized using Superscript II RT with the GeneRacer oligo(dT) primer at 42°C for 50 min. 3' RACE PCR was performed with the GeneRacer 3' primer and a genespecific primer (AS1) under the following conditions: one cycle of 94°C for 2 min, five cycles of 94°C for 30 s and 72°C for 1 min, five cycles of 94°C for 30 s and 70°C for 1 min, 30 cycles of 94°C for 30 s, 55°C for 30 s, 68°C for 2 min and one cycle of 68°C for 10 min. To obtain the 5' ends, the dephosphorylated and decapped mRNA was ligated with Gene Racer RNA oligonucleotides and the first-strand cDNA was reverse-transcribed using Thermoscript RT (Invitrogen) with AS2 as a primer at 65°C for 60 min. 5' RACE PCR was performed with the GeneRacer 5' primer and AS2 under the following conditions: one cycle of 94°C for 2 min, five cycles of 94°C for 30 s and 72°C for 1 min, five cycles of 94°C for 30 s and 70°C for 1 min, 30 cycles of 94°C for 30 s, 55°C for 30 s, 68°C for 1 min and one cycle of 68°C for 10 min.

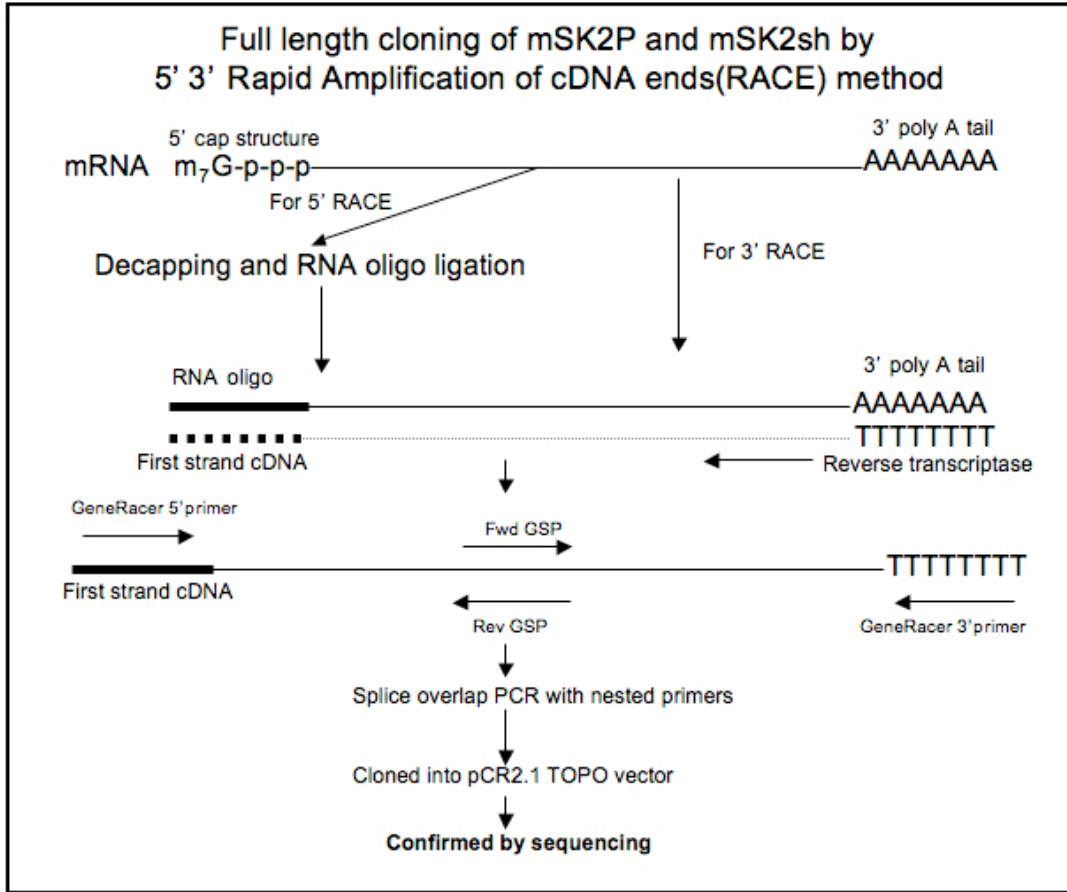


Fig. 6a: Diagrammatic representation of full length cloning of mSK2P and mSK2sh by 5' 3' RACE method. Mouse hippocampal mRNA was used to generate two separate reactions of 5' and 3' RACE. Forward gene specific primer (FwdGSP) and reverse gene specific primer (Rev GSP) were used to amplify 5' and 3' fragments respectively for SK2P and SK2sh. These two fragments were used to generate the full length cDNA by splice overlap PCR as these fragments had overlapping sequences at their ends.

After agarose gel electrophoresis of the 3' and 5' RACE PCR products, PCR products with the predicted length were purified from the gel with Wizard SV Gel and PCR Clean-Up System (Promega). PCR products were inserted into a pCR4-TOPO vector using a TOPO TA cloning kit for sequencing (Invitrogen), and then transformed into OneShot competent cells (Invitrogen). To avoid possible sequencing errors due to RACE artifacts, sequence analyses were performed on 25 (5' RACE) and 25 (3' RACE) independent clones derived from each RACE. DNA sequencing was performed on both

strands with an ABI PRISM terminator cycle sequencing ready reaction kit (Applied Biosystems) using an automated DNA sequence analyzer (model 310, Applied Biosystems). The full length cDNA was obtained by combining 5' RACE PCR and 3' RACE PCR product by splice overlap PCR with Pfx DNA polymerase (Invitrogen). The PCR product was cloned into pCR4-TOPO vector and confirmed by sequencing.

4.7. Construction of SK2sh His tagged expression vector and establishment of HEK293 transfectant expressing SK2sh. ORF of mSK2sh was amplified from mSK2sh/pCR4-TOPO vector with primers mSK2shFwd (5' ATG AGC AGC TGC AGG TAC 3') and mSK2shRev (5' GCT ACT CTC TGA TGA AGT TGG T 3') the PCR fragment was gel extracted and cloned into pcDNA3.1His vector (Invitrogen) in frame with the polyHistidine repeats and confirmed by sequencing. HEK293 cells maintained in Dulbecco's modified Eagle's medium (GIBCO) containing 10% fetal calf serum (GIBCO) and 2mM glutamine in a 37°C humidified incubator with 5% CO₂ and split 1:10 twice weekly. HEK293 cells were plated in 12-well plates and once 40 – 50% confluence had been reached, cells were transiently transfected using FuGene 6 (Roche Molecular Biochemicals, Indianapolis, IN, USA) with 6 μ g mSK2sh DNA construct in serum-free OptiMEM medium (Life Technologies, Inc.) as per the manufacturer's recommended protocol. Cells were plated 24 h following transfection for overnight growth and labeling studies were performed.

Identification of FITC-labeled mSK2sh in HEK293 cells

Cells were washed two times with cold phosphate buffered saline (PBS) containing 10 mm MgCl₂, 0.1% (w v⁻¹) D-glucose and 0.2% (w v⁻¹) bovine serum albumin (BSA). Cells were fixed with 100% methanol and washed twice in PBS. 10% Fetal Bovine serum in PBS was applied to block non-specific binding. Subsequently, cells were exposed to 10 nm anti-His (C-term)-FITC antibody (1:500 dilution) (Invitrogen) either alone or in the presence of excess cold, unlabelled anti-His(C-term) antibody (10 m). Cells were incubated for 1 hour at room temperature in the dark. After incubation cells were washed twice with PBS and examined under a fluorescent microscope (Carl Zeiss Inc., Thornwood, NY, U.S.A.) equipped with FITC filters. FITC

Materials and Methods

images were collected using appropriate bandpass filters at an excitation wavelength of 488 nm and an emission wavelength of 520 nm. The images were analyzed by AXIO image software.

4.8. *In-situ* hybridization of mouse SK2sh mRNA

Six C57BL/6J mice brains were removed, and frozen in liquid nitrogen. Coronal sections (20 μ m thick) were obtained with a microtome, thaw-mounted onto SuperFrost Plus slides (Fischer, Pittsburgh, PA), fixed in 4% PFA, followed by washing in PBS, and dehydration in graded series of ethanol. Oligonucleotide probes complementary to mouse pre-SK2shanti mRNA antisense strand (5'- GTG ACA TCC TGT TGA TCA TGG TAC TGT ATT TCC CTG GCG TGG TAC ACG AA -3') and SK2shsense (5'- ATC GTG TAC CAC GCC AGG GAA ATA CAG TAC CAT GAT CAA CAG GAT GTC AC -3') were end-labeled by ³³P at 37°C for 10 minutes using terminal deoxynucleotidyl transferase kit (Roche, Mannheim, Germany). The sections were incubated overnight in hybridization buffer (50% formamide, 10% dextran sulfate, 50 mM DTT, 0.3M NaCl, 30mM Tris HCl (pH 7.4), 4mM EDTA (pH 8), IX Denhardtts solution, 0.5 mg/ml salmon sperm DNA and 0.5 mg/ml Poly A DNA) at 48.6°C. Post-hybridization washes were carried out in 1x standard sodium citrate (SSC) (150mM NaCl, 30mM Na citrate, pH 7.2) for 2x2 min at room temperature, followed by a stringent wash at 57°C in 1xSSC for 45 minutes. The slides were subsequently washed in progressively diluted SSC buffers and then dehydrated in aqueous ethanol (50%-100%). After dehydration in an ascending ethanol series, the sections were air dried at room temperature and dipped in NBT-2 emulsion (Kodak) diluted 1:1 with distilled water. After exposure for 1 month at 4°C, the dipped slides were developed in Kodak D-19 developer and fixed. After images were captured in darkfield microscopy, the sections were stained with cresyl violet to confirm the cytoarchitectures and to capture brightfield images. Microscopic analysis was performed under a Zeiss microscope equipped with a darkfield condenser and a Zeiss Axioplan-2microscope (Carl Zeiss, Oberkochen, Germany). Digital images of each section were captured with a digital camera (Canon) and analyzed with WinROOF analysis software (Mitani Co., Fukui, Japan). Before emulsion staining, slides were air-dried and exposed to Kodak Biomax MR-Roentgen film for 24 hrs to 48 hrs.

4.9. Fluorescent *in situ* transcription (FIST) of mouse SK2P and SK2sh mRNAs

Oligonucleotide cDNA primers of 20 mer and ~50% GC content were designed for mouse SK2P, primer mSK2PFIST 5' TTA ATT TCC GAG CTT GAT GA 3' corresponding to nucleotides 1369-1384 of full length cDNA and for SK2sh, primer mSK2shFIST 5' ATG CCG GTG AGA AGA CAG ACA CCT TTC CCA CAG-3' corresponding to nucleotides 668-691 of the sense strand of the SK2sh full length cDNA were synthesized (IDT, Hawaii, USA). FIST was performed under sterile, RNase-free conditions. Fresh brain sections (10-15 μ m) were mounted on superfrost slides, fixed in 4% paraformaldehyde (10 min at room temperature), rinsed in 2 X SSC, dried and then stored at - 80°C until used. Tissues were permeabilized (10 min at room temperature) in 0.001% digitonin (Sigma Chemical, St. Louis, MO) and then covered in blocking buffer for 1 h at 37°C to control against potential random priming by unblocked 5'-nucleotide bases. Incorporation of a dideoxy-NTP renders the mRNA inactive for subsequent enzymatic extension by reverse transcriptase. The blocking buffer contained 50 mM Tris-HCl (pH 8.3), 6 mM MgCl₂, 120 mM KCl, 7 mM DTT, 200 μ M each of ddATP, ddCTP, ddGTP, and dTTP, 0.12 U/ μ l of RNase inhibitor (RNasin, Promega), 13 U/ μ l of avian reverse transcriptase (Promega). A pre-hybridization step was performed for 30 min at 20°C, followed by hybridization, which continued overnight at room temperature. Fluorescein-12-dUTP (Roche) was incorporated into the growing cDNA chain by avian reverse transcriptase and exogenous dNTPs. The enzymatic extension occurred for 30 min at 37°C, an additional 2 μ l of 3 μ M TTP was added, and incubation continued for 90 min. The enzymatic reaction was terminated by rinsing with 1 X SSC, followed by several dips in double-distilled water. After drying, cover slips were attached to the slides using mounting medium for fluorescence (Vectashield, Vector Labs, CA) . The tissue sections were examined under an fluorescent microscope (AXIO-Imager, Zeiss, Germany).

4.10. Fear Conditioning

The fear conditioning experiments were performed as previously described (Blank et al., 2002, 2003) using a computer-controlled fear conditioning system (TSE,

Materials and Methods

Bad Homburg, Germany). Fear conditioning was performed in a Plexiglas cage (36 x 21 x 20 cm) within a fear conditioning box constantly illuminated (12 V, 10 W halogen lamp, 100-500 lux). In the conditioning box, a high-frequency loudspeaker (Conrad, KT-25-DT, Hirschau, Germany) provided constant background noise [white noise, 68 dB sound pressure level (SPL)]. The training (conditioning) consisted of a single trial. The mouse was exposed to the tone-conditioning (10 kHz, 75 dB SPL, pulsed 5 Hz) context (180 sec) serving as conditional stimulus (CS) followed by a footshock (0.7 mA, 2 sec, constant current) serving as unconditional stimulus was delivered through a stainless steel grid floor. The mouse was removed from the fear conditioning box 30 sec after shock termination to avoid an aversive association with the handling procedure. Under these conditions, the context served as background stimulus. Background contextual fear conditioning but not foreground contextual fear conditioning, characterized by omission of the tone during training, has been shown to involve the hippocampus (Phillips and LeDoux, 1994). The mice were decapitated and whole brains or hippocampi were removed at 1 hour, 3 hours and 24 hours and frozen immediately after fear conditioning procedure.

4.11. Western Blotting

Hippocampi were dissected out and immediately homogenized at 4°C with a plastic homogenizer in a homogenization buffer containing 50 mM Tris-HCl (pH 8.0), 10 mM EDTA, 4 mM EGTA, 15 mM sodium phosphate, 100 mM β -glycerophosphate, 10 mM sodium fluoride and a protease inhibitor cocktail tablet (Boehringer Mannheim, Germany). The insoluble material was removed by centrifugation at 13 000 x g for 10 min at 4°C. Protein concentrations were determined by the Bradford method (BioRad, Munich, Germany). Equal amounts of protein for each group were separated on a 10% SDS gel and transferred to an Immobilon-P membrane (Millipore Corporation, Bedford, MA, USA). The blot was probed using crude serum of SK2(538-555) at a dilution of 1:5000 (Sailer et al., 2002). Western blots were developed using the chemiluminescence method. Bands were quantified by densitometry.

4.12. Excitotoxicity Experiment

Materials

Neurobasal medium and B27 supplements were purchased from Invitrogen (Invitrogen, Gibco BRL, Carlsbad, CA). Complete mini protease inhibitor cocktail tablets were obtained from Roche (Indianapolis, IN). Primary antibodies used were a rabbit polyclonal antibody specific for SK2 (kindly provided by Hans-Günther Knaus, University of Innsbruck) and a monoclonal mouse antibody specific for actin (MP Biomedicals, Irvine, CA, USA). The secondary antibodies used were alkaline phosphatase (AP)-conjugated goat anti-mouse (Tropix) and AP-conjugated goat anti-rabbit (Tropix). The chemiluminescence detection kit (Nitroblock and CDP-star) was purchased from Tropix. All other materials were from Sigma.

Animal experiments

All experiments were performed using C57BL/6J mice (Harlan, Horst, The Netherlands). The procedures concerning animal care were in accordance with the regulation of the ethical committee for the use of experimental animals of the University of Groningen, The Netherlands. Mice were individually housed in standard macrolon cages and maintained on a 12 hours light/dark cycle. They received food and water ad libitum.

4.13. Primary cortical neuronal culture

Cortical neurons were prepared from embryonic brains (E15-16) of C57Bl/6J mice. The meninges were removed and the cortical neurons were separated by mechanical dissociation. Cells were plated at a density of 2×10^6 cells/well (6 well plates) on $2 \mu\text{g/ml}$ poly-D-lysine coated plates. Neurobasal medium with B27-supplement, 0.5 mM glutamine, 1% penicillin/ streptomycin and $2.5 \mu\text{g/ml}$ amphotericin B was used as a culture medium. After 48 h cells were treated with $10 \mu\text{M}$ cytosine arabinoside for another 2 days, to inhibit non-neuronal cell growth. Subsequently, the medium was completely exchanged and after 6 days of in vitro culture, the neurons were used for experiments. Cells were incubated over a period of 24 h with 100 ng/ml TNF (kindly provided by L. Marchetti). Excitotoxicity was induced by different concentrations

Materials and Methods

of glutamate for 1 h. After treatment the media was completely removed and the neurons were lysated for Western blot analysis.

4.14. Protein analysis

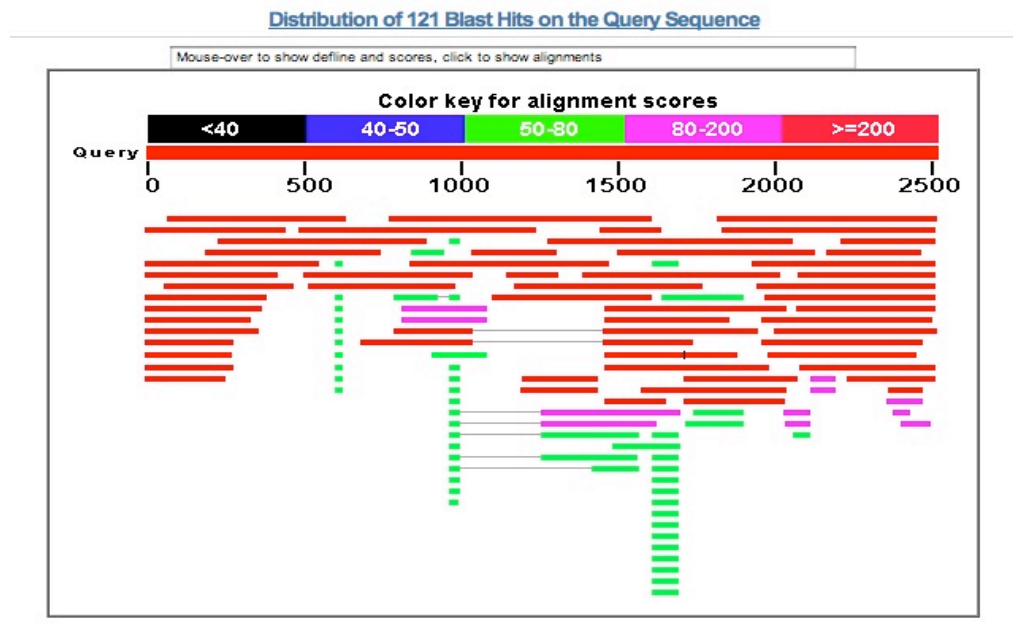
Primary cortical neurons from C57B16J mice were washed twice with ice cold phosphate-buffered saline (PBS) and subsequently lysed by the addition of 0.15 ml lysis buffer (20 mM Tris, 150 mM NaCl, 1 mM EDTA, 1 mM EGTA, 1% Triton, 2.5 mM sodium pyrophosphate, 1 mM sodium orthovanadate and Complete mini protease inhibitor cocktail tablet (one tablet in 10 ml). The samples were centrifuged at 9,000g for 10 min at 4° C and the supernatants were boiled for 5 min in Laemmli's sample buffer (2% SDS, 5% DTT). Twenty μ g of total protein was separated by 10% SDS-polyacrylamide gel electrophoresis. After transfer to a PVDF transfer membrane (Millipore Corporation, USA) proteins were detected with a specific primary antibody and an alkaline phosphatase labeled secondary antibody using the ECL detection system according to the manufacturer's instructions (Tropix). Primary antibodies used were a rabbit polyclonal antibody specific for SK2 (1:4000 dilution) and a monoclonal mouse antibody specific for actin (1:100000 dilution). The actin was taken as an internal control to correct for variations in protein content. The blots were incubated with alkaline phosphatase (AP) conjugated secondary antibodies: AP conjugated goat anti-mouse (1:10000 dilution) and AP conjugated goat anti-rabbit (1:10000 dilution). Integrated optical densities were measured by the Leica DFC 320 Image Analysis System (Leica, Cambridge, UK) and densitometric analysis was evaluated by the Leica Qwin program (Cambridge, UK).

5. Results

The primary aims of this study were: a) to identify and characterize SK2 alternative splice variants using computational and experimental methods and b) to evaluate their potential biological significance.

5.1. Bioinformatic analysis of SK2 alternative splice variants

A manual and exhaustive bioinformatics EST (Expressed Sequence Tag) analysis was carried out for human and mouse SK2 primary isoform (SK2std) cDNA and protein sequences (Fig. 1, 2). SK2std cDNA and protein sequences were taken as query for blastn and tblastn, respectively. Blastn tool uses the BLAST algorithm (Altschul et al., 1990) to compare a nucleotide query sequence, in this case SK2 cDNA against a nucleotide sequence database (EST database). TBLASTN tool uses a different BLAST algorithm, which converts the DNA sequence in the EST database to all 6 frames and finds a match for the protein query sequence (protein sequence of SK2) in the database. The BLAST hits were manually screened for the sequence alignment difference with SK2 cDNA or protein against EST sequences.



Results

Fig. 1: Graphic display of tblastn results for human SK2std amino acid sequence (query) against human EST database. One hundred and twenty one EST hits are shown as red, green and pink bars depending on their percentage of identity to SK2std cDNA. Color combinations for percentage identity to the query (SK2std protein) are shown in the color key alignment score bar. EST hits with gaps (represented as black thin lines in between red bars) are potential splice variants of the SK2 gene. These EST hits were selected and further bioinformatics analysis was carried out.

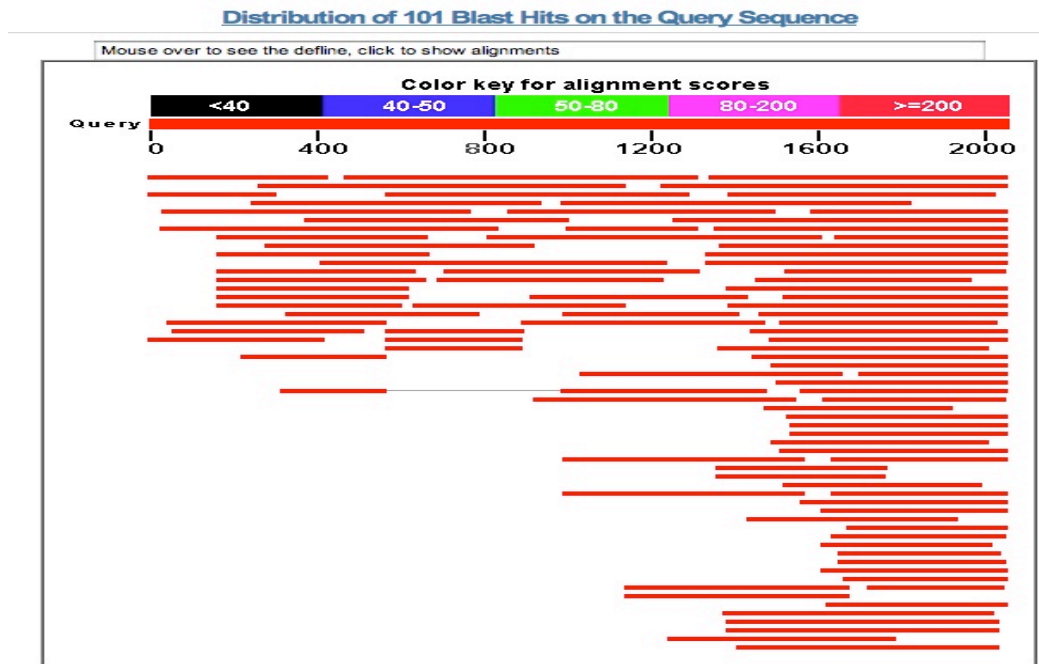


Fig.2: Graphic display of nucleotide blast (blastn) results for human SK2 primary isoform cDNA against human EST database. One hundred and one EST hits are shown as red bars depending on their percentage of identity to SK2std cDNA. This graphic display provides a rough idea about the number of EST hits for SK2std cDNA to be screened for further analysis. Screening individual ESTs is explained in the SK2P and SK2sh result sections of this thesis.

Gaps and inserts in the EST sequence compared to the cDNA were screened by the difference in the nucleotide or amino acid numbers of the EST sequences. Once a potential splice variant was found, the EST was further BLASTed against the genomic sequence database to confirm its exact alignment with exons of the SK2 gene locus. The ESTs were further subjected to comparative genomic analysis with the genomic database

Results

from other species. This revealed the conservation of the spliced variants in human, mouse, rat and other mammalian species. I was using this approach since evolutionarily conserved splice variants are most likely of major relevance to the organism's functionality (Modrek and Lee, 2003; Sorek et al., 2004; Pan et al., 2005; Yeo et al., 2005). A complete transcript structure of the splice variants was established using ORF analysis. In the ORF analysis the exons of new splice variants were arranged according to the EST evidence and a six frame reading was carried out using the EMBOSS sixpack translation structure. These complete transcript structures were experimentally verified by full length cloning using the RACE method. As a result, six new alternatively spliced variants were found in mouse (Fig. 2) by bioinformatics analysis and were verified by RT-PCR. The PCR fragments of these variants were confirmed by sequencing. Comparative genomic analysis confirmed that two of these variants (SK2sh and SK2P) were highly conserved across species.

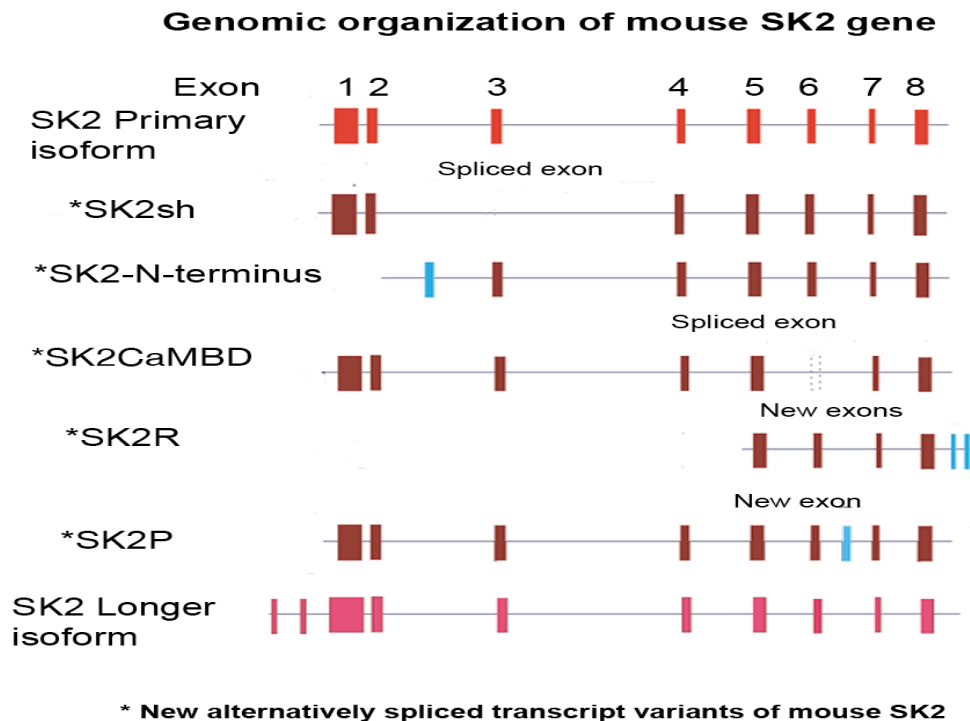


Fig. 3: SK2 splice variants predicted by EST analysis. Genomic organization of the mouse SK2 gene is represented as exons (bars) on the genomic sequence (lines). Six new

Results

alternatively spliced variants were predicted by exhaustively searching the EST databases. SK2 short (SK2sh) and SK2 Parkinson (SK2P) were found to be conserved in human, mouse and rat. SK2CaMBD, SK2-N-terminus SK2R and a longer isoform were mouse-specific variants. All the splice variants were found in brain, except for the SK2-N-terminus variant, which was found only in mouse heart tissue. SK2CaMBD had a premature stop codon in the calmodulin-binding domain, while SK2-N-terminus had an alternative initiation codon. SK2R has two new exons at the 3'UTR and exon 5 of the primary isoform was the first exon for this variant. SK2P has 9 nucleotides (3 amino acids, -Ala-Arg-Lys-) insertion in between exon 6 and 7 of the primary isoform.

Since SK2P and SK2sh had high conservation among species, individual analyses were carried out on these variants.

5.2. Characterizations of SK2 splice variants

5.2.1. SK2P variant

SK2P variant was primarily identified by EST analysis in the human Parkinson's disease EST database (Kim JM et al., 2006), hence the name SK2P (P for Parkinson). In the SK2P transcript a cassette exon of 9 nucleotides was identified by manually screening the SK2 cDNA and EST alignment (Fig.4). The tblastn and ORF analysis of the SK2P transcript revealed that the 9 nucleotide exons cassette in the SK2P variant introduces a 3 amino acid (-Ala-Arg-Lys-) long insert “in frame” between exons 6 and 7 relative to the primary SK2std isoform (Fig. 8). Human and mouse genomic analysis showed that the exon cassette is highly conserved with splice consensus sequences (AG-GT) (Fig. 5).



Fig. 4: Blast alignment of human SK2 primary isoform and EST of SK2P isoform.

Nucleotide sequence alignment (A) and protein sequence alignment (B) of SK2 primary isoform (or SK2std) and EST of SK2P variant has been shown. The 9-nucleotide cassette exon and three amino acid insert in the EST nucleotide and protein sequence respectively has been highlighted. The EST was 678 nucleotides long and aligned to exons 6, 7 and 8 of the SK2std variant.

Results

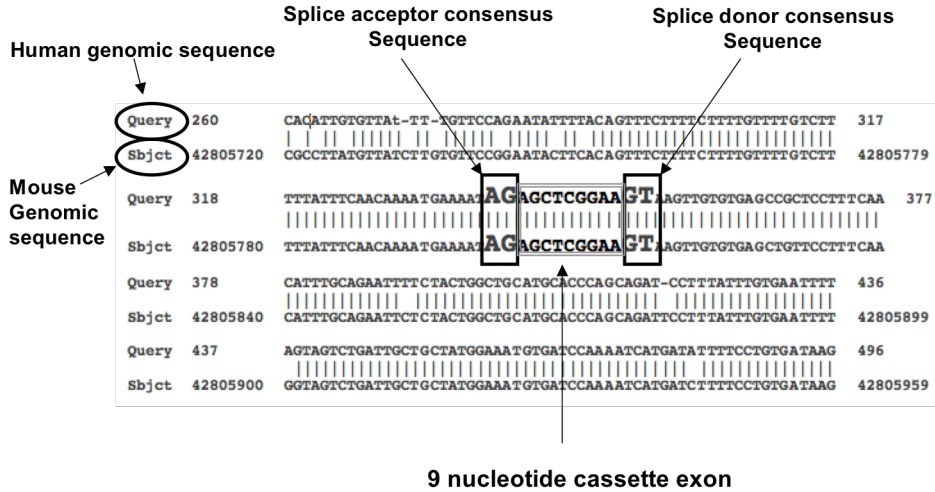


Fig. 5: Blast alignment of human and mouse genomic sequence at the 9-nucleotide exon cassette region of the SK2 gene.

There was a 100% conservation in the nucleotide sequence seen in the 9-nucleotide exon cassette region (thin lined box) and classic splice consensus sequences AG-GT (thick lined box) in human (query) and mouse (subject) genomic sequences.

Primers were designed (see Material and methods) to overlap the exon cassette and splice junctions of SK2P to get specific amplification of SK2P by reverse transcriptase PCR with human and mouse hippocampal cDNA samples. Conserved regions were selected to design one set of primers for all the three species. The expected band was detected on a 2% agarose gel and the amplified fragment was confirmed by sequencing (Fig. 6).

Results

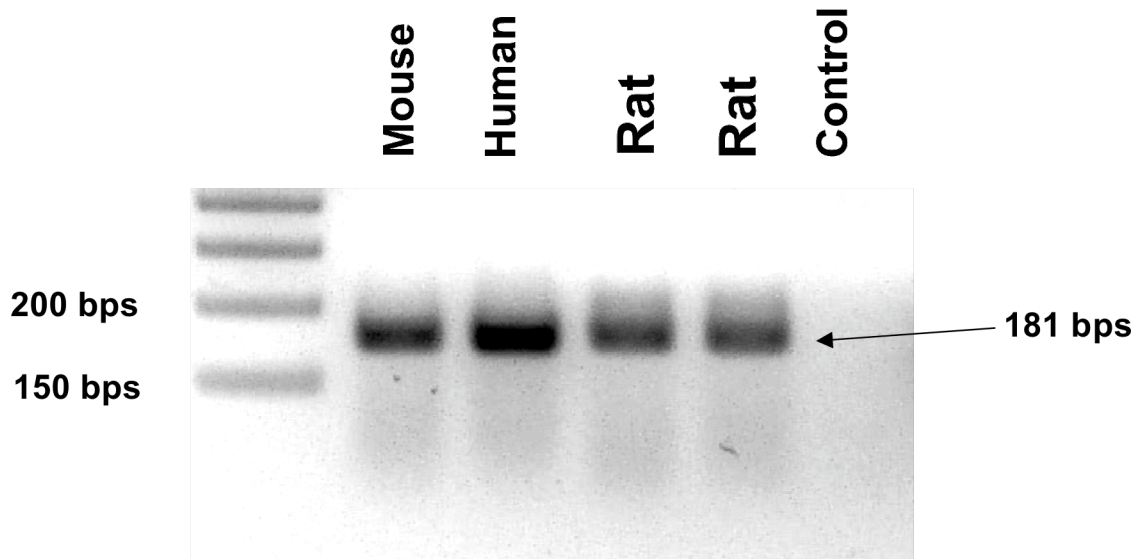


Fig. 6: RT-PCR of hippocampal mRNA from mouse, human and rat. Primers were designed at the exon junctions of the SK2P variant to amplify 181 bps of SK2P fragment from total RNA extracted from human, mouse and rat hippocampal tissues. The gel image indicates the presence of SK2P variant in all the above species and was confirmed by sequencing.

Primers were designed at the overlapping segments of SK2P exon cassette and neighboring exons and RACE full-length cloning of mouse SK2P was carried out as explained in the materials and methods section and was confirmed by sequencing. Based on the full-length sequence of SK2P, ORF was predicted and compared with SK2std protein sequence (Fig. 7)

A CLUSTAL W multiple protein sequence alignment of mSK2std and mSK2P

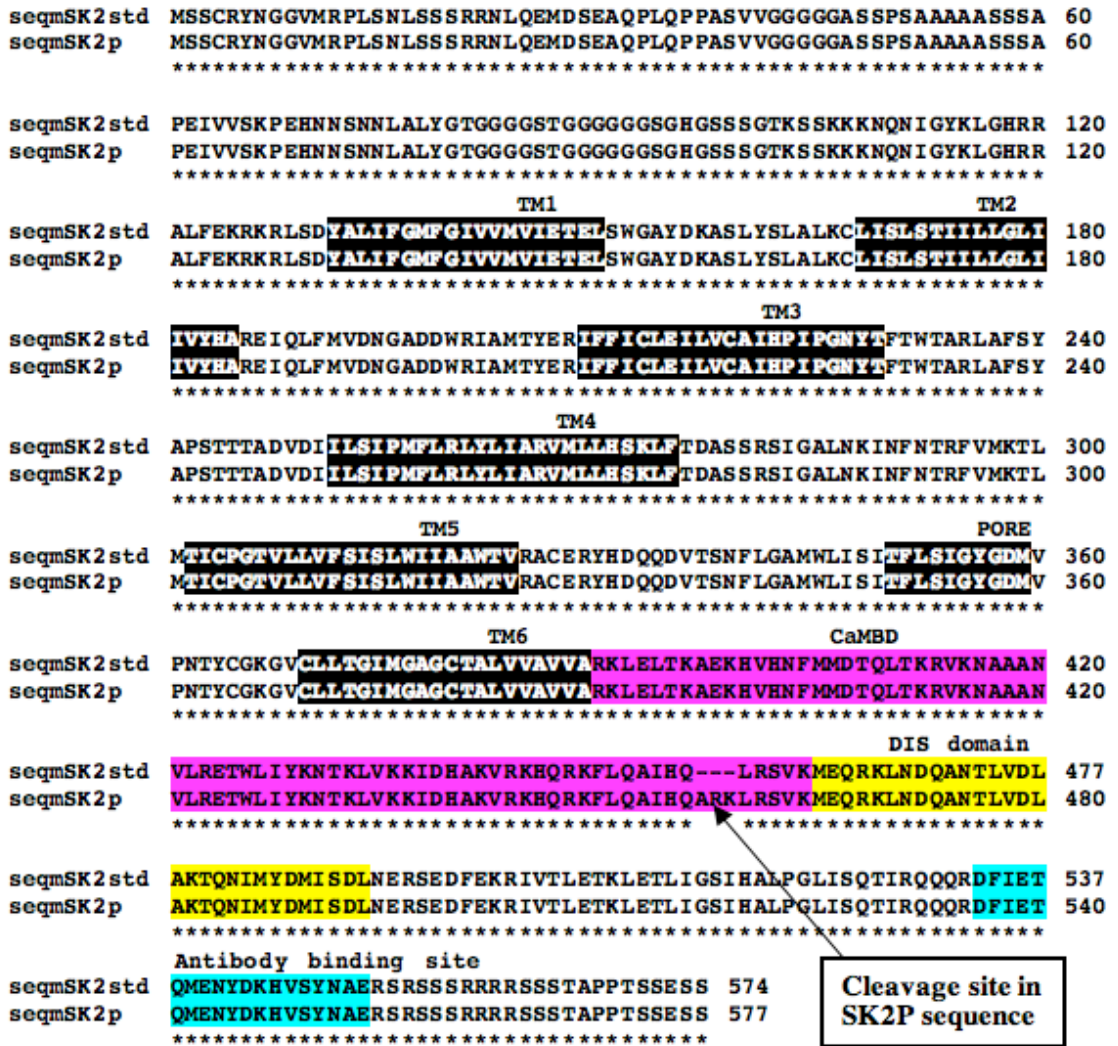


Fig. 7: Mouse protein sequence alignment of SK2P against SK2std.

Six trans membrane domains (TM) and pore forming regions are highlighted with black background. Calmodulin binding domain is highlighted with pink background and Dominant Inhibitor Sequence (DIS) domain is highlighted in yellow. Antibody binding site is also indicated to show that both the SK2 isoforms can be potentially identified with the same antibody. A box represents the 3 amino acids insert unique to the SK2P isoform. The arginine and lysine residues represent a classic posttranslational cleavage site.

The full length assembly and protein sequence prediction showed that mouse SK2P was similar to the SK2std isoform except for a 3 amino acids insert between exon 6

Results

and 7. The 3 amino acid insertion was further analyzed for any posttranslational modification, which may take place with alanine, arginine and lysine residues. Arginine-lysine residues are considered a classic cleavage site. Here, the ProP method (Duckert et al., 2004) of cleavage prediction method was used to predict cleavage sites on the SK2P protein sequence. High scoring cleavage motifs were screened at three different sites of the SK2P isoform (residues from 461-469, 497-501 and 504-511). Interestingly, all these sites were on the C-terminal region of SK2P.

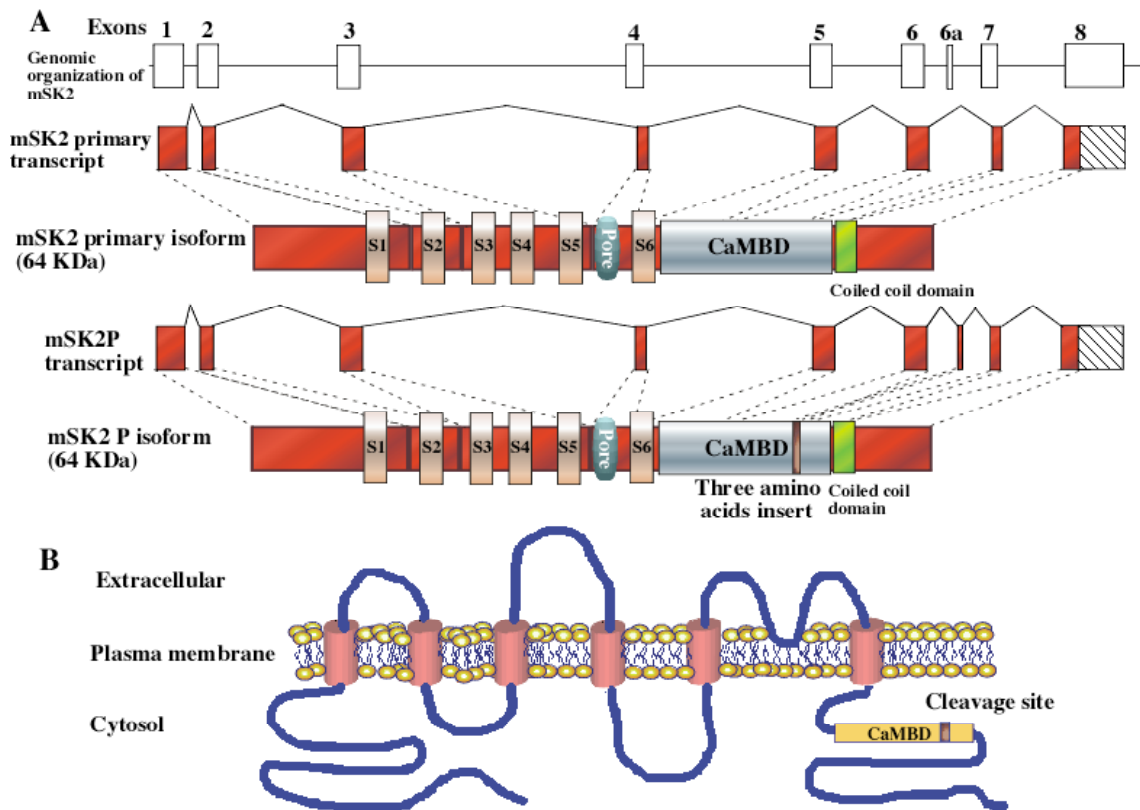


Fig. 8: Genomic organization and topology of SK2std and SK2P: (A) Schematic representation of exon-intron positions on the mouse genomic SK2 locus, mRNA transcripts of SK2std and SK2P. Between exon 6 and 7 in the SK2 locus a nine nucleotide cassette exon 6a, which introduces a 3 amino acid insert at the calmodulin binding domain (CamBD) forms a cleavage site in SK2P (Exons not to scale) (B) Topology of SK2sh in the plasma membrane.

Results

The 3 amino acid insert at the cassette exon (6a) introduces a posttranslational tryptic cleavage site (residues from 461-469) in the arginine-lysine residues at the C-terminus end of the calmodulin-binding site (Fig.8). By this cleavage, the release of a 10KDa protein was predicted and later observed using Western blots of mouse hippocampal tissue whole cell lysate. Further bioinformatic sequence analysis with SMART (Simple Modular Architecture Research Tool) online domain analysis tool (Schultz et al., 1998) showed that, the 10KDa protein fragment contained a domain homologous to the syntaxin 1A N-terminal domain (Fig. 10), which is implicated in the docking of synaptic vesicles at the presynaptic plasma membrane (Betz et al., 1997). The cleaved peptide has a high score for α -helix (Fig. 9) coiled-coil formation at the N-terminus from residue 2 to 97, similar to syntaxin 1A N-terminal domain and has an E-value (Expectation-value) of 2.86e+00, which is considered highly significant. The N-terminal region is likely to have a specific role in exocytosis (Fernandez et al., 1998). Pfam online domain analysis tool (Finn et al., 2005) predicted SNARE [soluble N-ethylmaleimide-sensitive factor (NSF) attachment protein (SNAP) receptors] (Poirier et al., 1998) for the domain from residue 44 to 105 of the cleaved peptide with an E-value of 5.40e+00, which is also considered significant (Fig.9).

Results

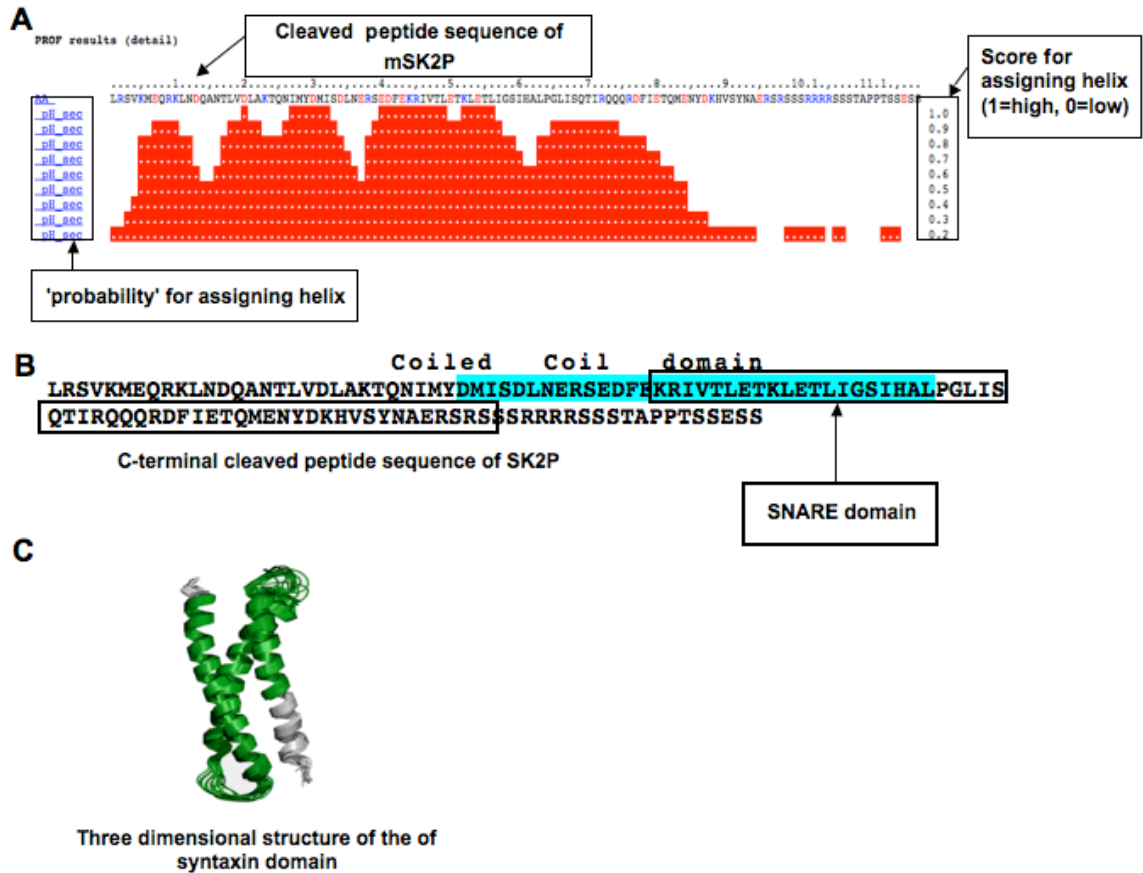


Fig. 9: Prediction of α -helical structure, coiled-coil region and SNARE domain at the N-terminus sequence of the cleaved peptide of SK2P protein. A) PROF prediction (Rost B, 1993) for SK2P cleaved peptide α -helix. There is a high scoring value for α -helix at the N-terminal residues. Probability for assigning helix (pH sec) for each residue is also shown. B) SMART software prediction for coiled coil region is highlighted in blue and Pfam software prediction of SNARE domain in the SK2P cleaved peptide is indicated in the box. C) Three dimensional structure of the of syntaxin domain.

Cleavage at the predicted site would generate a 10KDa protein. Further bioinformatic sequence analysis using the SMART online domain analysis tool showed that, the 10KDa protein fragment contained a domain homologous to the syntaxin 1A N-terminal domain (Fig. 10), which is implicated in the docking of synaptic vesicles at the presynaptic plasma membrane (Betz et al., 1997). However, even though the 10 KDa peptide is homologous to the N-terminal syntaxin proteins, not all the domains in this proteins are present in the 10 KDa fragment, but only the SNARE domain is present.

Results

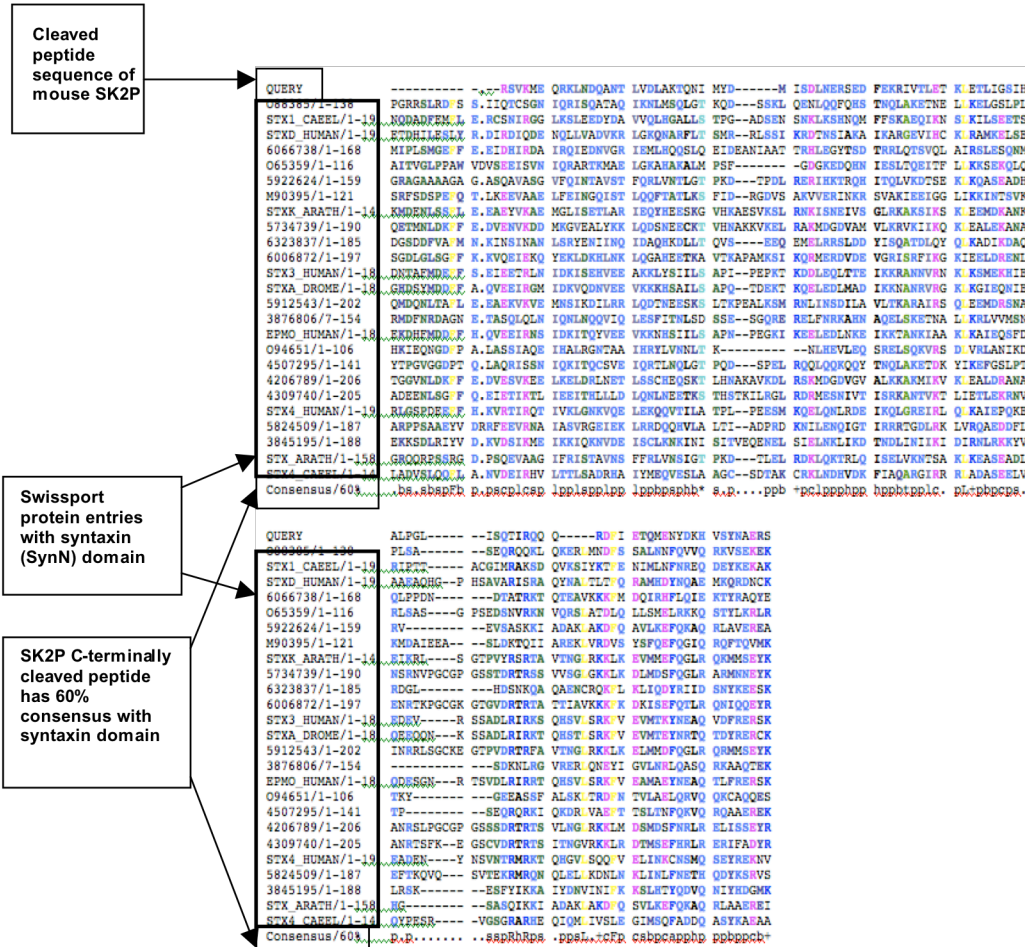
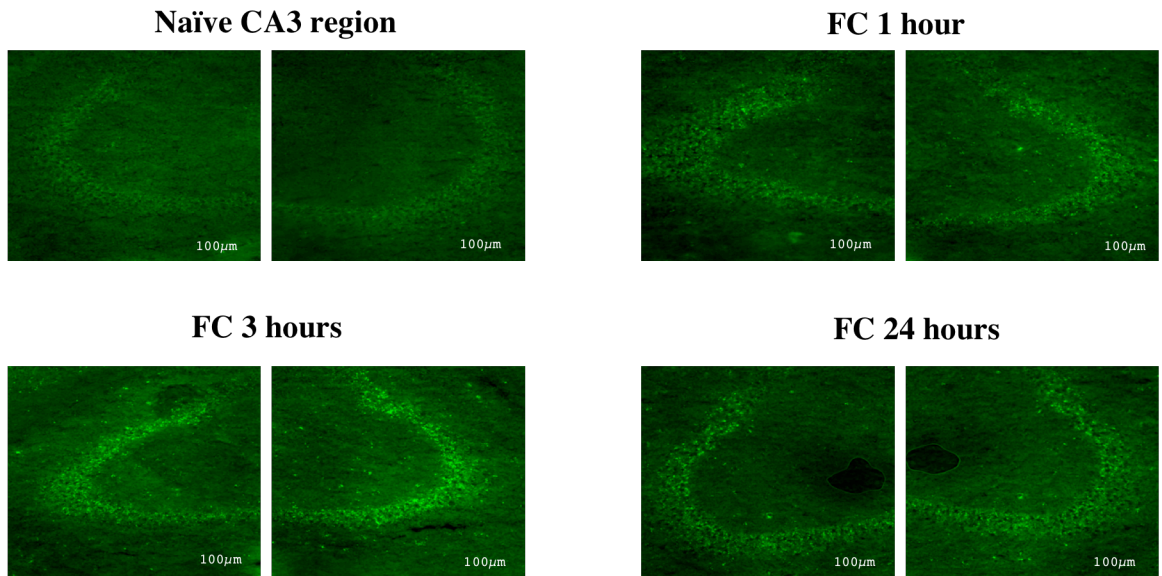


Fig. 10: Multiple alignments of selected Syntaxin N-terminal domains. A conserved region was found in the N-terminal region of C-terminally cleaved peptide of SK2P proteins with Syntaxin N-terminal domains. A PSI-BLAST search was performed using a region (residues 457-574) of mouse SK2P as query with $E < 0.01$ as a parameter. Predicted secondary structure and 60% consensus sequences are shown beneath the alignments. SwissProt/PIR/EMBL accession codes and residue limits are given after the alignments. Residues are colored according to the consensus sequence [green: hydrophobic (h), ACFGHIKLMRTVWY; blue: polar (p), AGS; cyan: turn-like (t), ACDEGHKNQRST; green: aliphatic (l), ILV; and, magenta: alcohol (o), ST).

Results

A main aim of this study has been to determine the biological significance of the new SK2 splice variants and here especially the contribution to learning and memory. Thus, SK2P mRNA expression was assessed in the hippocampus of C57BL/6J mice at different time points after fear conditioning by FIST (Fig.11). SK2P mRNA expression was more or less specific to the CA3 region of the mouse hippocampus.



FC: Hippocampus removal time points after fear conditioning training

Fig.11: Hippocampal SK2P mRNA expression at three different time points following fear-conditioning training. Fluorescent in situ transcription (FIST) analysis showing SK2P mRNA expression in the CA3 region of mouse hippocampus at 1, 3 and 24 hours after fear conditioning (FC) training. (Scale 100µm)

Furthermore, SK2P mRNA expression was up-regulated 1 hour and 3 hour after the training session in the CA3 region of the hippocampus. Even 24 hour after the training session SK2P expression level did not return to baseline levels.

SK2P expression was highest 3 hours after fear-conditioning (Fig. 11). The expression level was still elevated 24 hours after the training session when compared to baseline levels. The sham-handled group showed only a faint increase of SK2P expression 1 hour

Results

after training (data not shown). All other time points were indistinguishable from baseline conditions.

Western blots analysis of hippocampal tissue from fear conditioned mice showed an increase in the predicted 10 KDa fragment at 1, 3 and 24 hours time point after training (Fig.12).

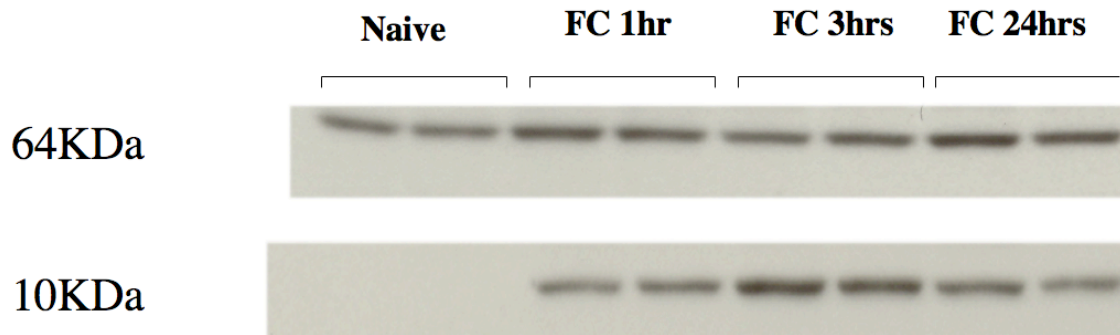


Fig. 12: Western blot analysis of SK2P after fear conditioning training. SK2P cleaved peptide at 10 KDa appeared at 1hour after fear conditioning training and significantly increased at 3 hours. The 10 KDa band was not found in the naïve group. The 64KDa band represents SK2std.

Mira et al., (2003) had shown that the synthetic peptide of synaptosomal associated protein of 25 kDa (SNAP25) was a potent inhibitor of SNARE complex formation and neuronal exocytosis, and suggested that this protects hippocampal SNARE complex formation and neuronal exocytosis. Taking into consideration that the hippocampus is one of the highly vulnerable tissues to neuroexcitotoxic attacks (Chinnaiyan and Dixit, 1996.), many neurodegenerative diseases have been proposed to result from the accumulation of high local concentrations of excitatory amino acids, particularly glutamate (Olney and Gubareff, 1978; Rothman SM, 1983; Simon et al., 1984; Choi DW, 1988; Choi DW, 1992; Meldrum BS, 2000; Chinnaiyan and Dixit, 1996), whose accumulation leads to an excessive level of Ca^{2+} influx and cell death. Taking all these findings into consideration, I examined the role of SK2P 10KDa peptide in a neuronal excitotoxicity experiment, since I hypothesized that the presence of SK2P C-terminally cleaved peptide, which is homologous to the SNARE domain at residues 41 to 97 could also be involved in glutamate release. To test the hypothesis that the SK2P 10KDa

Results

fragment could have a similar function in mouse hippocampal neurons, excitotoxicity experiments were conducted in primary cortical neurons from C57Bl6J mice (Fig.13).

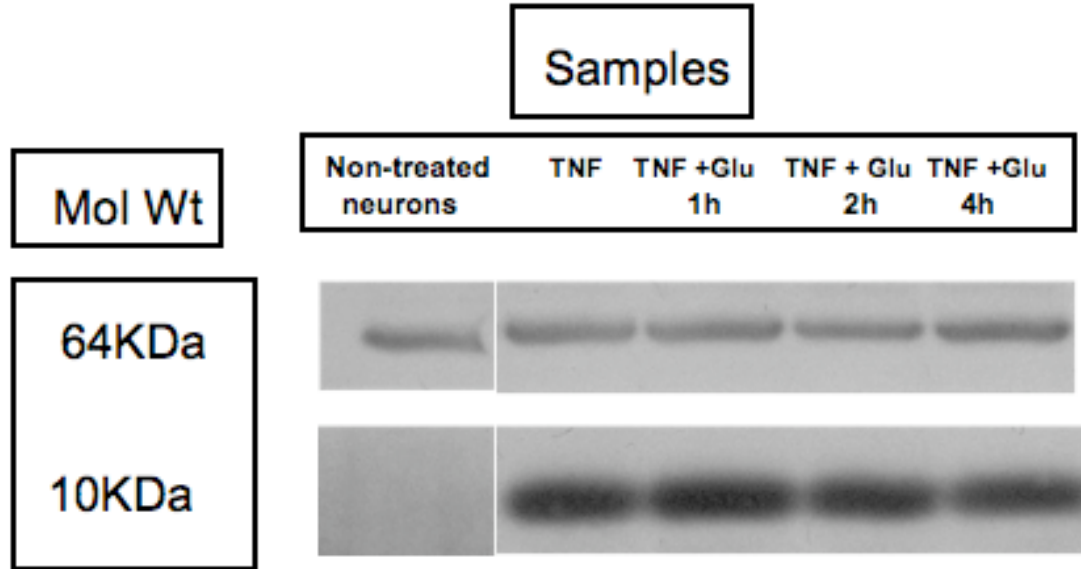


Fig. 13: Western blot immunodetection showing SK2 expression in mouse cortical neurons in response to cytotoxic insult: TNF and glutamate at $30\mu\text{g}$ concentration individually or combined were used to induce cytotoxicity. Western blots were analyzed using SK2 antibody. SK2std at 64KDa was detected in both, non-treated and TNF or/and glutamate treated sample at 1, 2 and 4 hours with no significant modulations. Interestingly, the predicted C-terminally cleaved peptide was detected at every time point following treatment with TNF and/or glutamate.

In this experiment we investigated the expressional change of the predicted 10 KDa peptide of SK2P in cultured primary cortical neurons during glutamate and TNF – induced excitotoxicity. The data showed that the predicted SK2P 10 KDa fragment appeared after TNF treatment or TNF in combination with glutamate.

In order to determine further potential biological significance I evaluated the effect of stress exposure on the expression of mRNA for novel SK2 splice variants.

C57BL/6J mice were subjected to acute immobilization stress for 1 hour and the hippocampus was removed at different subsequent time points. Total mRNA was extracted from the hippocampal samples and first strand cDNA was generated. Real time

Results

analysis was carried out with 1 μg of cDNA from each sample. SK2P mRNA expression showed a substantial reduction after 1 hour of immobilization stress and significant increase at the 2 hours recovery phase (Fig. 14). No significant change was found in the mRNA expression of SK2std (data not shown). The mRNA levels of the housekeeping gene HPRT were not affected by the stress stimulus, hence HPRT mRNA level were taken as standard to calculate the mRNA expression of SK2P and SK2std.

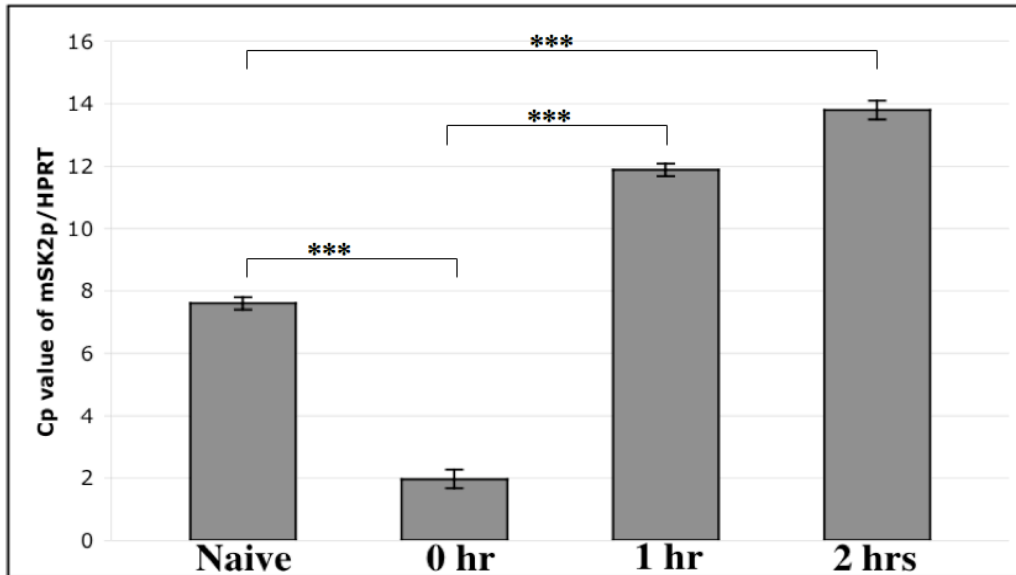


Fig. 14: Effects of stress on mSK2P mRNA expression in hippocampus: The mRNA level of mSK2P in the hippocampus of mice were significantly reduced immediately after stress exposure and significantly increased one and two hours after immobilization stress. The bar graph is shown as the relative crossing point of mSK2P mRNA normalized to the housekeeping gene HPRT mRNA. Statistical analysis was performed using Student's *t* test (***) $p < 0.0001$.

5.2.2. SK2 short (SK2sh) variant

In this study the second splice variant characterized was SK2 short (SK2sh), which is shorter than SK2std. In this study, primary identification of the SK2sh variant was done by EST analysis in the human EST database. Human EST DR003610 from hippocampus was identified by manual screening of the EST alignment results for SK2 cDNA against Human EST (Fig.15).

Results

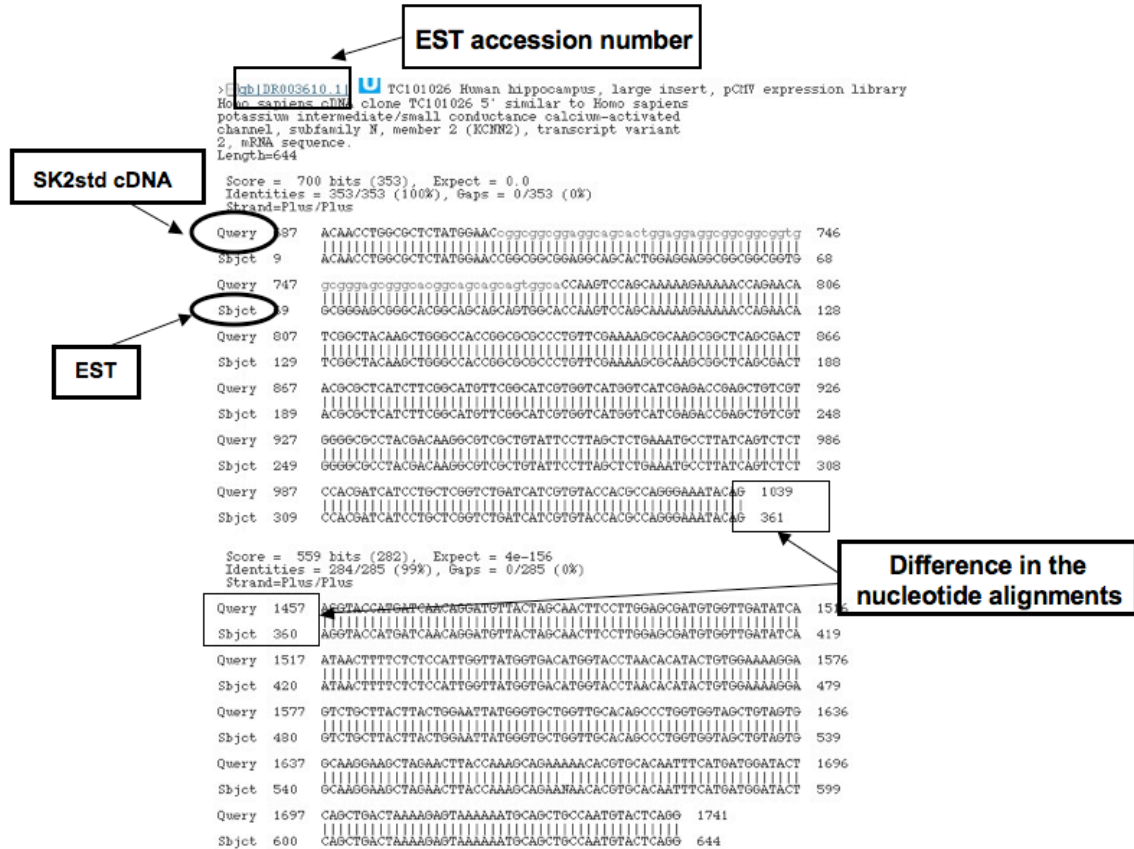


Fig. 15: Human SK2 cDNA aligned against a human EST from nucleotide blast results. Manual and exhaustive screening of human EST database identified a potential splice variant by the difference in the alignment between SK2 cDNA and the EST sequences of 420 bases (highlighted as blue squares).

Genomic BLAST confirmed that the EST DR003610 belongs to the SK2 locus on the chromosome 5 and exon 3 was spliced compared to the SK2std variant.

SK2std cDNA and EST sequences were further analyzed to confirm the exact difference in the alignment using the bl2seq tool (Tatusova et al., 1999). A Genomic BLAST of the selected EST was performed against Human genomic database with $E < 0.01$ and low complexity as parameters to find the distribution of the exons on the SK2 locus (Fig.16).

Results

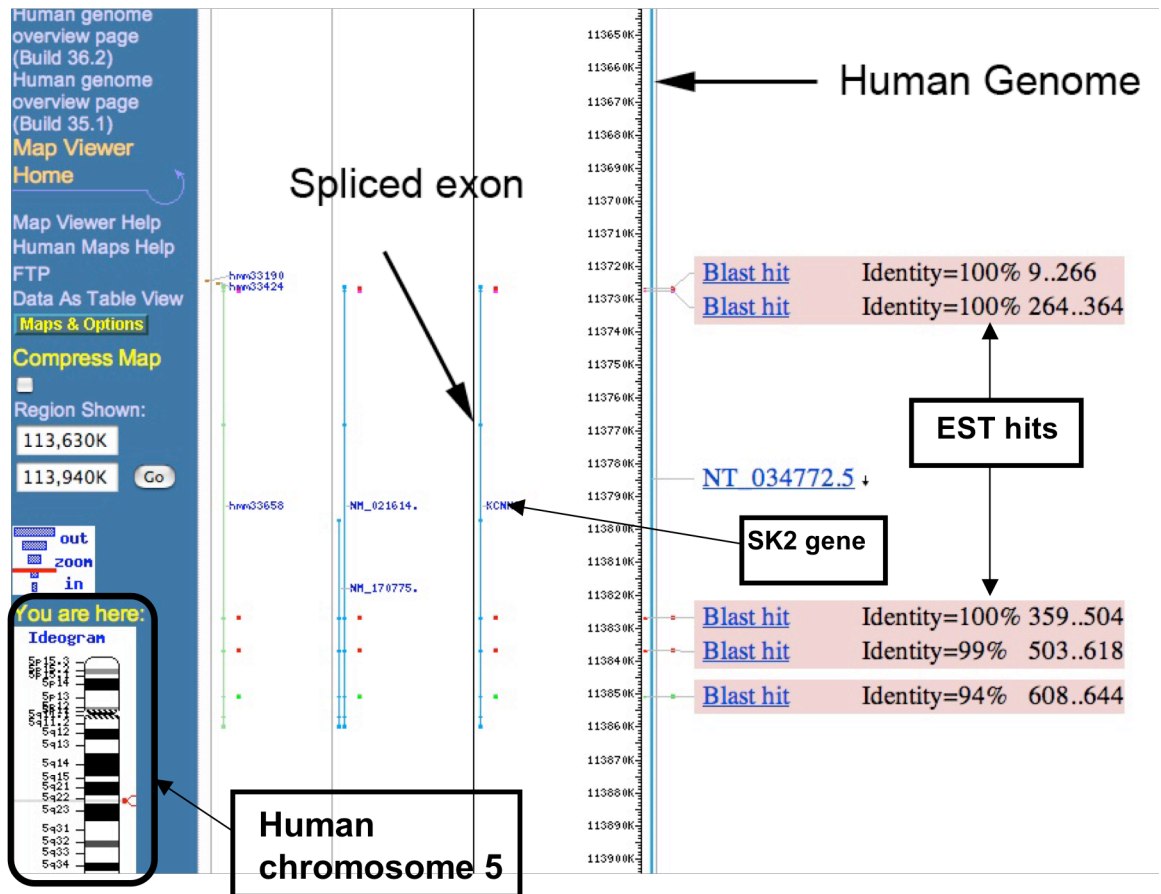


Fig. 16: Genomic alignment of the EST:

Screened EST from the previous analysis was used to align against the human genomic database using genomic BLAST tool. The BLAST hits on the map viewer are shown as red bars aligned against the human genomic sequence (indicated by arrows) on chromosome 5 (inset, SK2 locus position is indicated as red dot). Exon three (bold arrow), which is skipped in the alignment compared to SK2std, is indicated and the EST score is 100% for three exons, 99% and 94% for the other two exons.

The EST DR003610 alignment on the human genome stretched from the first exon to the sixth exon, skipping the third exon of 320 nucleotides in length of the SK2 gene.

To determine whether this splice variant is also present in mouse and rat, an EST search was performed on the EST databases of mouse and rat, taking human EST as query. However, no comparable EST was found. Comparative genomic search at the

Results

spliced region of the EST DR003610 in human, mouse and rat showed 100% conservation in all three organisms. The splice consensus sequence was also conserved across these species (Fig 17).

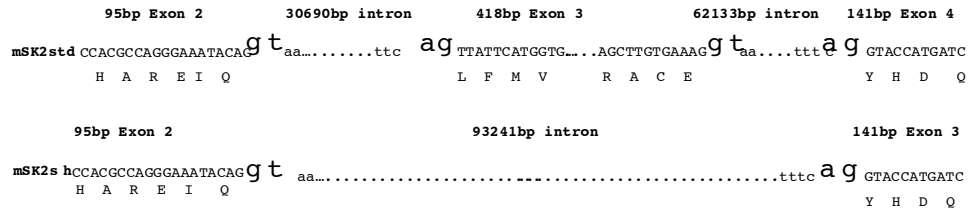


Fig. 17: Exon intron junction and splice consensus sequence of SK2std and SK2sh: A portion of the SK2 gene locus is shown from exon 2 to exon 4 (exons not to scale). Splicing of exon 3 in SK2sh leads to a 93.24 Kb intron. The splice consensus sequence of GT-AG has been conserved with a 100% identity also in the human SK2 gene.

In order to determine the expression of the SK2sh variant in mouse hippocampus, primers were designed at the specific splice exon junctions. A RT-PCR reaction was carried out with human, mouse and rat hippocampal total RNA. Bands of 151 bp were detected on a 2.0% agarose gel (Fig. 18B). PCR fragments were eluted and sequences were confirmed by sequencing. This experimental method showed that finding splice variants in the EST database from one species can be successfully used to find the same splice variant in another species without any prior EST evidence in the latter EST database. The copy number of this new variant was less compared to SK2std in all three species.

Results

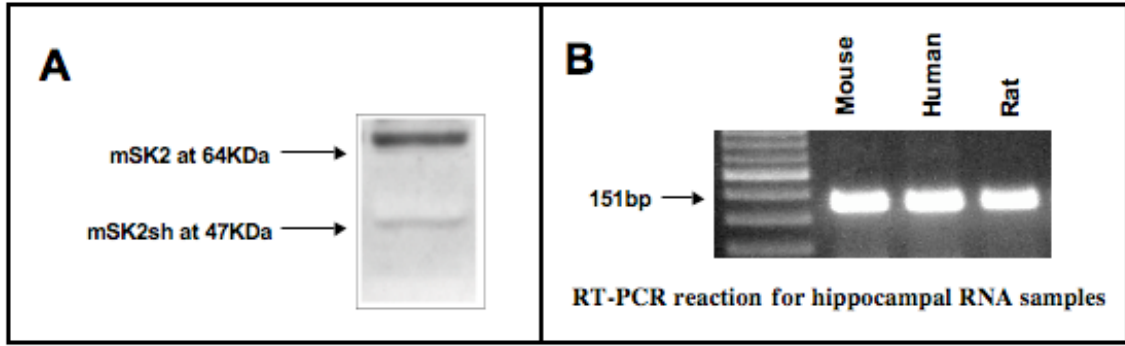


Fig. 18: Detection of SK2sh in hippocampal tissue using Western blot analysis and RT-PCR: (A) 64KDa and 47KDa bands of mSK2std and mSK2sh, respectively, were observed in Western blots from mouse hippocampal tissue using an antibody against mouse SK2. (B) SK2sh was amplified from hippocampal RNA samples prepared from mouse, human and rat tissue.

The RACE method of cloning was used to amplify the full length of mSK2sh as explained in the material and methods section and confirmed by sequencing. The full-length sequence was used to predict the ORF and the protein sequence was compared with SK2std protein sequence (Fig.19).

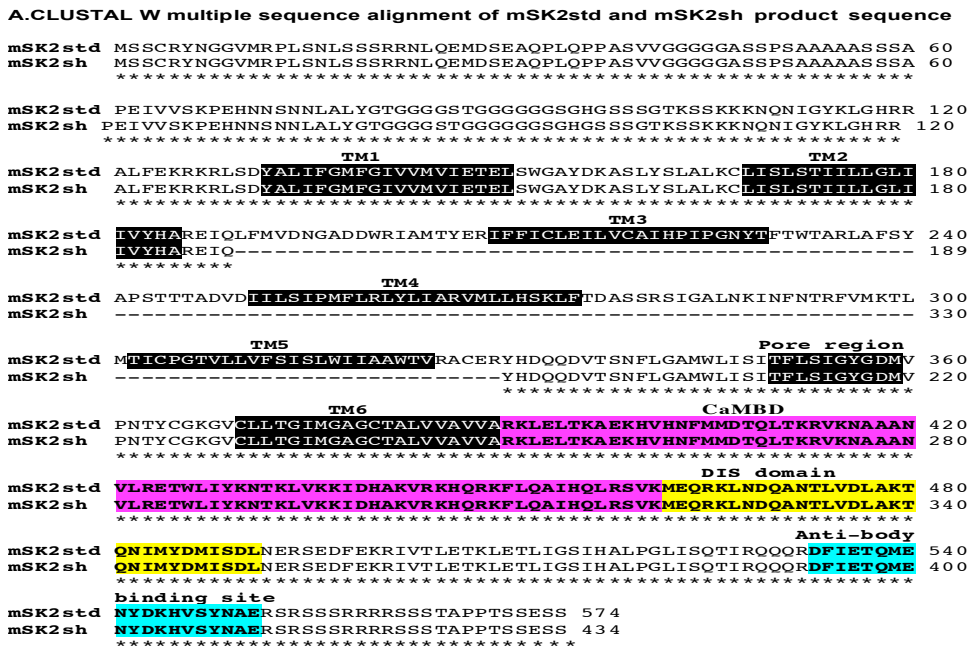


Fig. 19: Multiple alignment of mSK2std (primary isoform) and mSK2sh protein sequence: 140 amino acids have been spliced out as results of exon three being

Results

alternatively spliced. Otherwise, there were no differences to the primary isoform. Asterisks indicate amino acid residues that are identical between both sequences. Presence of Dominant Inhibitor Sequence (DIS) domains is shown, which is especially active in splice variants of many proteins and may sequester other subunits in the cytosol. SK2sh contains the specific epitope used to generate the antibody for SK2std. Six transmembrane domains, the pore forming region and the calmodulin-binding domain are also shown.

The predicted ORF had a molecular weight of 47 KDa and was present in mouse hippocampus as shown using Western blot technique (Fig. 18A). This confirmed the presence of a protein product for the SK2sh isoform even though the amount of SK2sh protein was less than SK2std. This data corresponds with the mRNA copy number of RT-PCR results. The domains were predicted as shown in Fig. 20. Since the SK2sh form lacks three transmembrane domains, it seems unlikely to function as a channel protein despite retention of the pore domain.

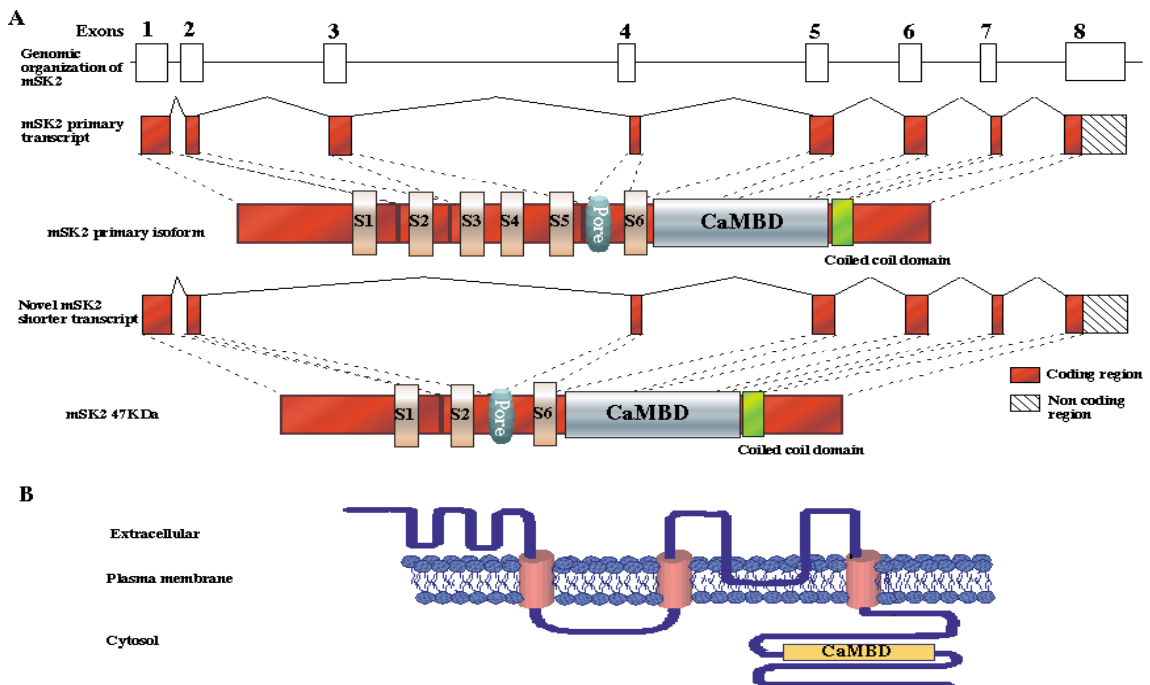


Fig. 20: Genomic organization, splice junction and topology of the SK2 primary isoform and SK2sh (47KDa): (A) Diagrammatic representation of exon-intron positions on the mouse genomic SK2 locus, mRNA transcripts of SK2 primary isoform and SK2 short form. Exons are numbered 1–8 (not to scale) and represented as boxes on the

Results

genome, which is represented as line. Splicing of exon 3 in SK2sh results in omission of the three transmembrane domains S3, S4 and S5 at the protein product, whereas the pore forming region, calmodulin binding domain (CamBD) and coiled coil regions are retained as in the SK2 primary isoform. (B) Predicted membrane topology of SK2sh.

The SK2sh protein sequence was further analyzed for any posttranslational modifications, which might contribute to the function of this variant. ProP method (Duckert et al., 2004) for cleavage prediction was used to predict cleavage sites on the SK2sh protein sequence. High scoring cleavage motifs were screened at three different sites in the SK2P isoform (residues within 368-376) at the C-terminal region of SK2sh. Isotopical averaged molecular weight of the cleaved peptide was 10 KDa, the same molecular weight as found for the SK2P cleaved peptide. Bioinformatic sequence analysis was done using the SMART online domain analysis tool (Schultz et al., 1998). For the 10 KDa protein-fragment it showed a high score for an α -helix coiled-coil formation at the N-terminus from residue 6 to 39 (Fig. 20). Pfam online domain analysis tool predicted SNARE [soluble N-ethylmaleimide-sensitive factor (NSF) attachment protein (SNAP) receptors] for the domain from residue 20 to 81 of the cleaved peptide with an E-value of 5.40e+00, which is considered a significant score. Most, if not all vesicular membrane fusion events in eukaryotic cells are mediated by a conserved fusion machinery involving SNARE. These SNARE domains are thought to act as protein-protein interaction modules in the assembly of a SNARE protein complex (Weimbs et al., 1997). Since the cleaved peptide of SK2sh had a SNARE domain, it seemed important to evaluate the distribution pattern of SK2sh in the mouse brain.

In vivo expression analysis of SK2sh mRNA was carried out to determine the distribution of SK2sh in mouse brain by radiolabelled in situ hybridization (Fig.21) and FISH (Fig.22). We found that SK2sh expression was predominantly in the white matter area rather than in the gray matter of mouse brain. SK2sh mRNA was found in the fimbria (fi), which is a main output pathway of the hippocampus and in the corpus callosum (cc). The overall expression pattern of SK2sh mRNA in mouse brain sections suggested that it was mainly expressed in regions rich in astrocytes and microglia.

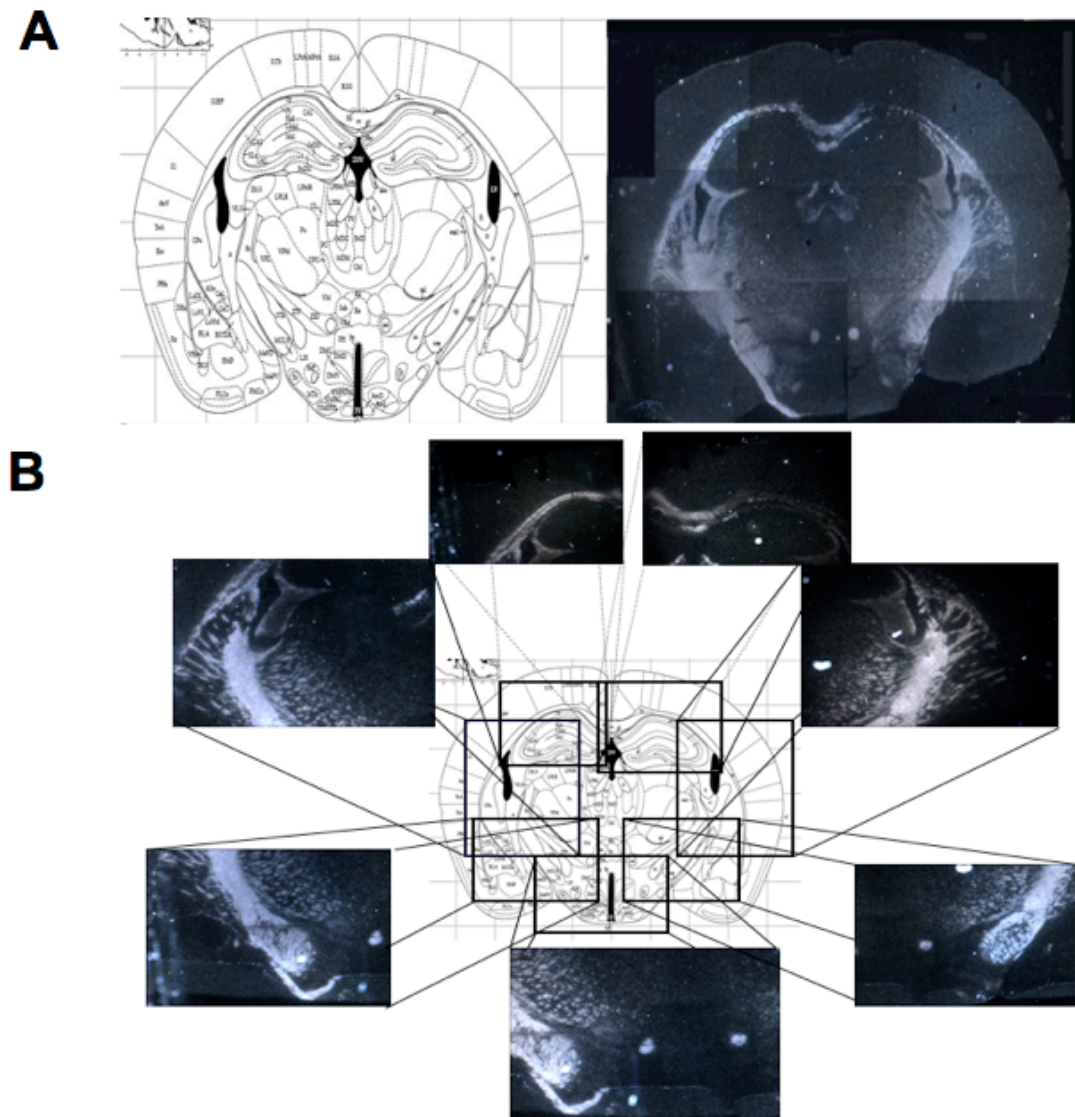


Fig. 21: Distribution of mSK2sh in mouse brain: *In situ* hybridization and emulsion staining of coronal sections from mouse brain was performed using ^{33}P labeled antisense mSK2sh probes. (A) George Paxinos and Keith B. J. Franklin mouse brain stereotactic coordinates figure 46 indicates distinct brain regions present in the brain section. mSK2sh mRNA were found in (B) fi, fimbria of the hippocampus; st, stria terminalis; cg, cingulum; cc, corpus callosum; ec, external capsule; LHbL, lateral habenular nucleus lateral part; LHbM, lateral habenular nucleus, medial part; mt, mammillothalamic tract; STh, subthalamic nucleus; MCLH, magnocellular nucleus of the lateral hypothalamus; ic, internal capsule.

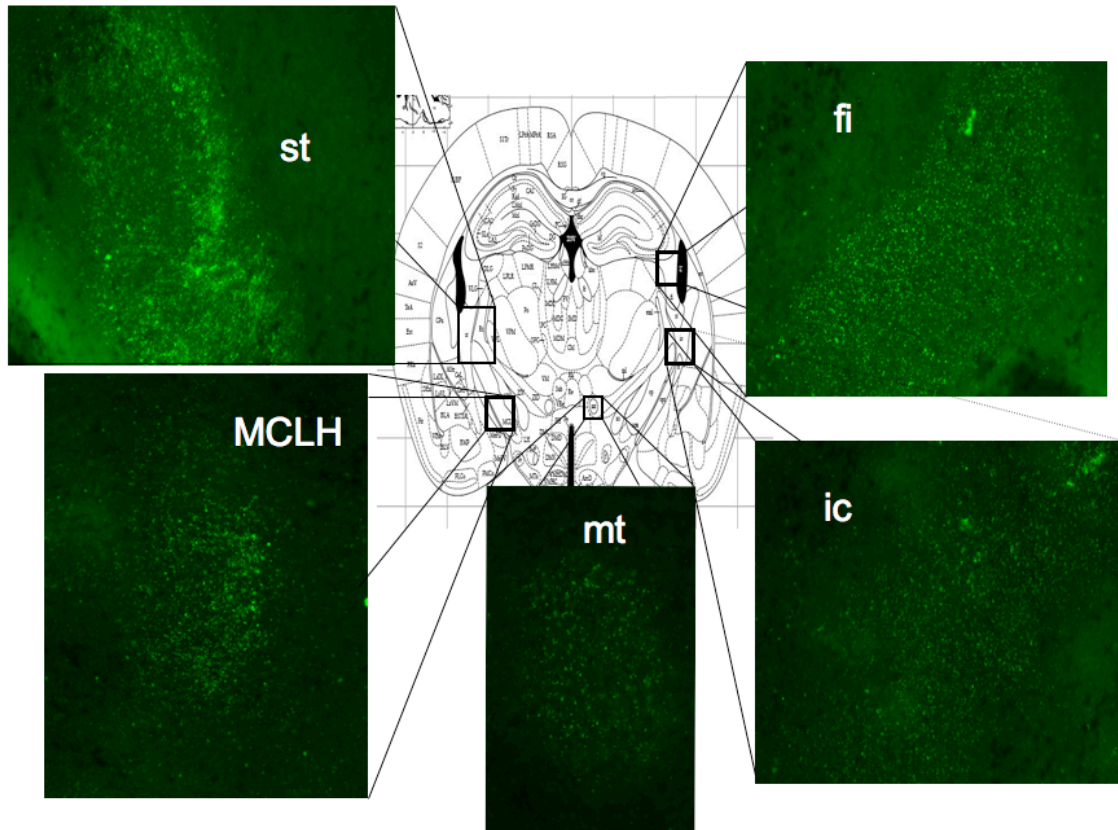


Fig. 22: Fluorescent *in situ* transcription (FIST) in mouse brain section: Fluorescein dUTP was used to amplify mSK2sh *in situ* in mouse brain sections. mSK2sh mRNA was amplified in fi, fimbria of the hippocampus; st, stria terminalis; MCLH, magnocellular nucleus of the lateral hypothalamus; mt, mammillothalamic tract and ic, internal capsule.

Since the expression pattern of SK2sh in mouse was identical to that of apolipoprotein D (ApoD), which is thought to be involved in the neuropathology of Alzheimer's disease (Drayna et al. 1986; Boyles et al. 1990; Thomas et al. 2001), the expression level of SK2sh was investigated in hippocampal tissue samples from Alzheimer's patients (Fig. 23). A total of 14 human hippocampal tissue samples were analyzed, in which three samples were from young controls (ages ranging from 33 years to 40 years), 5 samples were from aged controls (ranging from 73 years to 91 years) and 6 samples were from Alzheimer's disease patients, (ranging from 73 to 84 years). Interestingly SK2sh mRNA expression was significantly increased in the Alzheimer's

Results

disease samples. These data suggest that SK2sh may play a role as a glial cell compensatory response during Alzheimer's disease.

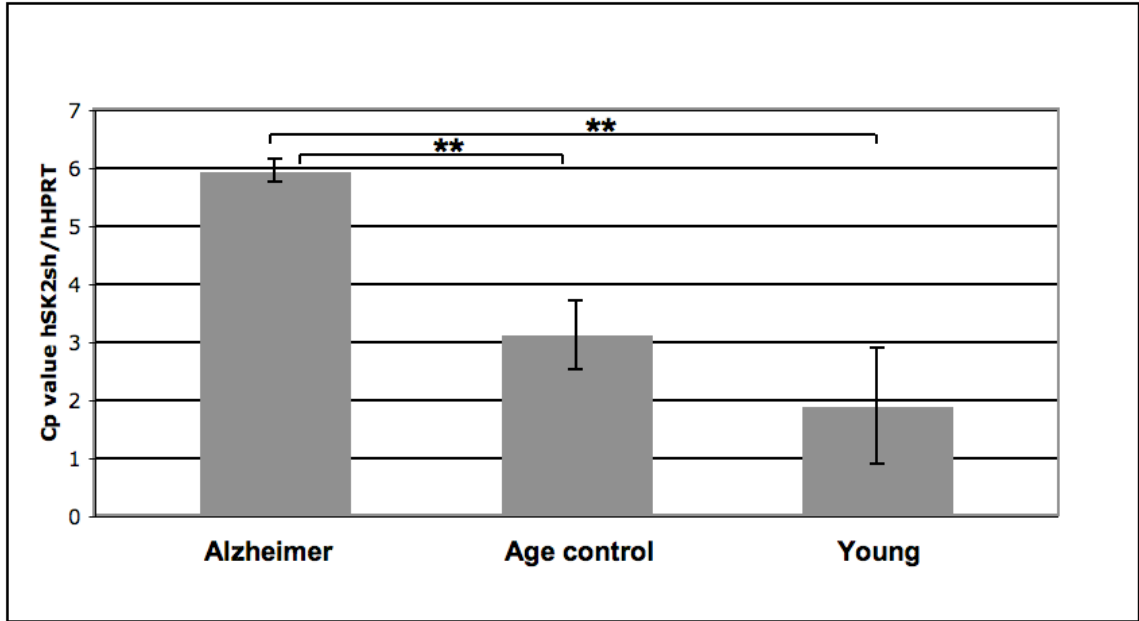


Fig. 23: Analysis of hSK2sh mRNA expression in Alzheimer's, age control and young human hippocampal tissue samples. The age range for Alzheimer's and age control samples were from 75 to 90 years, whereas young adult control group was within 33 to 40 years. A total of 14 hippocampal tissue samples were analyzed. Relative mRNA expression levels were calculated relative to HPRT. Statistical analysis was carried out by Student's test where data are the threshold crossing point (Cp) of the sample in real time PCR reaction. Data are means \pm SD from three separate PCR experiments performed in triplicate. (** $p < 0.01$)

To elucidate the cellular localization of SK2sh, SK2sh cDNA was His-tagged in pcDNA3.1/His vector (Invitrogen). After transfection into HEK293 cells SK2sh was localized at the plasma membrane and showed only scattered distribution in the cytosol (Fig. 24).

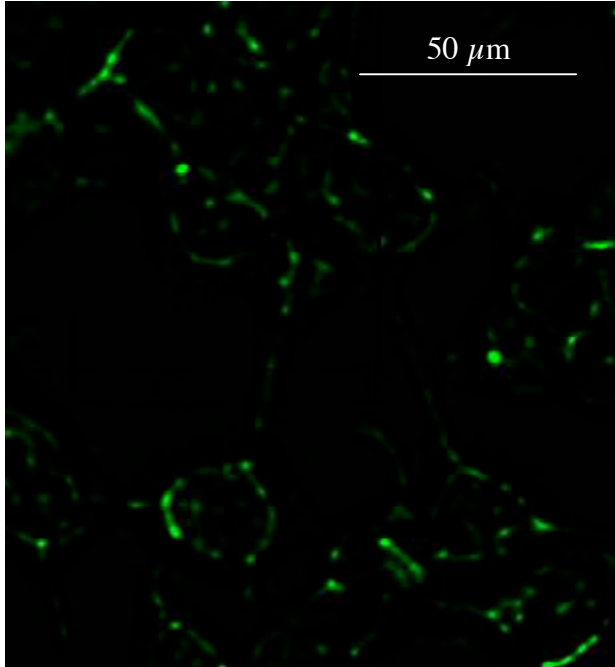


Fig. 24: Expression of His-tagged mSK2sh in HEK293 cells: Anti-His antibody coupled to fluorescein was used to determine the cellular localization of the mSK2sh/His tagged construct transfected into HEK293 cells. mSK2sh was predominantly found in or close to the cell membrane. Only minor signals were detected in the cytosol.

In order to investigate SK2sh mRNA regulation, C57BL/6J mice were subjected to acute immobilization stress for 1 hour and hippocampi were removed at different time points following the end of the stress session. SK2sh mRNA level showed no significant changes at any time point (Fig. 25).

Results

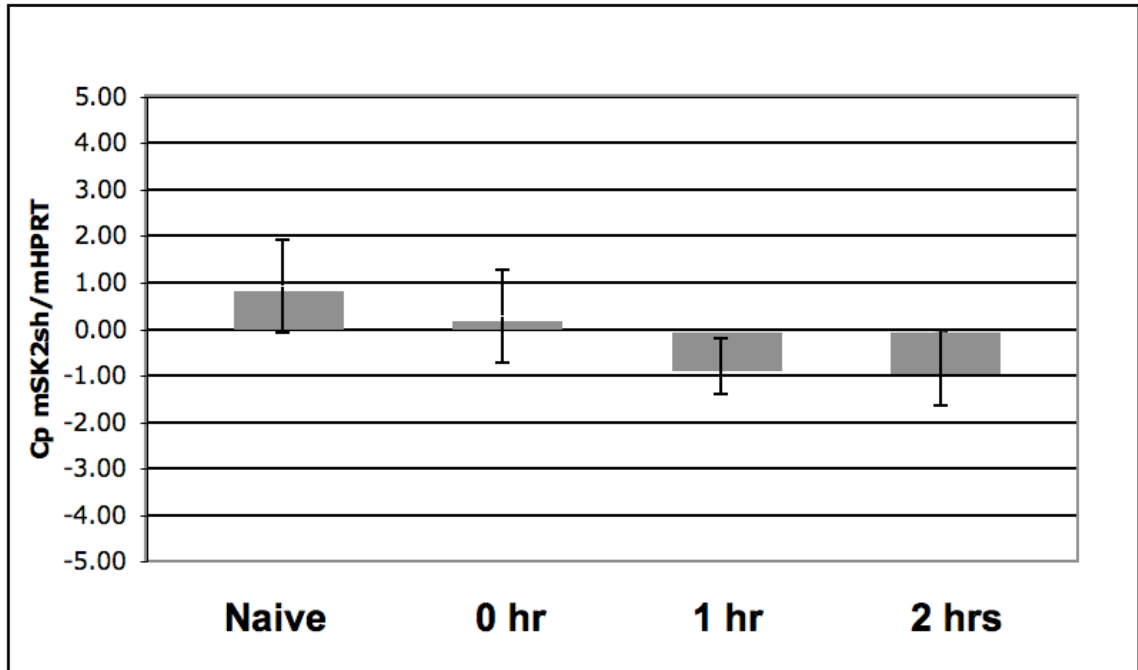


Fig. 25: RT-PCR analysis of hippocampal mSK2sh mRNA following acute stress: mSK2sh mRNA (grey bars) were normalized to mHPRT. No significant changes in mSK2sh expression were detected. Standard deviations are shown as bar-lines on the graph.

Since SK2sh is a new variant of the SK2 gene, we characterized the expression of SK2sh in various other mouse tissues. The data indicated that SK2sh was predominantly expressed in brain and heart tissue (Fig. 26)

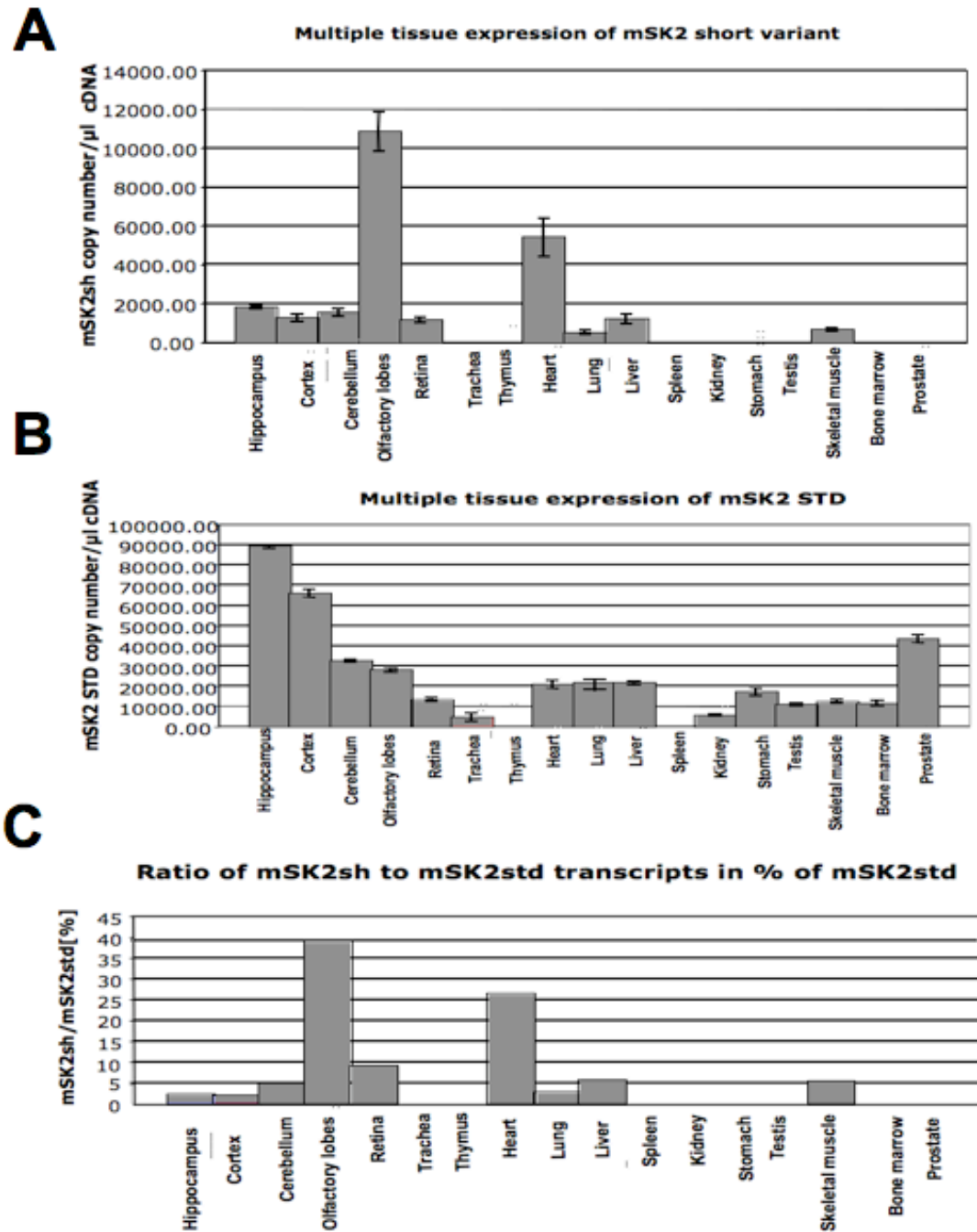


Fig. 26: Distribution of mSK2std and mSK2sh in different mouse tissues determined by DNA Master-PLUS SYBR Green quantitative RT-PCR: mRNA copy numbers are shown per microlitre of cDNA from various tissues in mouse for (A) mSK2sh and (B) mSK2std. The ratio between mSK2sh and mSK2std is given in percentage(C).

5.2.3. SK2 Long variant (SK2L)

The third splice variant characterized in this study was SK2L, which is longer than SK2std. Primary identification of SK2L was done by cDNA analysis in the mouse nucleotide database. A mouse RIKEN full-length enriched library, clone (GenBank™ accession number AK033158) from testis was identified by manual screening of the cDNA alignment results for SK2 cDNA against mouse nucleotide database. SK2std cDNA and RIKEN cDNA sequences were further analyzed to confirm the exact difference in the alignment using the bl2seq tool section.. A Genomic BLAST of the selected cDNA was performed against mouse genomic database with $E < 0.01$ and low complexity as parameters to find the distribution of the exons on the SK2 locus.

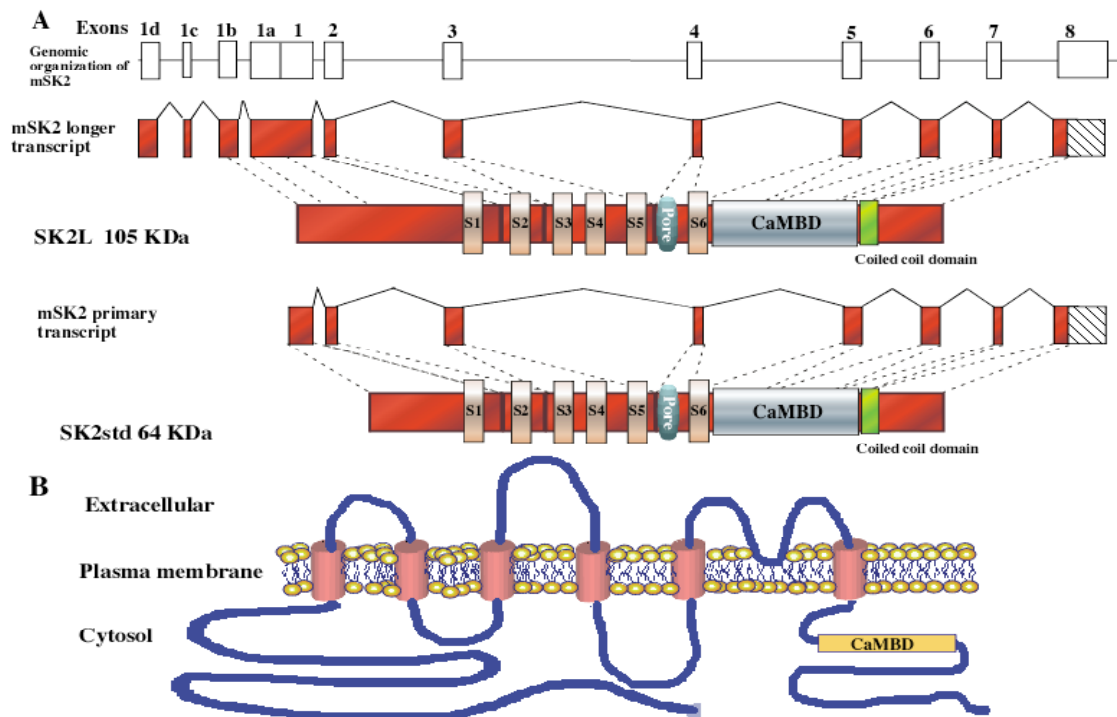


Fig. 27: Genomic organization and topology of SK2std and SK2L: (A) Diagrammatic representation of exon-intron positions on the mouse genomic SK2 locus, mRNA transcripts of SK2L and SK2std. Exon 1b, 1c and 1d are the three extra exons and 1a is the extended exon of SK2L at the 5' region compared to SK2std (exons are not to scale). 275 amino acids are in-frame with ORF of the initial methionine relative to the SK2std

Results

isoform. (B) Predicted membrane topology of SK2L.

The genomic alignment showed that SK2L has 3 new upstream exons and an extended first exon relative to the SK2std transcript. If the most 5'-translational initiation codon is used, the coding sequence is extended by 275 amino acids (Fig. 27). Comparative genomic analysis with human genomic sequence showed that the SK2L transcript was not conserved across species and specific to the mouse genome. Based on the RIKEN full-length sequence of SK2L, ORF was predicted and compared with the SK2std protein sequence (Fig. 28). The SK2L amino acid sequence was calculated and a 105 KDa protein product was predicted.

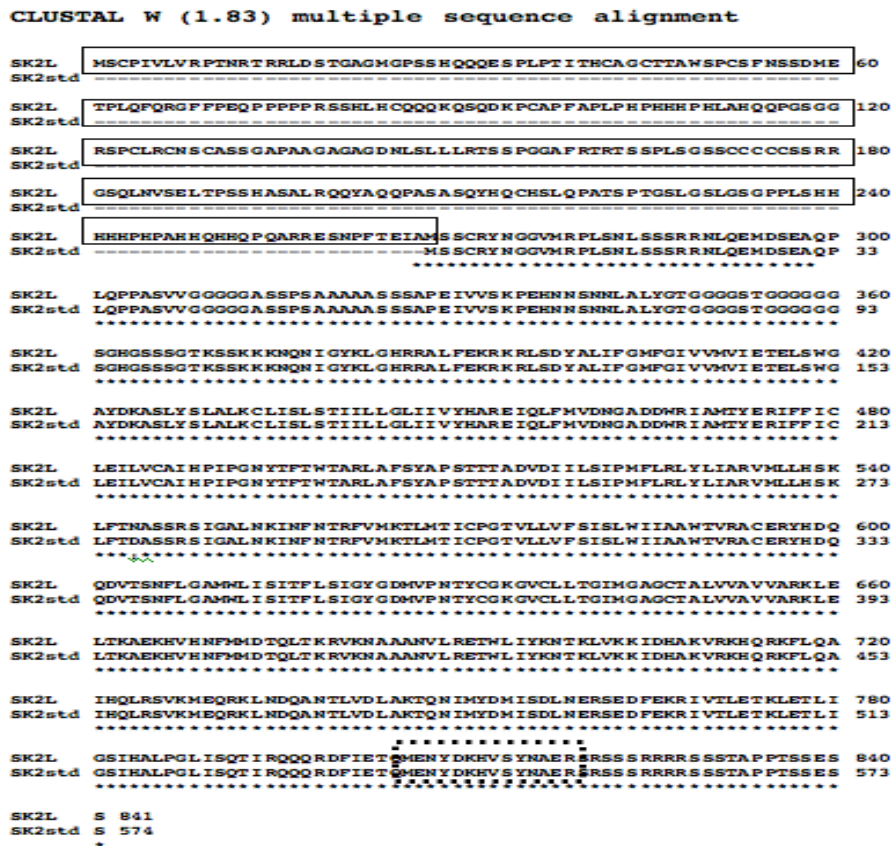
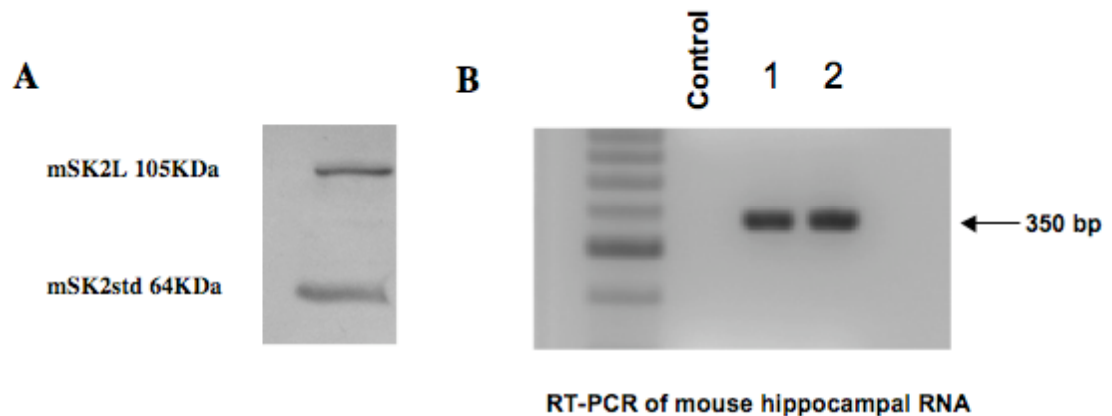


Fig. 28: Multiple alignment of mSK2L and mSK2std protein sequence: SK2L had additional 250 amino acids (box) up stream to the initial methionine in comparison to SK2std. The epitope (dotted box) used to generate the antibody for SK2std is shown and is common to both isoforms.

Results

Domain and motif analysis for the additional 250 amino acids of SK2L did not give any high scoring domains or motifs. To check for the presence of the SK2L variant in mouse hippocampus, primers were designed at the upstream exons unique to SK2L and a RT-PCR reaction was carried out with total RNA isolated from mouse hippocampus. Bands of 350 bp were detected on a 1.5% agarose gel (Fig. 29B). PCR fragments were eluted and sequenced. Hippocampal fractions were subjected to Western blot analysis using anti-SK2 antibody. The band of 105 KDa fitted the expected size of



mSK2L (Fig.29A).

Fig. 29: Detection of SK2 in hippocampal tissue using Western blot analysis and RT-PCR: (A) 105 KDa and 64 KDa bands of mSK2L and mSK2std respectively were found in the Western blot analysis of mouse hippocampal tissue using an anti-SK2 antibody. (B) RT-PCR amplification of SK2L mRNA (1 and 2) from mouse hippocampal tissue showed a single band at 350 bp, indicating that cDNA was devoid of genomic DNA.

In order to investigate SK2L mRNA regulation, C57BL/6J mice were subjected to acute immobilization stress for 1 hour and hippocampi were removed at different time points following the end of the stress session. SK2L mRNA level showed no significant changes at any time point (Fig. 30).

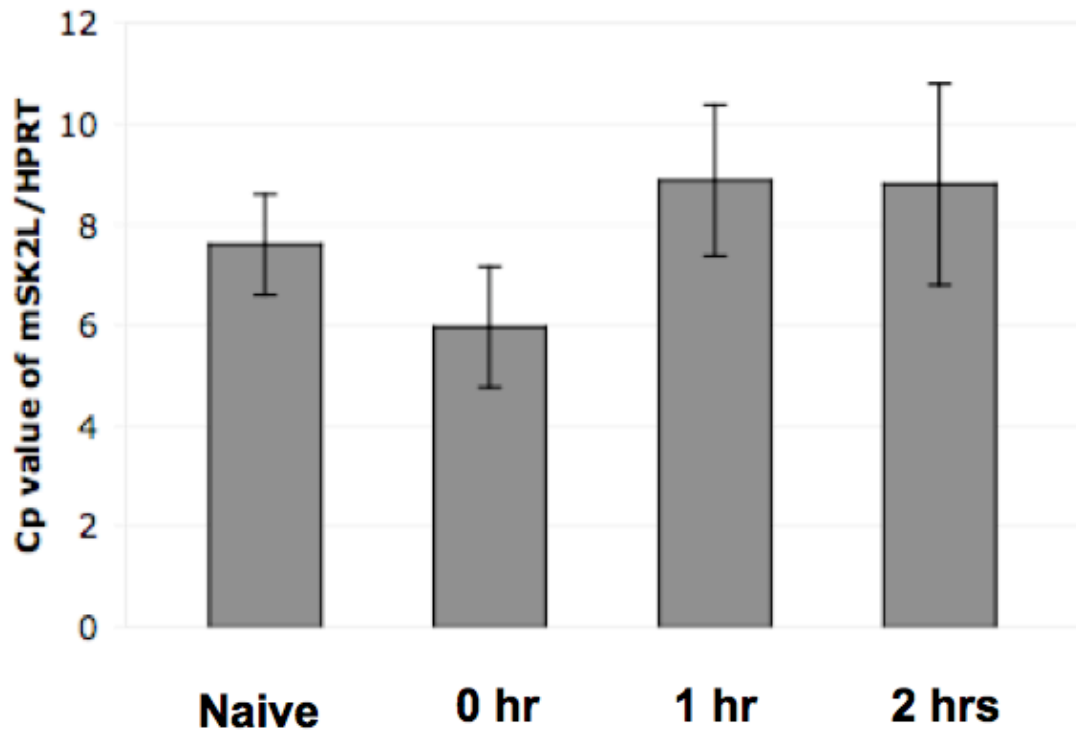


Fig. 30: RT-PCR analysis of hippocampal mSK2L mRNA following acute stress: The relative mRNA levels of mSK2L are represented as bars. The bar graph is shown as the relative crossing point of mSK2L mRNA normalized to the housekeeping gene HPRT mRNA. The statistics was performed by Student's *t* test. Error bars are shown as bar-lines on the graph.

5.2.4. SK2 calmodulin binding domain variant (SK2CaMBD), SK2 regulatory variant (SK2R) and SK2-N-terminus variant.

In this study the fourth, fifth and sixth splice variants characterized were SK2 CaMBD, which has an exon spliced at the calmodulin domain, SK2 regulatory (SK2R), which we predicted may have regulatory function at the post transcriptional level and SK2-N-terminus, which has an alternative first exon. Primary identification of these variants was done by EST analysis in the mouse EST database by manual screening of SK2 cDNA against mouse EST alignment. SK2std cDNA and these EST sequences were

Results

further analyzed to confirm the exact difference in the alignment using the bl2seq tool. A Genomic BLAST of the selected cDNA was performed against mouse genomic database with $E < 0.01$ and low complexity as parameters to find the distribution of the exons on the SK2 locus. SK2 CaMBD was identified by the EST (GenBank accession number: CO797528) analysis and had exon six spliced out relative to the SK2std variant. An alternative splice event introduced a premature stop codon, which was analyzed by ORF analysis. RT-PCR reaction showed the presence of SK2 CaMBD in mouse hippocampus at very low levels. It is well known that splice variants with premature stop codon undergo nonsense-mediated degradation. Thus, a functional product from this variant was not expected. SK2R was identified by the EST (GenBank accession number: CK332073) analysis and had two more exons at the 3' untranslated region relative to the SK2std variant. This variant did not disturb the protein-coding region. RT-PCR reactions showed the presence of SK2R in mouse hippocampus at very low levels. Thus, further analysis was not carried out. SK2-N-terminus was identified by the EST (GenBank accession number: AA209646; AA238176; DT915212) analysis and had an alternative first exon relative to the SK2std variant. RT-PCR reaction showed no presence of SK2-N-terminus in mouse hippocampus. Further screening of other tissues showed that this variant was only present in heart and liver.

6. Discussion:

It has been known for some time that members of the SK1 and SK3 gene family undergo extensive alternative splicing. Surprisingly, until recently there was no scientific evidence for alternative splicing of the SK2 gene. Within the framework of my thesis I was able to identify six novel splice variants of SK2. The findings indicate that SK2 is highly regulated at the post-transcriptional level and suggest a much broader functional spectrum for SK2 beyond the classical function as small-conductance calcium activated potassium channel. All six predicted splice variants are predominantly expressed in mouse brain tissue, except for the SK2-N-terminus variant, which was only found in mouse heart and liver tissues. The high conservation of two splice variants, SK2P and SK2sh, across mice, rats and humans makes them particularly interesting so that they were the main focus of this thesis.

6.1. SK2P

SK2P has a three amino acid (-Ala-Arg-Lys-) cassette exon, which inserts a tryptic cleavage site at the calmodulin-binding domain. Enzymatic cleavage of SK2P can generate a 10 KDa peptide. This precursor cleavage occurs frequently at motifs containing multiple basic residues like arginine or lysine (Seidah and Chretien, 1999). Many of the involved proteases are identified: PC1, PC2, furin, PC4, PC5, PACE4 and PC7 (Fuller et al., 1989; Bresnahan et al., 1990; van de Ven et al., 1990). A similar mechanism of C-terminal cleavage has been reported in voltage-gated sodium channels (Kim DY et al., 2007). It was shown by Kubalski et al. (1989) that application of proteases to the cytoplasmic face of the channel caused an irreversible increase in channel activity without affecting unit conductance. Moreover, trypsin and protease similarly removed the Ca²⁺ dependence of channel activation, while thermolysin removed the channel's voltage dependence. Further experiments are necessary to determine the effect of C-terminal cleavage on SK2P channel function.

6.2. Presence of SNARE domain in C-terminal region of SK2P

The SK2P cleaved 10 KDa peptide shows a homologous region to the N-terminal domain of syntaxin. This N-terminal domain of syntaxin constitutes an independently

Discussion

folded domain with a three-helix bundle structure. The C-terminal region consists of a core (Fernandez et al., 1998). Syntaxins are nervous system-specific proteins implicated in the docking of synaptic vesicles with the presynaptic plasma membrane and anchor the channel forming proteins to the cytoplasmic surface of cellular membranes. Association of syntaxin with large conductance calcium activated potassium channel was shown to enhance channel gating and kinetics (Ling s et al., 2003). The 10 KDa peptide of SK2P was homologous to the helical structure. The SNARE domain is present, but additional domains present in syntaxin proteins are absent. Data from various research groups has led to the formulation of the SNAP1 receptors (SNARE) model to describe the final steps of the secretion cascade (Matthews G, 1996; Calakos et al., 1996; Jahn et al., 1994; Südhof TC, 1995; O'Connor et al., 1994; Schweizer et al., 1995; Bark et al., 1994; Rothmann JE, 1994; Söllner et al., 1993). The SNARE hypothesis distinguishes three distinct stages in the pathway, namely docking, priming, and fusion. Vesicle docking refers to the process by which cargo vesicles are targeted to the plasma membrane at the active zone, although they are not competent for Ca²⁺-triggered fusion (Südhof TC, 1995). After docking, vesicles are activated by an ATP-dependent step known as vesicle priming. Primed vesicles are readily releasable in response to a transient Ca²⁺ elevation that triggers the fusion event. Trafficking of the excitatory amino acid carrier 1 (EAAC1), which plays a role as a precursor for the synthesis of the inhibitory neurotransmitter GABA (Sepkuty et al., 2002; Mathews and Diamond, 2003), was inhibited by a dominant-negative variant of SNAP-23, which lacks a domain required for SNARE complex assembly (Fournier KM and Robinson MB, 2006). The SNARE domain in the SK2P cleaved peptide is similar to the domain present in a dominant-negative variant of SNAP-23. This might explain, why the Western blot analysis of hippocampal tissue showed only a 10 KDa band, presumably the cleaved peptide. This appeared only after fear conditioning training or glutamate treatment in cultured neurons, which suggests that the tryptic cleavage of SK2P has a role in either inducing neuronal cell death or cell survival.

Synthetic peptides that mimic the amino acid sequence of SNARE segments from synaptotagmin (DeBello et al., 1993; Geppert et al., 1994), SNAPs (DeBello et al., 1995), synaptobrevin (Cornille et al., 1995) and SNAP-25 (Gutierrez et al., 1995; Metha et al.,

Discussion

1996) were all shown to be specific inhibitors of neurosecretion. These peptides, for which the term “Excitation-Secretion Uncoupling Peptides” (ESUP) (Gutierrez et al., 1997) was coined to highlight their activity (Gutierrez et al., 1995), are useful pharmacological tools to probe the functional role of distinct protein components in the secretory machinery and to dissect the contribution of specific domains in the protein-protein interactions that mediate this process, as well as to identify steps in the exocytotic cascade. We propose a similar homologous segment in the SNARE domain of the cleaved peptide, which could interact with the SNARE complex. Further studies are necessary to determine the exact function of the cleaved peptide in the exocytotic pathway.

6.3. Specific expression of SK2P in CA3

In situ experiments show that SK2P was specifically localized at the CA3 region of the hippocampus, unlike the primary isoforms, which is localized in the CA1 and CA2 regions (Stocker and Pedarzani, 2000; Sailer et al., 2004). This specific expression pattern of SK2P in the hippocampus may be the answer for the discrepancy observed between Stocker and Pedarzani, (2000) and Sailer et al. (2004). Given that these two studies had observed discrepancies between *in situ* hybridization and immunohistochemical staining data, the present study provides an answer for these discrepancies by showing that the SK2P variant has specific expression at the CA3 region of hippocampus where as the SK2std variant is found predominantly in CA1 and CA2. We note that the hybridization probe designed in Stocker and Pedarzani, (2000) bound to both SK2std and SK2P, whereas the antibody used in the immunohistochemical study conducted by Sailer et al., (2004) recognized only the SK2std protein product expressed in CA1 and CA2. In this present study we designed specific probes for SK2P and SK2std variants, which differentiated these localizations.

Recently, a set of papers from three research groups has demonstrated striking differences in the ensemble activity of CA3 and CA1 neurons in behavioral animal models (Lee et al. 2004; Leutgeb et al. 2004 and Vazdarjanova and Guzowski 2004). It was shown in lesion studies, that the involvement of CA3 is important at the earliest stage of acquisition, presumably for developing instant representation of a context and

Discussion

consolidation of contextual fear conditioning, as was also reported by Daumas et al., 2004. The role of CA3, however, was minimal in retrieving contextual memory after a long time period (i.e., 24 h), whereas the other subregions (i.e., CA1 and dentate gyrus) were critically involved (Lee and Kesner, 2004; Daumas et al., 2005) in such retrieval processes. Hence, SK2P may be involved in acquisition rather than retrieval of contextual memory. It is specifically expressed in CA3 and shows a clear increase after fear-conditioning training. Thus SK2 channel variants seem to be localized in distinct hippocampal subregions and seem to contribute differently to memory acquisition, consolidation and retrieval.

6.4. Regulation of SK2P after stress

Stress is proposed to induce CA3 dendritic retraction, which then disrupts hypothalamic-pituitary-adrenal axis activity, leading to dysregulated glucocorticoid release (Conrad CD, 2006). Real time PCR analysis shows that the SK2P variant is highly up-regulated after stress and is the major variant undergoing high modulation of cumulative effects of SK2 mRNA. It has been shown in previous studies in our lab that SK2 is regulated by glucocorticoids (GC) and it is well known that GC- and stress-mediated dendritic atrophy involves increased glutamate release (De Bruin et al., 1990; Lowy et al., 1993; Moghaddam et al., 1994 and Benson and Cohen 1996). Of relevance, glutamate is the major neurotransmitter present in mossy fiber-CA3 pyramidal neuron synapses (Storm-Mathisen et al., 1983), and stress appears to be associated with enhanced interaction of synaptic vesicles with the presynaptic membrane at these synapses (Magarinos et al., 1997). It seems possible that increased SK2P expression after stress may contribute to a mechanism underlying stress- and GC-mediated dendritic atrophy of CA3 pyramidal neurons, involving either increased or decreased glutamate release. The resulting excessive/decreased excitatory input into CA3 pyramidal neurons may, in turn, lead to adaptational changes in those neurons to limit the excitotoxic stimulus. It would be interesting to determine whether the 10 KDa cleaved peptide of SK2P facilitates or impairs the interaction of synaptic vesicles with the presynaptic SNARE complex.

Assembly of the SNARE complex involves coiling of the SNARE proteins from

Discussion

their distal to their proximal ends in a parallel fashion, which pulls the apposing membranes together (Hanson et al 1997 and Hanson et al 1997). This problem could be addressed by using site-directed mutagenesis at the Arg or Lys residues, which are in the cassette exon insert or by injecting the synthesized C-terminal peptide of SK2P *in vivo* into the mouse dorsal hippocampus. SK2P EST was primarily identified in Parkinson's disease substantia nigra tissue EST library and also SK2P mRNA expression was observed in substantia nigra of mouse brain in this study (data not shown). Role of substantia nigra in Parkinson's disease is very well documented in the literature (Eriksen JL et al., 2005). It would be interesting to study the role of SK2P in Parkinson's disease.

6.5. SK2sh

The SK2sh variant, which has 3 transmembrane domain spliced out (140 amino acid), appears to be a non-channel forming subunit of SK2 channel. SK2 expression has been described previously in mouse and rat brains (Sailer et al., 2004; Stocker and Pedarzani, 2000.), which concluded that SK channel subunits (SK1, SK2 and SK3) were expressed only in the gray matter areas of the brain. SK2sh mRNA distribution suggests that it is predominantly localized in astrocytes and microglial cells of mouse brain. SK2sh mRNA levels after immobilization stress made no significant contribution toward the SK2 mRNA population, since SK2sh is only expressed in fimbriae hippocampus at low levels. Different tissue distribution gives a clue that the regulation at the promoter level of SK2sh is quite different from that SK2std or SK2P.

However, recent evidence suggests that astrocytes are involved in the active control of neuronal activity and synaptic transmission. Astrocytes and neurons may function as a network where bi-directional communication takes place (Pasti et al., 1997; Araque et al., 1999). It is well known that neuronal transmitters evoke Ca^{2+} elevations in astrocytes (Cornell-Bell et al., 1990; Verkhratsky et al., 1996) and gliotransmitters synchronize neuronal activity (Fellin et al., 2004) and modulate synaptic transmission. There is evidence that gliotransmitters are released through SNARE protein-dependent mechanisms (Araque et al., 2000; Bezzi et al., 2004; Pasti et al., 2001). The roles of other SK channel subunits have been discussed previously (Armstrong et al., 2005). The SNARE domain in the C-terminally cleaved peptide of SK2sh, plus its increased

Discussion

expression in glia-rich regions suggests it may have an important role in gliotransmitter release. Astrocytes can respond to neuronal activity with increased intracellular Ca^{2+} (Dani et al., 1992; Porter and McCarthy, 1996; Pasti et al., 1997) that can propagate to neighboring astrocytes as a Ca^{2+} wave (Cornell-Bell et al., 1990; Charles et al., 1991; Newman and Zahs, 1997).

Furthermore, an elevation of astrocyte Ca^{2+} can signal to neurons, inducing neuronal Ca^{2+} elevations (Nedergaard, 1994; Parpura et al., 1994; Hassinger et al., 1995; Pasti et al., 1997; Bezzi et al., 1998), regulating neuronal excitability (Araque et al., 1998, 1999; Newman and Zahs, 1998) and modulating synaptic transmission (Araque et al., 1998; Kang et al., 1998). Therefore, astrocytes and neurons may function as a network where bi-directional communication takes place (Pasti et al., 1997; for review see Araque et al., 1999). Recently it was shown that Ca^{2+} -dependent glutamate release from astrocytes is a SNARE protein-dependent process (Araque et al., 2000). The presence of a SNARE domain in the cleaved peptide of SK2sh should play an important role in the exocytotic pathway in astrocytes. Furthermore, small-conductance Ca^{2+} /calmodulin-activated K^{+} channel KCNN4/ $\text{KCa}3.1/\text{SK4}/\text{IK1}$ is highly expressed in microglia, and is involved in microglia activation and neurotoxicity (Kaushal et al., 2007).

However, it was not shown in this study whether the SK4 channel has a SNARE domain similar to the domain present in the SK2sh peptide. In the present study I have also shown that SK2sh is overexpressed during Alzheimer's disease (AD). A commonly observed feature of AD is the presence of activated astrocytes and microglia, which is also a common feature of other neurodegenerative disorders. It is possible that SK2sh is elevated to counteract detrimental effects of amyloid deposition. This supports the theory that Abeta amyloids deposition has neurodegenerative consequences, as opposed to neuroprotective effects, as others have suggested (Campbell 2001). Compensatory functions of SK2sh in the CNS are consistent with proposed functions of other genes having identical mRNA expression patterns in the brain (Calero et al. 2000; Poirier 2000).

6.6. SK2L

The SK2 longer isoform was shown to co-assemble with SK2 primary isoform in

Discussion

the CA2 region of mouse hippocampus. The extended N-terminal sequence unique to SK2-L contains an SH3-binding site as well as a potential MAP kinase substrate and several serine and threonine residues that may also serve as targets for phosphorylation. It also contains a motif with a core sequence of CXXC that has homology to regions in enzymes that transfer sulfur-containing moieties to metabolites, MoeZ and MoeB, which are molybdopterin synthase activating enzymes in the molybdopterin cofactor biosynthesis pathway. The N-terminal extension of SK2-L described here is similar in length and shows some sequence homology with the N-terminal domain of SK3 (Adelman et al., 2005). Substantial differences in SK2L mRNA modulation were not found in the mouse hippocampus during immobilization stress experiments and the specific role of SK2L in the CNS has yet to be determined.

6.7. SK2CaMBD

The SK2CaMBD variant was found only in mouse brain and had an in-frame premature termination codon (PTC), which will lead to degradation of the transcript by nonsense-mediated decay mechanisms (Lewis et al., 2003) in the cell. However, studies have shown that some protein factors, including splicing factors that bind RNA, can auto regulate their levels by binding to their own pre-mRNA to promote increased levels of PTC-containing splice variants (Soergel et al., 2005). Thus, it is probable that SK2CaMBD transcripts may be involved in auto regulation of other mRNA transcripts of SK2.

6.8. SK2-N-terminus and SK2R

The SK2-N-terminus variant was only found in mouse heart and liver tissues, which was not within the scope of the current study. The extra two exons at 3' UTR of SK2R did not contribute to the protein coding relative to the SK2std isoform. Hence, no further analysis was performed with these variants.

6.9. Future perspectives

The present study provides several potentially important concepts. First, the SK2P C-terminally cleaved peptide can be involved in synaptic transmission and

Discussion

neurotransmitter release via the SNARE complex, which in turn can be involved in memory consolidation. Second, the SK2sh C-terminally cleaved peptide can be involved in bi-directional communication within an astrocyte-neuronal network via SNARE complex. Third, we propose a peptide, which can be used as a pharmacological tool in neurosecretion pathways studies. Fourth, this study has given clues concerning discrepancies observed in previous studies as to the expression of SK2 in mouse brain. Fifth, this study provides preliminary data suggestive of a role for SK channels in neuroglia interaction and synaptic transmission. Sixth, this study shows that the SK2sh variant may have an important role in the pathogenesis of Alzheimer's disease and deciphering the role of the SK2P variant in Parkinson's disease would be particularly interesting for future studies.

This study has successfully highlighted the computational findings and experimental verification of six novel SK2 splice variants. Additional studies are necessary to fully outline the contribution of these novel splice variants to SK channel signaling and cognitive processes. However, the data presented here clearly indicate that members of the SK2 channel family mediate their physiological function in several additional ways besides acting only as classical small conductance, calcium activated potassium channel. This methodology, starting from a bioinformatics approach, cloning, RNA and protein detection and finally closing in whole-animal experiments represents a powerful tool, which can also be used to identify novel and functionally important splice variants of other genes involved in health and disease.

7. Summary

In this study I have found six novel splice variants of mouse SK2 channel through bioinformatics analysis, indicating that SK2 is highly regulated at the post transcriptional level. Two of these variants, SK2P and SK2sh, were highly conserved across species and seem to have potentially novel function within the SK channel family. The SK2CaMBD variant had a premature stop codon, the SK2R variant did not alter the protein-coding region relative to SK2std and the SK2-N-terminus variant was found only in heart and liver tissues. Post translational cleavage within a three amino acid insert at the C-terminus of SK2P results in a 10 KDa peptide, which has a SNARE domain that may interfere with the SNARE complex formation, ultimately modulating exocytosis and glutamate release. SK2P is specifically localized in the CA3 region of the mouse hippocampus and is up-regulated after fear conditioning training. A 10 KDa peptide, which is most likely cleaved off at the C-terminal region of SK2P was found at several time points after training in hippocampal fractions. Since the 10 KDa peptide was not detected in the hippocampus of naïve animals, a role in memory consolidation can be expected. The SK2sh variant, which has three transmembrane domains spliced out (a total of 140 amino acid), appears to be a non-channel forming subunit and is localized in regions rich in astrocytes and microglial in the brain. Since SK2P plays a potential role in glutamate release and memory consolidation and SK2sh might play a role in gliotransmitter release, functions of these variants could be the reason for the seemingly contradictory roles of SK2 channels in hippocampal LTP and contextual fear memory. This study also showed that SK2P is highly up-regulated after stress and is the major variant undergoing high modulation in the cumulative effects of SK2 mRNA. Alternative splicing of the SK2 primary transcript thus adds unexpected complexity to SK2 channel functions in the CNS.

8. References

- Akker SA, Smith PJ and Chew SL. Nuclear postranscriptional control of gene expression. *J Mol Endocrinology*. (2001) 27:123-31.
- Altschul SF, Gish W, Miller W, Myers EW and Lipman, D.J. "Basic local alignment search tool." *J. Mol. Biol.* (1990) 215:403-410.
- Araque A, Parpura V, Sanzgiri RP and Haydon PG. Tripartite synapses: glia, the unacknowledged partner. *Trends Neurosci* (1999) 22:208-215.
- Araque A, Li N, Doyle RT and Haydon PG. SNARE protein-dependent glutamate release from astrocytes. *J Neurosci*. (2000) Jan 15;20(2):666-73.
- Armstrong WE, Rubrum A, Teruyama R, Bond CT and Adelman JP. Immunocytochemical localization of small-conductance, calcium-dependent potassium channels in astrocytes of the rat supraoptic nucleus. *J Comp Neurol*. (2005) Oct 24;491(3):175-85.
- Barford ET, Moore AL, Lidofsky SD. Cloning and functional expression of a liver isoform of the small conductance Ca²⁺-activated K⁺ channel SK3. *Am J Physiol Cell Physiol*. (2001) Apr;280(4):C836-42.
- Bark C, Bellinger FP, Kaushal A, Mathews JR, Partridge LD and Wilson M.C. Developmentally regulated switch in alternatively spliced SNAP-25 isoforms alters facilitation of synaptic transmission, *J Neurosci* 24 (2004), pp. 8796–8805.
- Benson DL and Cohen PA. Activity-independent segregation of excitatory and inhibitory synaptic terminals in cultured hippocampal neurons, *J Neurosci* 16 (1996), pp. 6424–6432.

References

Blanes-Mira C, Merino JM, Valera E, Fernández-Ballester G, Gutiérrez LM, Viniegra S, Pérez-Payá E, Ferrer-Montiel A. Small peptides patterned after the N-terminus domain of SNAP25 inhibit SNARE complex assembly and regulated exocytosis. *J Neurochem.* (2004) Jan;88(1):124-35.

Blatz AL and Magleby KL. Single apamin-blocked Ca²⁺ activated K channels of small conductance in cultured rat skeletal muscle *Nature (London)* (1986) 323:718-720

Blatz AL and Magleby KL. Calcium-activated potassium channels. *Trends Neurosci.* (1987) 10:463-467.

Blencowe BJ. Exonic splicing enhancers: mechanism of action, diversity and role in human genetic diseases. *Trends Biochem Sci* (2000) 25:106-10.

Boguski MS, Lowe TM, Tolstoshev CM. dbEST—database for expressed sequence tags. *Nature Genetics* (1993) 4:332—33.

Bairoch A, Apweiler R, Wu CH, et al. The Universal Protein Resource (UniProt). *Nucleic Acids Res* (2005) 33:D154-59.

Bezzi P, Gunderson V, Galbete JL, Seifert G, Steinhauser C, Pilati E, Volterra A. Astrocytes contain a vesicular compartment that is competent for regulated exocytosis of glutamate. *Nat Neurosci.* (2004) Jun;7(6):613-20.

Betz A, Okamoto M, Benseler F, Brose N. Direct interaction of the rat unc-13 homologue Munc13-1 with the N terminus of syntaxin. *J Biol Chem* (1997) 272: 2520-2526.

Boise et al., Bcl-x, a bcl-2-related gene that functions as a dominant regulator of apoptotic cell death. *Cell* 74 (1993), pp. 597–608.

Bond CT, Maylie J, and Adelman JP. Small-conductance calcium-activated potassium

References

channels *Ann N Y Acad Sci.* (1999) 370-378.

Black DL. Protein diversity from alternative splicing: a challenge for bioinformatics and post-genome biology. *Cell* 103 (2000), pp. 367–370.

Black DL, Grabowski PJ. Alternative pre-mRNA splicing and neuronal function. *Prog Mol Subcell Biol.* (2003); 31:187-216.

Blank T, Nijholt I, Kye MJ, Radulovic J, Spiess J. Small-conductance, Ca²⁺-activated K⁺ channel SK3 generates age-related memory and LTP deficits, *Nat Neurosci* (2003) **6**:911–912.

De Bruin LA, Schasfoort EM, Steffens AB and Korf J. Effects of stress and exercise on rat hippocampus and striatum extracellular lactate, *Am J Physiol* 259 (1990), pp. R773–R779.

Boyles JK, Notterpek LM, Wardell MR and Ball SCJ. Identification, characterization, and tissue distribution of apolipoprotein D in the rat. *J. Lipid Res.* (1990) 31, 2243-2256.

Boue S, Letunic I, Bork P. Alternative splicing and evolution. *Bioessays.* (2003) 25:1031–1034. doi: 10.1002/bies.10371.

Bresnahan PA, Leduc R, Thomas L, Thorner J, Gibson HL, Brake AJ, Barr PJ, Thomas G. Human fur gene encodes a yeast KEX2-like endoprotease that cleaves pro-beta-NGF in vivo. *J Cell Biol.* (1990) Dec;111 (6 Pt 2):2851-9.

Burgess RW, Nguyen QT, Son YJ, Lichtman JW and Sanes JR. Alternatively spliced isoforms of nerve and muscle derived agrin: their roles at the neuromuscular junction. *Neuron* 23 (1999), pp. 33–44.

Burge CB, Tuschl T and Sharp PA. Splicing of precursors to mRNAs by the

References

spliceosomes. In: *The RNA World* (1999), pp. 525–560.

Cartegni et al 2002. Listening to silence and understanding nonsense: exonic mutations that affect splicing. *Nature Reviews Genetics* 3: 285-298.

Chalfant CE, Mischak H, Watson JE, Winkler BC, Goodnight J, Farese RV and Cooper DR. Regulation of alternative splicing of protein kinase C beta by insulin. *J. Biol. Chem.* 270 (1995), pp. 13326–13332.

Chang CP, Pearse RV, O’Connell S and Rosenfeld MG. Identification of a seven transmembrane helix receptor for corticotropin-releasing factor and sauvagine in mammalian brain. *Neuron.* 11 (1993) 1187-1195.

Chetkovich DM, Bunn RC, Kuo SH, Kawasaki Y, Kohwi M and Brecht DS. Postsynaptic targeting of alternative postsynaptic density-95 isoforms by distinct mechanisms, *J Neurosci* 22 (2002), pp. 6415–6425.

Chinnaiyan AM, Dixit VM. The cell-death machine. *Curr Biol.* (1996) May 1;6(5):555-62.

Choi DW. Excitotoxic cell death. *J Neurobiol.* (1992) Nov;23(9):1261-76.

Choi DW. Glutamate neurotoxicity and diseases of the nervous system. *Neuron.* (1988) Oct;1(8):623-34.

Chong JA et al., REST: a mammalian silencer protein that restricts sodium channel gene expression to neurons. *Cell* 80 (1995), pp. 949–957.

Claverie JM. Gene number. What if there are only 30,000 human genes?. *Science* 291 (2001), pp. 1255–1257.

References

Clark RE and Squire LR Classical conditioning and brain systems: the role of awareness
Science (1998) 280: 77- 81.

Coetzee et al., Molecular diversity of K⁺ channels. *Ann. NY Acad. Sci.* 868 (1999), pp. 233–285.

Collett JW and Steele RE. Alternative splicing of a neural-specific Src mRNA (Src+) is a rapid and protein synthesis-independent response to neural induction in *Xenopus laevis*. *Dev. Biol.* 158 (1993), pp. 487–495.

Cornell-Bell AH, Finkbeiner SM, Cooper MS, Smith SJ. Glutamate induces calcium waves in cultured astrocytes: long-range glial signaling. *Science.* (1990) Jan 26;247(4941):470-3.

Cornille F, Deloye F, Fournie-Zaluski, MC. Roques, B. P., and Poulain, B. Inhibition of Neurotransmitter Release by Synthetic Proline-rich Peptides Shows That the N-terminal Domain of Vesicle-associated Membrane Protein/Synaptobrevin Is Critical for Neuroexocytosis. (1995) *J. Biol. Chem.* 270, 16826-16832

Conti LH and Foote SL, Effects of pretreatment with corticotropin-releasing factor on the electrophysiological responsivity of the locus coeruleus to subsequent corticotropin-releasing factor challenge. *Neuroscience* 69 (1995), pp.209-219.

Cortright DN, Nicoletti A and Seasholtz AF, Molecular and biochemical characterization of the mouse brain corticotropin-releasing hormone-binding protein. *Mol.Cell.Endocrinol.* 111 (1995) pp. 147-157.

Dal Toso R, Sommer B, Ewert M, Herb A, Pritchett DB, Bach A, Shivers BD and Seeburg PH. The dopamine D2 receptor: two molecular forms generated by alternative splicing. *EMBO J.* 8 (1989), pp. 4025–4034.

References

Daumas S, Halley H, Francés B, Lassalle JM. Encoding, consolidation, and retrieval of contextual memory: differential involvement of dorsal CA3 and CA1 hippocampal subregions. *Learn Mem.* (2005) Jul-Aug;12 (4):375-82.

Daumas S, Halley H, Lassalle JM. Disruption of hippocampal CA3 network: effects on episodic-like memory processing in C57BL/6J mice. *Eur J Neurosci.* (2004) Jul;20(2):597-600.

de Kloet ER, Rots NY, van den Berg DT and Oitzl MS Brain mineralocorticoid receptor function *Ann N Y Acad Sci.* (1994) 746: 8- 20.

de Kloet ER, Vreugdenhil E, Oitzl MS and Joels M Brain corticosteroid receptor balance in health and disease *Endocr Rev.* (1998) 19: 269- 301.

DeBello WM, Betz H, Augustine GJ. Synaptotagmin and neurotransmitter release. *Cell.* (1993) Sep 24;74(6):947-50.

DeBello WM, O'Connor V, Dresbach T, Whiteheart SW, Wang SS, Schweizer FE, Betz H, Rothman JE, Augustine GJ. SNAP-mediated protein-protein interactions essential for neurotransmitter release. *Nature.* (1995) Feb 16; 373 (6515): 626-30.

De Bruin LA, Schasfoort EM, Steffens AB and Korf J. Effects of stress and exercise on rat hippocampus and striatum extracellular lactate, *Am J Physiol* 259 (1990), pp. R773–R779.

De Cesare D and Sassone-Corsi P. Transcriptional regulation by cyclic AMP-responsive factors. *Progr. Nucl. Acid Res. Mol. Biol.* 64 (2000), pp. 343–369.

de Kloet ER, Vreugdenhil E, Oitzl MS and Joels M Brain corticosteroid receptor balance in health and disease *Endocr Rev.* (1998) 19: 269- 301.

References

Denzer AJ, Gesemann HD, Ruegg MA. Synaptic differentiation: the role of agrin in the formation and maintenance of the neuromuscular junction. *Cell Tissue Res* (1997) 290, 357–365.

DeSouza S, Fu J, States B.A and Ziff E.B. Differential palmitoylation directs the AMPA receptor-binding protein ABP to spines or to intracellular clusters, *J Neurosci* 22 (2002), pp. 3493–3503.

Drayna D, Fielding C, McLean J, Baer B, Castro G, Chen E, Comstock L, Henzel W, Kohr W, Rhee L. Cloning and expression of human apolipoprotein D cDNA. *J Biol Chem.* (1986) Dec 15;261(35):16535-9.

Duckert P, Brunak S, Blom N. Prediction of proprotein convertase cleavage sites. *Protein Eng Des Sel.* (2004) Jan;17(1):107-12.

Ehlers MD, Tingley WG and Huganir RL. Regulated subcellular distribution of the NR1 subunit of the NMDA receptor. *Science* 269 (1995), pp. 1734–1737.

Ehlers MD, Bernhardt ZS, Huganir RL. Inactivation of NMDA receptors by direct interaction of calmodulin with the NR1 subunit. *Cell* (1996) 84, 745–755.

Eichenbaum H, Dudchenko P and Wood E The hippocampus, memory, and place cells: it spatial memory or a memory space? *Neuron* (1999) 23: 209-226.

Fasshauer D, Sutton RB, Brunger AT, Jahn R "Conserved structural features of the synaptic fusion complex: SNARE proteins reclassified as Q- and R-SNAREs". *Proceedings of the National Academy of Sciences* (1998) 95: 15781-15786.

Fettiplace R and Fuchs PA. Mechanisms of hair cell tuning. *Annu. Rev. Physiol.* 61 (1999), pp. 809–883.

References

Flames N, Long JE, Garratt AN, Fischer TM, Gassmann M, Birchmeier C, Lai C, Rubenstein JL and Marin O. Short- and long-range attraction of cortical GABAergic interneurons by neuregulin-1, *Neuron* 44 (2004), pp. 251–261.

Florea L, Hartzell G, Zhang Z, et al. A computer program for aligning a cDNA sequence with a genomic DNA sequence. *Genome Res* (1998) 8:967-74.

Florea L, Di Francesco V, Miller J, et al., Gene and alternative splicing annotation with AIR. *Genome Research* (2005) 15:54-66.

Foulkes NS and Sassone-Corsi P. More is better: activators and repressors from the same gene. *Cell* 68 (1992), pp. 411–414.

Francesconi A and Duvoisin RM. Alternative splicing unmasking dendritic and axonal targeting signals in metabotropic glutamate receptor 1, *J Neurosci* 22 (2002), pp. 2196–2205.

Fellin T, Pascual O, Gobbo S, Pozzan T, Haydon PG, Carmignoto G. Neuronal synchrony mediated by astrocytic glutamate through activation of extrasynaptic NMDA receptors. *Neuron*. (2004) Sep 2;43 (5):729-43.

Fernandez I, Ubach J, Dulubova I, Zhang X, Südhof TC, Rizo J. Three-dimensional structure of an evolutionarily conserved N-terminal domain of syntaxin 1A. *Cell*. (1998) Sep 18;94(6):841-9.

Fuller RS, Brake AJ, Thorner J. Intracellular targeting and structural conservation of a prohormone-processing endoprotease. *Science*. (1989) Oct 27;246(4929):482-6.

Garcia-Blanco MA, Tiaraniak AP, Lasda EL. Alternative splicing in disease and therapy. *Nature Biotechnology* (2004) 22: 535-46.

References

Geppert M, Goda Y, Hammer RE, Li C, Rosahl TW, Stevens CF, Südhof TC. Synaptotagmin I: a major Ca²⁺ sensor for transmitter release at a central synapse. *Cell*. (1994) Nov 18;79(4):717-27.

W. Gilbert , Why genes in pieces?. *Nature* 271 (1978), p. 501.

Giros B SP, Martres MP, Riou JF, Emorine LJ, Schwartz JC. Alternative splicing directs the expression of two D2 dopamine receptor isoforms. *Nature* (1989) 342, 923–926.

Gautam et al., Defective neuromuscular synaptogenesis in agrin-deficient mice. *Cell* 85 (1996), pp. 525–535.

Godfrey EW, Roe J and Heathcote RD. Overexpression of agrin isoforms in *Xenopus* embryos alters the distribution of synaptic acetylcholine receptors during development of the neuromuscular junction. *Dev. Biol.* 205 (1999), pp. 22–32.

Grandy DK, MM, Makam H, Stofko RE, Alfano M, Frothingham L, Fischer JB, BHK, Bunzow JR, Server AC, et al.,. Cloning of the cDNA and gene for a human D2 dopamine receptor. *Proc Natl Acad Sci USA* (1989) 86, 9762–9766.

Guiramand J, MJ, Ceraline J, Bhatia M, Borrelli E. Alternative splicing of the dopamine D2 receptor directs specificity of coupling to G-proteins. *J Biol Chem* (1995) 270, 7354–7358.

Gutierrez LM, Canaves JM, Ferrer-Montiel AV, Reig JA, Montal M and Viniegra S. A peptide that mimics the carboxy-terminal domain of SNAP-25 blocks Ca²⁺-dependent exocytosis in chromaffin cells. (1995) *FEBS Lett.* 372, 39-43.

Gutierrez LM, Viniegra S, Rueda J, Ferrer-Montiel AV, Canaves JM, Montal M. A peptide that mimics the C-terminal sequence of SNAP-25 inhibits secretory vesicle docking in chromaffin cells. *J Biol Chem.* (1997) Jan 31;272(5):2634-9.

References

Haas SA, Beissbarth T, Rivals E, et al. GeneNest: automated generation and visualization of gene indices. *Trends Genetics* (2000);16:521-23.

Hammond RS, Bond CT, Strassmaier T, Ngo-Anh TJ, Adelman JP, Maylie J, Stackman RW. Small-conductance Ca²⁺-activated K⁺ channel type 2 (SK2) modulates hippocampal learning, memory, and synaptic plasticity. *J Neurosci.* (2006) Feb 8;26(6):1844-53.

Harris AS, Croall DE, Morrow JS. The calmodulin-binding site in alpha-fodrin is near the calcium-dependent protease-I cleavage site. *J Biol Chem.* (1988) Oct 25;263(30):15754-61.

Hille B. *Ionic channels of Excitable Membranes.* Sinauer Associates Sunderland MA (1992).

Hisatsune H, Umemori T, Inoue T, Michikawa K, Kohda K, Mikoshiba and Yamamoto T. Phosphorylation-dependent regulation of N-methyl--aspartate receptors by calmodulin. *J. Biol. Chem.* 272 (1997), pp. 20805–20810.

Hollrigel GS, Chen K, Baram TZ and Soltesz I. The pro-convulsant actions of corticotropin-releasing hormone in the hippocampus of infant rats. *Neuroscience.* (1998) May;84(1):71-9.

Hu GK, Madore SJ, Moldover B. et al. Predicting splice variant from DNA gene expression data. *Genome Res* (2001) 11:1237-45.

Huerta PT, Sun LD, Wilson M, and Tonegawa S Formation of temporal memory requires NMDA receptors within CA1 pyramidal neurons *Neuron* (2000) 25:473-380.

Ichtchenko K, Hata Y, Nguyen T, Ullrich B, Missler M, Moomaw C and Sudhof T.C.

References

Neurologin 1: a splice site-specific ligand for beta-neurexins. *Cell* 81 (1995), pp. 435–443.

Jaskolski F, Coussen F, Nagarajan N, Normand E, Rosenmund C and Mulle C. Subunit composition and alternative splicing regulate membrane delivery of kainate receptors, *J Neurosci* 24 (2004), pp. 2506–2515.

Jiang ZH and Wu J. Alternative splicing and programmed cell death. *Proc. Soc. Exp. Biol. Med.* 220 (1999), pp. 64–72.

Jiang ZH, Zhang WJ, Rao Y, Wu JY. Regulation of Ich-1 pre-mRNA alternative splicing and apoptosis by mammalian splicing factors. *Proc. Natl. Acad. Sci. USA* 95 (1998), pp. 9155–9160.

Joels M and de Kloet ER Effect of corticosteroid hormones on electrical activity in rat hippocampus *J Steroid Biochem Mol Biol.* (1991) 40: 83- 86.

Joels M, Heslen W and de Kloet ER Mineralocorticoid hormones suppress serotonin induced hyperpolarization of rat hippocampal CA1 neurons *J Neurosci.* (1991) 11: 2288-2294.

Joels M, Velzing E, Nair S, Verkuyl JM and Karst H Acute stress increases calcium current amplitude in rat hippocampus: temporal changes in physiology and gene expression *Eur J Neurosci.* (2003) 18:1315- 1324.

Jones EM, Gray-Keller M and Fettiplace R. The role of Ca²⁺-activated K⁺ channel spliced variants in the tonotopic organization of the turtle cochlea. *J. Physiol. (London)* 518 (1999), pp. 653–665.

Karst H and Joels M The induction of corticosteroid actions on membrane properties of hippocampal CA1 neurons requires protein synthesis *Neurosci Lett.* (1991) 130: 27- 31.

References

Karst H, Wadman WJ and Joels M Corticosteroid receptor-dependent modulation of calcium currents in rat hippocampal CA1 neurons *Brain Res.* (1994) 649: 234- 242.

Kent WJ. BLAT-the BLAST-like alignment tool *Genome Research* (2002) 12:656-64.

Kiyosawa H, Mise N, Iwase S, et al. Disclosing hidden transcripts: mouse natural sense-antisense transcripts tend to be poly (A) negative and nuclear localized. *Genome Research* (2005) 15:463-74.

Kim N, Shin S, Lee S. ECgene: genome-based EST clustering and gene modeling for alternative splicing. *Genome Research* (2005) 15:566-76.

Kole MH, Swan L. and Fuchs E. The antidepressant tianeptine persistently modulates glutamate receptor currents of the hippocampal CA3 commissural associational synapse in chronically stressed rats, *Eur J Neurosci* 16 (2002), pp. 807–816.

Köhler M, Hirschberg B, Bond CT, Kinzie JM, Marrion NV, Maylie J and Adelman JP. (1996) *Science* 273, 1709–1714

Krämer A. The structure and function of proteins involved in mammalian pre-mRNA splicing. *Annu. Rev. Biochem.* 65 (1996), pp. 367–409.

Krishek BJ, Xie X, Blackstone C, Huganir RL, Moss SJ, Smart TG. Regulation of GABAA receptor function by protein kinase C phosphorylation. *Neuron* 12 (1994), pp. 1081–1095.

Koike M, Tsukada S, Tsuzuki K, Kijima H and Ozawa S. Regulation of kinetic properties of GluR2 AMPA receptor channels by alternative splicing. *J. Neurosci.* 20 (2000), pp. 2166–2174.

References

Kolski-Andreaco A, Tomita H, Shakkottai VG, Gutman GA, Cahalan MD, Gargus JJ, Chandy KG. SK3-1C, a dominant-negative suppressor of SKCa and IKCa channels. *J Biol Chem.* (2004) Feb 20;279(8):6893-904.

Konig H, Ponta H and Herrlich P. Coupling of signal transduction to alternative pre-mRNA splicing by a composite splice regulator. *EMBO J.* 17 (1998), pp. 2904–2913.

Ladd AN and Cooper TA. Finding signals that regulate alternative splicing in the post-genomic era, *Genome Biology* (2002) 3 (11): reviews 0008.1-0008.16.

Lambolez B, Ropert N, Perrais D, Rossier J and Hestrin S. Correlation between kinetics and RNA splicing of alpha-amino-3-hydroxy-5-methylisoxazole-4-propionic acid receptors in neocortical neurons. *Proc. Natl. Acad. Sci. USA* 93 (1996), pp. 1797–1802.

Lancaster B and Adams PR. Calcium-dependent current generating the afterhyperpolarization of hippocampal neurons *J Neurophysiol.* (1986) 55: 1268- 1282

Lee BT, Tan TW, Ranganathan S. MGAlignIt: a web service for the alignment of mRNA/EST and genomic sequences. *Nucleic Acids Res* 2003 Jul 1;31(13):3533-6.

Lee I, Yoganasimha D, Rao G, Knierim JJ. Comparison of population coherence of place cells in hippocampal subfields CA1 and CA3. *Nature.* (2004) Jul 22;430 (6998):456-9.

Lee I and Kesner RP. Differential contributions of dorsal hippocampal subregions to memory acquisition and retrieval in contextual fear-conditioning. *Hippocampus.* (2004);14(3):301-10.

Lee Y and Tsai J, Sunkara S, et al. The TIGR Gene Indices: clustering and assembling EST and known genes and integration with eukaryotic genomes. *Nucleic Acids Research* (2005) 33(Database issue) D71-4.

Leipzig J, Pevzner P and Heber S. The Altenianve Splicing gallery (ASCI); bridging the gap between genome and transcriptome. *Nucleic Acids Res* (2004) 32:3977-83.

References

- Leutgeb S, Leutgeb JK, Treves A, Moser MB, Moser EI. Distinct ensemble codes in hippocampal areas CA3 and CA1. *Science*. (2004) Aug 27;305(5688):1295-8.
- Liang F, Holt I, Pertea G. *et al.* An optimized protocol for analysis of EST sequences. *Nucleic Acids Research* (2000) 28;2657-65.
- Lin Z, Haus S, Edgerton J, Lipscombe D. Identification of functionally distinct isoforms of the N-type Ca²⁺ channel in rat sympathetic ganglia and brain. *Neuron* 18 (1997), pp. 153–166.
- Lin Z, Lin Y, Schorge S, Pan JQ, Beierlein M, Lipscombe D. Alternative splicing of a short cassette exon in alpha1B generates functionally distinct N-type calcium channels in central and peripheral neurons. *J. Neurosci.* 19 (1999) pp. 5322–5331.
- Lingle C.J, Solaro C.R, Prakriya M and Ding J.P. Calcium-activated potassium channels in adrenal chromaffin cells. *Ion Channels* 4 (1996), pp. 261–301.
- Livak KJ, Schmittgen TD. Analysis of relative gene expression data using real-time quantitative PCR and the 2(-Delta Delta C(T)) method. *Methods* (2001) 25:402–408.
- Lopez AJ. Developmental role of transcription factor isoforms generated by alternative splicing. *Dev. Biol.* 172 (1995), pp. 396–411.
- Lopez AJ. Alternative splicing of pre-mRNA: developmental consequences and mechanisms of regulation. *Annu. Rev. Genet.* 32 (1998), pp. 279–305.
- Lowy MT, Gault L and Yamamoto BK. Adrenalectomy attenuates stress-induced elevations in extracellular glutamate concentrations in the hippocampus, *J Neurochem* 61 (1993) pp. 1957–1960.
- Lynch KW and Weiss A. A model system for activation-induced alternative splicing of CD45 pre-mRNA in T cells implicates protein kinase C and Ras. *Mol. Cell. Biol.* 20 (2000), pp. 70–80.
- Madison DV and Nicoll RA Control of the repetitive discharge of rat CA1 pyramidal

References

neurons in vivo *J Physiol.* (1984) 354: 319-331.

Maniatis T and Tasic B. Alternative pre-mRNA splicing and proteome expansion in metazoans. *Nature.* (2002) Jul 11;418(6894):236-43.

Matter N, Herrlich P and Konig H. Signal-dependent regulation of splicing via phosphorylation of Sam68. *Nature* (2003) 420, 691-695.

McEwen BS, De Kloet ER and Rostene W Adrenal steroid receptors and actions in the nervous system *Physiol Rev.* (1986) 66: 1121- 1188.

Mehta MR, Barnes CA and McNaughton BL Experience-dependent, asymmetric explanation of hippocampal place fields *Proc. Natl. Acad. Sci. USA* (1997) 8918-8921.

Meldrum BS. Glutamate as a neurotransmitter in the brain: review of physiology and pathology. *J Nutr.* (2000) Apr; 130 (4S Suppl):1007S-15S.

Metha PP, Battenberg E and Wilson MC. SNAP-25 and synaptotagmin involvement in the final Ca²⁺-dependent triggering of neurotransmitter exocytosis. (1996) *Proc. Natl. Acad. Sci. U. S. A.* 93, 10471-10476.

Missler M and Sudhof T.C. Neurexins: three genes and 1001 products. *Trends Genet.* 14 (1998), pp. 20–26.

Moghaddam B, Bolinao ML, Stein-Behrens B and Sapolsky R. Glucocorticoids mediate the stress-induced extracellular accumulation of glutamate, *Brain Res* 655 (1994), pp. 251–254.

Mott R. EST_GENOME: a program to align spliced ONA sequences to unspliced genomic DNA. *Comput Appl Biosciences* (1997) 3:477-78.

Mpari B, Regaya I, Escoffier G, Mourre C. Differential effects of two blockers of small conductance Ca²⁺-activated K⁺ channels, apamin and lei-Dab7, on learning and memory in rats. *J Integr Neurosci.* (2005) Sep;4(3):381-96.

Mu Y, Otsuka T, Horton A.C., Scott DB and Ehlers MD. Activity-dependent mRNA

References

splicing controls ER export and synaptic delivery of NMDA receptors, *Neuron* 40 (2003), pp. 581–594.

Navaratnam DS, Bell TJ, Tu TD, Cohen EL, Oberholtzer JC. Differential distribution of Ca²⁺-activated K⁺ channel splice variants among hair cells along the tonotopic axis of the chick cochlea. *Neuron* 19 (1997), pp. 1077–1085.

Nijholt I, Farchi N, Kye M, Sklan EH, Shoham S, Verbeure B, Owen D, Hochner B, Spiess J, Soreq H, Blank T. Stress-induced alternative splicing of acetylcholinesterase results in enhanced fear memory and long-term potentiation. *Mol Psychiatry*. (2004) Feb; 9 (2):174-83.

Olney JW, de Gubareff T. Glutamate neurotoxicity and Huntington's chorea. *Nature*. (1978) Feb 9; 271 (5645) : 557-9.

Owens MJ and Nemeroff CB. Physiology and pharmacology of corticotropin-releasing factor. *Pharmacol. Rev.* 43 (1991) 425-473.

Palm K, Belluardo N, Metsis M, Timmusk T. Neuronal expression of zinc finger transcription factor REST/NRSF/XBR gene. *J. Neurosci.* 18 (1998), pp. 1280–1296.

Pasti L, Volterra A, Pozzan T, Carmignoto G. Intracellular calcium oscillations in astrocytes: a highly plastic, bidirectional form of communication between neurons and astrocytes in situ. *J Neurosci* (1997) 17:7817-7830.

Pasti L, Zonta M, Pozzan T, Vicini S, Carmignoto G. Cytosolic calcium oscillations in astrocytes may regulate exocytotic release of glutamate. *J Neurosci.* (2001) Jan 15;21(2):477-84.

Philipps DL, Park JW, Graveley BR. A computational and experimental approach toward a priori identification of alternatively spliced exons. *RNA.* (2004) 10:1838–1844.

Poirier MA, Xiao W, Macosko JC, Chan C, Shin YK, Bennett MK. The synaptic SNARE complex is a parallel four-stranded helical bundle. *Nat Struct Biol.* 1998 Sep;5(9):765-9.

References

Ponting CP, Schultz J, Milpetz F, Bork P. SMART: identification and annotation of domains from signalling and extracellular protein sequences. *Nucleic Acids Res.* (1999) Jan 1;27(1):229-32.

Potter E, Behan DP, Fischer WH, Linton EA, Lowry PJ and Vale WW, Cloning and characterization of the cDNA for human and rat corticotropin releasing factor-binding proteins. *Nature.* 349 (1991), pp.423-426.

Pruitt KD, Tatusova T, Maglott DR. NCBI Reference Sequence project: update and current status. *Nucleic Acids Res* (2003) 31:34-37.

Puschel AW and Betz H. Neurexins are differentially expressed in the embryonic nervous system of mice. *J. Neurosci.* 15 (1995), pp. 2849–2856.

Quinlan JJ, Firestone LL and Homanics GE. Mice lacking the long splice variant of the gamma 2 subunit of the GABA(A) receptor are more sensitive to benzodiazepines. *Pharmacol. Biochem. Behav.* 66 (2000), pp. 371–374.

Quirk MC, Blum KI and Wilson MA Experience-dependent changes in extracellular spike amplitude may reflect regulation of dendritic action potential back-propagation in rat hippocampal pyramidal cells. *J Neurosci.* (2001) 21:240-248

Resch A, Xing Y, Alekseyenko A, Modrek B, Lee C. Evidence for a subpopulation of conserved alternative splicing events under selection pressure for protein reading frame preservation. *Nucleic Acids Res.* (2004) 32:1261–1269.

Rodger J, Davis S, Laroche S, Mallet J, Hicks A. Induction of long-term potentiation in vivo regulates alternate splicing to alter syntaxin 3 isoform expression in rat dentate gyrus. *J. Neurochem.* 71 (1998), pp. 666–675.

Rosenblatt KP, Sun ZP, Heller S and Hudspeth AJ. Distribution of Ca²⁺-activated K⁺ channel isoforms along the tonotopic gradient of the chicken's cochlea. *Neuron* 19 (1997), pp. 1061–1075.

Rost B and Sander C. Prediction of protein secondary structure at better than 70%

References

accuracy. *J Mol Biol.* (1993) Jul 20;232(2):584-99.

Rothman SM. Synaptic activity mediates death of hypoxic neurons. *Science.* (1983) Apr 29;220(4596):536-7.

Ruegg MA, Tsim KW, Horton SE, Kroger S, Escher G, Gensch EM and McMahan UJ. The agrin gene codes for a family of basal lamina proteins that differ in function and distribution. *Neuron* 8 (1992), pp. 691–699.

Sah P and Bekkers JM Apical dendritic location of slow afterhyperpolarization current on hippocampal pyramidal neurons: implications for the integration of long-term potentiation *J Neurosci.* (1996) 16: 4537- 4542

Sailer CA, Kaufmann WA, Marksteiner J and Knaus HG. Comparative immunohistochemical distribution of three small-conductance Ca²⁺-activated potassium channel subunits, SK1, SK2, and SK3 in mouse brain. (2004) *Mol.Cell. Neurosci.* 26, 458–469.

Scheiffele P, Fan J, Choih J, Fetter R and Serafini T. Neuroligin expressed in nonneuronal cells triggers presynaptic development in contacting axons. *Cell* 101 (2000), pp. 657–669.

Schmucker D, Clemens JC, Shu H, Worby CA, Xiao J, Muda M, Dixon JE, Zipursky SL. *Drosophila Dscam* is an axon guidance receptor exhibiting extraordinary molecular diversity. *Cell* 101 (2000), pp. 671–684.

Schoenherr CJ and Anderson D.J. The neuron-restrictive silencer factor (NRSF): a coordinate repressor of multiple neuron-specific genes. *Science* 267 (1995), pp. 1360–1363.

Seidah NG, Chrétien M. Proprotein and prohormone convertases: a family of subtilases generating diverse bioactive polypeptides. *Brain Res.* (1999) Nov 27;848(1-2):45-62.

References

Seidah NG, Day R, Marcinkiewicz M, Chrétien M. Precursor convertases: an evolutionary ancient, cell-specific, combinatorial mechanism yielding diverse bioactive peptides and proteins. *Ann N Y Acad Sci.* (1998) May 15;839:9-24.

Shmukler BE, Bond CT, Wilhelm S, Bruening-Wright A, Maylie J, Adelman JP, Alper SL(2001) Structure and complex transcription pattern of the mouse SK1 K(Ca) channel gene, KCNN1 *Biochim Biophys Acta.* (2001) Mar 19;1518 (1-2):36-46.

Shaham S and Horvitz HR. An alternatively spliced *C. elegans* ced-4 RNA encodes a novel cell death inhibitor. *Cell* 86 (1996), pp. 201–208.

Shifrin V.I and Neel B.G. Growth factor-inducible alternative splicing of nontransmembrane phosphotyrosine phosphatase PTP-1B pre-mRNA. *J. Biol. Chem.* 268 (1993), pp. 25376–25384.

Schuler GD. Pieces of the puzzle: expressed sequence tags and the catalog of human genes. *J Mol Med* (1997) 75:694-98.

Schumacher MA, Rivard AF, Bachinger HP and Adelman JP. Structure of the gating domain of a Ca²⁺-activated K⁺ channel complexed with Ca²⁺/calmodulin. *Nature* (2001) 410, 1120–1124.

Schultz J, Milpetz F, Bork P, Ponting CP. SMART, a simple modular architecture research tool: identification of signaling domains. *Proc Natl Acad Sci U S A.* (1998) May 26;95(11):5857-64.

Shapiro ML, Tanila H and Eichenbaum H Cues that hippocampal place cells encode: dynamic and hierarchical representation of local and distal stimuli *Hippocamps* (1997) 7: 624-642

Simth C. Valcarcel J. Alternative pre-mRNA splicing: the logic of combinatorial control.

References

Trends Biochem Sci (2000) 25:381-88.

Simon RP, Swan JH, Griffiths T, Meldrum BS. Blockade of N-methyl-D-aspartate receptors may protect against ischemic damage in the brain. *Science*. (1984) Nov 16;226(4676):850-2.

Smith MA and O'Dowd DK. Cell-specific regulation of agrin RNA splicing in the chick ciliary ganglion. *Neuron* 12 (1994), pp. 795–804.

Smith MA, Fanger GR, O'Connor LT, Bridle P and Maue RA. Selective regulation of agrin mRNA induction and alternative splicing in PC12 cells by Ras-dependent actions of nerve growth factor. *J. Biol. Chem.* 272 (1997), pp. 15675–15681.

Sorek R, Ast G. Intronic sequences flanking alternatively spliced exons are conserved between human and mouse. *Genome Res.* (2003) 13:1631–1637.

Sorek R, Shemesh R, Cohen Y, Basechess O, Ast G, Shamir R. A non-EST-based method for exon-skipping prediction. *Genome Res.* (2004) 14:1617–1623.

Spiess J, River J, River C and vale W, Primary structure of corticotropin-releasing factor from ovine hypothalamus. *Proc.Natl.Acad.Sci.* 78 (1981), pp.6517-6521.

Squire LR and Zola-Morgan S The medial temporal lobe memory system *Science* (1991) 253:1380-1386.

Staley JP and Guthrie C. Mechanical devices of the spliceosome: motors, clocks, springs, and things. *Cell* 92 (1998), pp. 315–326.

Stamm S, Zhu J, Nakai K, Stoilov P, Stoss O, Zhang MQ. An alternative exon database and its statistical analysis. *DNA Cell Biol.* 19 (2000), pp. 739–756.

References

Stocker M and Pedarzani P. Differential distribution of three Ca(2+)-activated K(+) channel subunits, SK1, SK2, and SK3, in the adult rat central nervous system. (2000) *Mol. Cell. Neurosci.* 15, 476–493.

Strassmaier T, Bond CT, Sailer CA, Knaus HG, Maylie J, Adelman JP. A novel isoform of SK2 assembles with other SK subunits in mouse brain. *J Biol Chem.* (2005) Jun 3;280(22):21231-6.

Strausberg RL, Feingold EA, Klausner RD, et al. The mammalian gene collection. *Science* 1999;286:455-57.

Südhof TC. The synaptic vesicle cycle: a cascade of protein-protein interactions. *Nature.* (1995) Jun 22;375(6533):645-53.

Sugnet CW, Kent Wj, Ares Jr M, et al. Transcriptome and genome conservation of alternative splicing events in humans and mice. *Pac.Symp Biocomput* 2004;9:66-77.

Sutton RB, Fasshauer D, Jahn R, Brünger AT. "Crystal structure of a SNARE complex involved in synaptic exocytosis at 2.4 Å resolution". *Nature* (1998) 395: 347-353.

Suzuki K. *Biomed. Biochim. Acta* (1991) 50,483486.

Suzuki K, Imajoh S, Emori Y, Kawasaki H, Minami Y and Ohno S. (1987) *FEBS Lett.* 220,271-277.

Sweatt JD. *Mechanisms of memory* Elsevier Academic Press (2003)

Tanila H, Shapiro ML and Eichenbaum H Discordance of spatial representation in ensembles of hippocampal place cells *Hippocamps* (1997) 7: 613-623.

Tatusova TA, Madden TL. BLAST 2 Sequences, a new tool for comparing protein and

References

nucleotide sequences. *FEMS Microbiol Lett.* (1999) May 15;174(2):247-50.

Teng FY, Wang Y, Tang BL. The syntaxins. *Genome Biol.* (2001) 2(11): REVIEWS.

Thaler C, Gray AC and Lipscombe D. Cumulative inactivation of N-type CaV2.2 calcium channels modified by alternative splicing, *Proc Natl Acad Sci USA* 101 (2004), pp. 5675–5679.

Thomas EA, Danielson PE, Nelson PA, Pribyl TM, Hilbush BS, Hasel KW, Sutcliffe JG. Clozapine increases apolipoprotein D expression in rodent brain: towards a mechanism for neuroleptic pharmacotherapy. *J Neurochem.* (2001) Feb;76(3):789-96.

Thomas EA, Sautkulis LN, Criado JR, Games D, Sutcliffe JG. Apolipoprotein D mRNA expression is elevated in PDAPP transgenic mice. *J Neurochem.* (2001) Dec;79(5):1059-64.

Thomas G. Furin at the cutting edge: from protein traffic to embryogenesis and disease. *Nat Rev Mol Cell Biol.* (2002) Oct;3(10):753-66.

Thomas WS, O'Dowd DK and Smith MA. Developmental expression and alternative splicing of chick agrin RNA. *Dev. Biol.* 158 (1993), pp. 523–535.

Togneri J, Cheng YS, Munson M, Hughson FM, Carr CM. Specific SNARE complex binding mode of the Sec1/Munc-18 protein, Sec1p. *Proc Natl Acad Sci U S A.* (2006) Nov 21;103(47):17730-5.

Tomita H, Shakkottai VG, Gutman GA, Sun G, Bunney WE, Cahalan MD, Chandy KG, Gargus JJ.(2003) Novel truncated isoform of SK3 potassium channel is a potent dominant-negative regulator of SK currents: implications in schizophrenia. *Mol Psychiatry.* (2003) May;8(5):524-35, 460.

References

Ullrich B, Ushkaryov YA and Sudhof TC. Cartography of neurexins: more than 1000 isoforms generated by alternative splicing and expressed in distinct subsets of neurons. *Neuron* 14 (1995), pp. 497–507.

Usuka J, Zhu W, Brendel V, Optimal spliced alignment of homologous cDNA to a genomic DNA template. *Bioinformatics* (2000) 16:203-11.

Vale W, Spiess J, Rivier C and Rivier J Characterization of 41-residue ovine hypothalamic peptide that stimulates secretion of corticotropin and beta-endorphin. 213 (1981), pp. 1394-1397.

van de Ven WJ, Voorberg J, Fontijn R, Pannekoek H, van den Ouweland AM, van Duijnhoven HL, Roebroek AJ, Siezen RJ. Furin is a subtilisin-like proprotein processing enzyme in higher eukaryotes. *Mol Biol Rep.* (1990) Nov;14(4):265-75.

Vergara C, Latorre R, Marrion N.V and Adelman J.P. Calcium-activated potassium channels. *Curr. Opin. Neurobiol.* 8 (1998), pp. 321–329.

Verkhatsky A, Kettenmann H. Calcium signalling in glial cells. *Trends Neurosci.* (1996) Aug;19(8):346-52. Review.

Wafford KA, Bain CJ, Whiting PJ, Kemp JA. Functional comparison of the role of gamma subunits in recombinant human gamma-aminobutyric acidA/benzodiazepine receptors. *Mol. Pharmacol.* 44 (1993), pp. 437–442.

Wang Z, Grabowski PJ. Cell- and stage-specific splicing events resolved in specialized neurons of the rat cerebellum. *RNA* 2 (1996), pp. 1241–1253.

Wang A, Cohen D.S, Palmer E and Sheppard D. Polarized regulation of fibronectin secretion and alternative splicing by transforming growth factor. *J. Biol. Chem.* 266 (1991), pp. 15598–15601.

References

Wang H, Hubbell E, Hn J. et.al. Gene structure-based splice variant deconvolution using a microarray platform. *Bioinformatics* 2003;19 (Suppl.1):i315-22.

Weimbs T, Low SH, Chapin SJ, Mostov KE, Bucher P, Hofmann K; A conserved domain is present in different families of vesicular fusion proteins: a new superfamily. *Proc Natl Acad Sci U S A* (1997) 94:3046-3051.

Wheelan SJ, Church DM, Ostell JM. Spidey: a tool for mRNA-to-genomic alignments. *Genome Res* (2001) 11:1952-57.

Whiting P, McKernan R.M and Iversen L.L. Another mechanism for creating diversity in gamma-aminobutyrate type A receptors: RNA splicing directs expression of two forms of gamma 2 phosphorylation site. *Proc. Natl. Acad. Sci. USA* 87 (1990), pp. 9966–9970.

Winson J. Loss of hippocampal theta rhythm results in spatial memory deficit in the rat *Science* (1978) 201:160-160

Wittekindt OH, Dreker T, Morris-Rosendahl DJ, Lehmann-Horn F, Grissmer S (2004). A novel non-neuronal hSK3 isoform with a dominant-negative effect on hSK3 currents. *Cell Physiol Biochem.* (2004) 14(1-2):23-30.

Woodbury DJ, Rognlien K. "The t-SNARE syntaxin is sufficient for spontaneous fusion of synaptic vesicles to planar membranes". *Cell Biology International* (2000) 24 (11): 809-818.

Wu HY, Tomizawa K, Oda Y, Wei FY, Lu YF, Matsushita M, Li ST, Moriwaki A, Matsui H. Critical role of calpain-mediated cleavage of calcineurin in excitotoxic neurodegeneration. *J Biol Chem.* (2004) Feb 6;279(6):4929-40.

Wu TD, Watanabe CK. GMAP: a genomic mapping and alignment program for mRNA and EST sequences. *Bioinformatics* (2005) 21:59-75

References

Xie GX, Jones K, Peroutka SJ and Palmer PP. Detection of mRNAs and alternatively spliced transcripts of dopamine receptors in rat peripheral sensory and sympathetic ganglia. *Brain Res.* 785 (1998), pp. 129–135.

Yeo GW, Van Nostrand E, Holste D, Poggio T, Burge CB. Identification and analysis of alternative splicing events conserved in human and mouse. *Proc Natl Acad Sci U S A.* (2005) 102:2850–2855.

Zacharias DA and Strehler EE. Change in plasma membrane Ca²⁺(+)-ATPase splice-variant expression in response to a rise in intracellular Ca²⁺. *Curr. Biol.* 6 (1996), pp. 1642–1652.

Zhang L, Liu W and Grabowski PJ. Coordinate repression of a trio of neuron-specific splicing events by the splicing regulator PTB. *RNA* 5 (1999), pp. 117–130.

9. Curriculum Vitae (Lebenslauf)

Name: Saravana Radha Krishna Murthy
Geburtsdatum: 02. October 1977
Geburtsort: Bangalore, Indien
Staatsbürgerschaft: Indisch
Wohnort: Honolulu, USA

Bildungsweg:

1982 - 1991 Besuch der St. Antony's Primary and Middle School, Bangalore, Indien

1991 - 1994 Besuch der Lowry Memorial High School, Bangalore, Indien

1994 - 1997 Besuch des Pre-university college (biology) Dr. B. R. Ambedkar Pre-university college, Bangalore, Indien

1997 -2000 Bachelor of Science, Department of Microbiology Government Science College, Bangalore University, Bangalore, Indien

2000 -2002 Master of Science, Department of Microbiology, Bangalore University, Bangalore, Indien
Titel: "Survey On Human Genome Project"

2004 - 2007 Dissertation am Max-Planck-Institut für Experimentelle Medizin in Göttingen in der Abteilung *Molekulare Neuroendokrinologie* and John A Burns School of Medicine in Specialized Neuroscience Research Program II (Headed by Prof. Dr. Joachim Spiess), University of Hawaii, Honolulu, Hawaii U.S.A.
Titel: "Characterization of Small-Conductance, Calcium-Activated Potassium Channel 2 (SK2) Isoforms in Mouse Brain".

10. Acknowledgements

It was the September of 2004 when I first came to Goettingen, Germany. This was the first time I ever boarded a plane, the first time I ever stepped into other country and many more things I did and experienced for the first time. I still remember very vividly the first thing that made an impression on me: there were very few people around unlike any Indian city. Coming from a country with a warm climate, I was shivering even in September as soon as I got down the train in Goettingen Bahnhof (railway station). Yet, unfamiliar as the terrain was, I could not help but feel a rush of excitement under my skin. The university town was the perfect place to do science. Three years later, I stand at the end of yet another personal milestone, that of completing my doctoral studies. These have been three interesting years, full of challenges, new people, new places and new experiences. This environment was total different for me and it was not always easy. I had to adjust from an Indian cultural environment and code of living to the sometimes-intimidating fluidity of situations and characters. In the process, I have grown (and still growing) both as a person and as a scientist. Amidst all these changes, though, there still is one feeling that remains the same as the first day I came to Goettingen and later to the beautiful paradise, Honolulu: I am still excited and this is a very important chapter in my life. For that, I am thankful. There are two groups of people that I would like to thank: those that had something to do with my thesis and those with no relation to it what so ever.

Starting with the first group, I extend my gratitude to Max Planck Institute for Experimental Medicine, for supporting me financially all these years. Without this support I would probably not have been here in the first place. I would also like to thank Georg-August-University and John A Burns School Of Medicine (JABSOM). The work presented in this dissertation started in Max Planck Institute for Experimental Medicine, Goettingen, Germany and finished in JABSOM, Honolulu, Hawaii, U.S.A, literally I have come a very long way. Apart from providing the infrastructure needed for my research, Max Planck Institute and JABSOM provided me an intellectually stimulating environment in which to perform this research. Working one year in the Max Planck Institute and rest in JABSOM, I had the opportunity to interact with several talented people. I am thankful to all of them for sharing their ideas and visions with me.

Acknowledgements

At an individual level, there are several people that I had the pleasure and the privilege to work with and learn from. First, my advisor Dr. Thomas Blank (I call him Thamu). Thamu has been a delight to work with and I am thankful to him for sharing his ideas and experience.

My first advisor, Prof. Dr. Joachim Spiess, the man who inspired me the most. I should be blessed to work under his guidance. He was the one who drew my attention to focus and discover biology in different angles and opened doors for many new scientific avenues. I had directly worked under him for a very short period. Even during this short time, I have come to appreciate his innovative thinking, his ability to quickly concentrate on the most crucial aspects of a problem, his knack for identifying important problems as well as his focus and dedication to whatever problem we are working on. Without him, completion of my PhD would have been questionable. One of the most important lessons I had learnt from Prof. Dr. Spiess is “**Never give up until you get what you want**”.

Prof. Dr. Hardeland, my referent at the Georg-August-University in Goettingen, has been a source of inspiration. I am grateful to him for being my advisor and the support he provided during my doctoral work. I had learnt a lot from him even though we had brief meetings. I was astonished by the knowledge he has about the latest advances in biological sciences, which I realized during my oral examination to matriculate in Georg-August-University. I want to thank Prof. Dr. Wimmer, my co-referent at the Georg-August-University, for accepting my request to be my co-referent. I would also like to thank Prof. Dr. Braus, Prof. Dr. Doenecke, Prof. Dr. Hustert and Prof. Dr. Ficner for accepting to be members of my thesis committee. Special thanks to Prof. Dr. Braus and Prof. Dr. Doenecke for being my oral examiners. I am grateful to Prof. Dr. Martin Rayner, for helping to shape up my thesis. I have no words to thank Dr. Tessi Sherrin, who as been a very great friend and supported me a lot. Dr. Tessi made me feel that I am not very far from India. We have traded ideas and often cracked jokes.

I would like to thank my parents, without whom I wouldn't have come into this world. They have always been there for me, giving me their unconditional love and supporting me in all my decisions. My mother's and late father's blessing has brought me so far and will carry me all through my life. There are no words to express my gratitude to them. Their affection has been a source of energy for me both during good and bad

Acknowledgements

times. I want to thank my sister Kalaivani and brother Gokul for supporting and encouraging me all the time. I want to specially thank and I am very grateful to Chandrasekhar uncle for helping our family in all our hard times, sharing happiness and constantly encouraging me by e-mails.

I want to take this opportunity to thank Ms. Farahnaz Shakoori and Ms. Angela Meister, for all their support in the administrative work. Ms. Farahnaz was of great help in solving all my administrative problems. I will never forget the timely help she had given, when I twisted my ankle and was in need for medical help. I admire Ms. Farahnaz for her timeous attitude in her work. I want to thank all our Max Planck group members and SNRP2 group members for making my life easy. I want to thank Dr. Akhilesh Pandey, who helped me vision and dream about scientific discoveries during my tenure at IOB (Institute Of Bioinformatics). My special thanks to Prof. Dr. M.R.N.Murthy for introducing me to the fascinating world of research, during my project work in his lab at Indian institute of science in Bangalore, India.

I consider myself lucky because I have been blessed with good friends. With my college buddies and my IOB buddies. We remain good friends even after all these years that we have been apart. Having them around made coping with things so much easier. Our common experiences and mutual support has helped our bond grow stronger and I am sure that it will stay like that for years to come.

11. Publications and abstracts

Full Papers:

Saravana R, Blank T, Spiess J. Involvement of a novel SK2 splice variant (SK2P) in contextual fear conditioning. (In preparation)

Saravana R, Spiess J, Blank T. Cloning and characterization of a novel splice variant of SK2 channel: SK2short. (In preparation)

Gandhi TKB, Chandran S, Peri S, **Saravana R**, Amanchy R, Prasad TSK and Pandey A. A bioinformatics analysis of protein tyrosine phosphatases in humans. DNA Research. (2005) 12, 79-89.

Harsha HC, Suresh S, Amanchy S, Deshpande K, Shanker K, Yatish AJ, Muthusamy B, Vrushabendra V, Rashmi BP, Chandrika KN, Padma N, Sharma S, Badano JS, Ramya MA, Shivashankar HN, Peri S, Choudhury DR, Kavitha MP, **Saravana R**, Niranjana V, Gandhi TKB, Ghosh N, Chandran S, Menezes M, Joy M, Mohan SS, Katsanis N, Deshpande KS, Raghothama C, Prasad CK, and Pandey A. A. Manually Curated Functional Annotation of the Human X Chromosome. Nature Genetics. (2005) 37, 331-332.

Peri S, Navarro JD, Kristiansen TZ, Amanchy R, Surendranath V, Muthusamy B, Gandhi TKB, Chandrika KN, Deshpande N, Suresh S, Rashmi BP, Shanker K, Padma N, Niranjana V, Harsha HC, Talreja N, Vrushabendra BM, Ramya MA, Yatish AJ, Joy M, Shivashankar HN, Kavitha MP, Menezes M, Choudhury DR, Ghosh N, **Saravana R**, Chandran S, Mohan S, Jonnalagadda CK, Prasad CK, Kumar-Sinha C, Deshpande KS and Pandey A. Human Protein Reference Database as a Discovery Resource for Proteomics. Nucleic Acids Research (2004) 32, 497-501.

Publications and abstracts

Peri S, Navarro JD, Amanchy R, Kristiansen TZ, Jonnalagadda CK, Surendranath V, Niranjana V, Muthusamy B, Gandhi TKB, Gronborg M, Ibarrola N, Deshpande N, Shanker K, Shivashankar HN, Rashmi BP, Ramya MA, Zhao Z, Chandrika KN, Padma N, Harsha HC, Yatish AJ, Poovaiah KM, Menezes M, Choudhury DR, Suresh S, Ghosh N, **Saravana R**, Chandran S, Krishna S, Joy M, Anand SK, Madavan V, Joseph A, Wong GW, Schiemann WP, Constantinescu SN, Huang L, Khosravi-Far R, Steen H, Tewari M, Ghaffari S, Blobel GC, Dang CV, Garcia JGN, Pevsner J, Jensen ON, Roepstorff P, Deshpande KS, Chinnaiyan AM, Hamosh A, Chakravarti A and Pandey A. Development of Human Protein Reference Database as an initial platform for approaching systems biology in humans. *Genome Research*. (2003) 13, 2363-2371.

Abstracts:

Saravana R, Spiess J, Blank T (2007). Cloning and characterization of a novel conserved splice variant of SK2 Channel (SK2sh). *Soc. Neurosci. Abstr.* 246

Saravana R, Andres MA, Spiess J, Blank T (2005) Interaction Network Map of Proteins Involved in Learning and Memory Under Non-Stressed and Stressed Conditions. *Soc. Neurosci. Abstr.* 571.15.

Saravana R, Spiess J, Blank T (2006) Interaction Network Map of Proteins Involved in Learning and Memory Under Non-Stressed and Stressed Conditions in Mouse brain. JABSOM symposium.